January 2016

The Impact Of Anterior Gradient 2 (AGR2) Expression In Models Of Arsenite And Cadmium Induced Breast And Bladder Cancers

Jamie Lynn Van Gieson

THE IMPACT OF ANTERIOR GRADIENT 2 (AGR2) EXPRESSION IN MODELS OF ARSENITE AND CADMIUM INDUCED BREAST AND BLADDER CANCERS

by

Jamie Lynn Van Gieson
Bachelor of Science, York College, 2010

A Dissertation

Submitted to the Graduate Faculty

of the

University of North Dakota

in partial fulfillment of the requirements

for the degree of

Doctor of Philosophy

Grand Forks, North Dakota
December
2016

This dissertation, submitted by Jamie L. Van Gieson in partial fulfillment of the requirements for the Degree of Doctor of Philosophy from the University of North Dakota, has been read by the Faculty Advisory Committee under whom the work has been done and is hereby approved.

Seema Somji, Ph.D.

Scott H. Garrett, Ph.D.

John Shabb, Ph.D.

Kurt Zhang, Ph.D.

Jane R. Dunlovy, Ph.D.

This dissertation is being submitted by the appointed advisory committee as having met all of the requirements of the School of Graduate Studies at the University of North Dakota and is hereby approved.

Grant McGimpsey
Dean of the School of Graduate Studies

October 13, 2016
Date

PERMISSION

Title The Impact of Anterior Gradient 2 (AGR2) Expression in Models of Arsenite and Cadmium Induced Breast and Bladder Cancers

Department Biochemistry and Molecular Biology

Degree Doctor of Philosophy

In presenting this dissertation in partial fulfillment of the requirements for a graduate degree from the University of North Dakota. I agree that the library of this University shall make it freely available for inspection. I further agree that permission for extensive copying for scholarly purposes may be granted by the professor who supervised my dissertation work or, in her absence, by the Chairperson of the department or the dean of the School of Graduate Studies. It is understood that any copying or publication or other use of this dissertation or part thereof for financial gain shall not be allowed without my written permission. It is also understood that due recognition shall be given to me and to the University of North Dakota in any scholarly use with may be made of any material in my dissertation.

Jamie L. Van Gieson
July 18, 2016

TABLE OF CONTENTS

LIST OF FIGURES

LIST OF TABLES

Table Page

ACKNOWLEDGEMENTS

I wish to express my sincere appreciation to the members of my advisory committee for their assistance during my time in the doctorate program at the University of North Dakota. I appreciate Dr. Kurt Zhang for his willingness to serve on my committee. My thanks to Dr. Jonathan Shabb for his guidance and for reminding me of why I love to learn. My sincere appreciation goes to Dr. Jane Dunlevy for her support and assistance, including the opportunity to explore the realm of all things confocal microscopy. I would like to extend my gratitude to Drs. Scott Garrett and Seema Somji for their advising, guidance, and support without which this dissertation would not have been possible. Many thanks to Dr. Donald Sens for his support and assistance without which it would not have been possible for me to pursue or complete my graduate education, enabling me to further pursue my career goals.

My appreciation goes to Dr. Xudong Zhou for his technical expertise and assistance with immunohistochemistry. I would also like to extend my thanks to the graduate students with whom I have had the opportunity to work and from whom I have received much gracious support and encouragement.

To My Loving and Supportive Family

ABSTRACT

Bladder cancer constitutes one of the most prevalent cancers and is among the leading causes of cancer-related deaths in the United States. This work sought to better characterize and understand the role of the proto-oncogene anterior gradient 2 (AGR2) in bladder cancers. Immunohistochemical analysis of AGR2 expression in a range of bladder cancer specimens indicated that the expression of AGR2 decreases with an increase in the stage and grade of bladder cancers. The environmental carcinogens arsenic and cadmium (Cd^{2+}) have been implicated in various cancers. This laboratory has demonstrated that arsenite (As^{3+}) and Cd^{2+} can malignantly transform the bladder epithelium cell line UROtsa. This study therefore sought to determine AGR2 expression in six As^{3+} and seven Cd^{2+}-transformed UROtsa cell lines in which real-time PCR and western blotting data indicated that AGR2 expression was increased in several of the transformed cell lines. Next AGR2 expression was evaluated in mouse heterotransplant tumors arising from the injection of the previously transformed UROtsa cell lines in athymic nude ($Foxn1^{nu}$) mice. Results from real-time PCR analysis and immunohistochemistry on tumor samples demonstrated that AGR2 expression remained increased in most of the Cd^{2+} heterotransplants but was significantly increased in only a couple of the As^{3+} heterotransplants. UROtsa cells were further exposed to 2, 4, or 6 μM As^{3+} or to 1, 2, or 4 μM Cd^{2+} for up to 72 hours and real-time PCR analysis was performed to evaluate AGR2 expression. While AGR2 exhibited increased expression in

response to 48 hours As^{3+} exposure, expression was not induced to the same extent in Cd^{2+} exposed UROtsa cells. Spheroids containing cancer initiating cells (CICs) were generated from the transformed and the parent UROtsa cells and the expression of AGR2 was determined. The results obtained suggested that there was an increase in the expression of AGR2 in all of the spheroids isolated from the As^{3+}-transformed cells whereas some of the spheroids isolated from the Cd^{2+}-transformed cells expressed high levels of AGR2 when compared to the spheroids isolated from the parent UROtsa cells.

This laboratory has also shown that As^{3+} and Cd^{2+} can cause malignant transformation of a breast epithelial cell line, MCF-10A. Previous studies have shown that the expression of AGR2 promotes breast tumorigenesis in mice. This gene is known to play a role in promoting cellular transformation, tumor growth, and metastasis in various cancers. This study was interested in determining the expression level of AGR2 in As^{3+} and Cd^{2+}-transformed MCF-10A cells. Real-time PCR and Western analysis indicated that the expression of AGR2 was significantly increased in the MCF-10A cells transformed with As^{3+} when compared to the Cd^{2+}-transformed cells. Exposure of the parent MCF-10A cells to 4, 8, and 16 μM As^{3+} for 48 hours resulted in a significant increase in the expression of AGR2 whereas exposure to Cd^{2+} did not increase the expression of AGR2, suggesting that As^{3+} has the potential to induce AGR2 in MCF-10A cells. In order to further investigate the effects of AGR2 expression on breast epithelial cells, MCF-10A cells were transfected with the AGR2 gene. Overexpression of AGR2 in the MCF-10A cells increased the ability of the cells to migrate faster in the wound scratch assay when compared to the blank vector transfected cells. In addition, MTT and scratch assays revealed increased growth and migration in the As^{3+}-transformed cells

when compared to the parent MCF-10A cells and the Cd^{2+}-transformed MCF-10A cells further implicating AGR2 in enhancing cell growth and migration. Treatment of the MCF-10A cells with the histone deacetylase inhibitor MS-275 and the demethylating agent, 5-Aza-2'-deoxycytidine (5-AZC) increased the expression of AGR2 suggesting that epigenetic modifications may be involved in regulating the expression of AGR2 in MCF-10A cells. These data also suggest that the expression of AGR2 in the MCF-10A cells may be regulated independently of the estrogen receptor status of the cells. Seeking to gain a better understanding of the relationship between AGR2 expression and breast cancer grade and stage, immunohistochemical staining was performed on a range of breast cancer specimens. Results showed elevated AGR2 expression with increasing grade of breast carcinoma. In conclusion, this study demonstrated the usefulness of AGR2 expression as a biomarker for bladder and breast cancers, further characterized the effect of AGR2 on the growth and migration of MCF-10A cells, and began to evaluate possible mechanisms by which AGR2 expression may be induced.

CHAPTER 1

INTRODUCTION

1.1 Bladder Cancer

Bladder cancer is the fourth most common type of cancer among men (Jacobs, B.L., Lee, C.T., Montie 2010). Bladder cancer has previously been linked to cigarette smoking as well as various chemicals and occupational exposures. Bladder cancer is also of concern for women among whom it was estimated that 17,770 new cases would be diagnosed in 2010 (Jemal et al. 2009). The variances between risk for men and women are partially due to the fact that men were more likely to work in industrial jobs. One study reported that the R198 cell line, a model of transitional cell carcinoma, produced fewer tumors when transplanted into female or estrogen-treated male nude mice. This suggests the possibility that androgens have a role in the formation of bladder cancers which, in turn, may partially explain an increased prevalence of bladder cancers in men over women (Reid et al. 1984).

Among the candidates for roles in bladder cancer is arsenic, which may be involved in bladder carcinogenesis. In addition, most diagnosed bladder cancers are of a papillary type, exhibiting low grade and stage. The concern is that most diagnosed bladder cancers also have a high likelihood of recurrence (Johansson and Cohen 1997). Bladder cancer risk has been associated with chemical and occupational carcinogen exposure, cigarette smoking, certain chemotherapeutic drugs, urinary tract infections, and

Schistosomiasis infections. Upon diagnosis, bladder cancer is classified as one of two main subtypes: superficial (non-muscle invasive) or muscle invasive (Droller 1998).

1.1.1 Diagnosis of Bladder Cancer

There are still several challenges to diagnosing and treating bladder cancer, among the most impactful are the need for better early detection methods. While most newly-diagnosed cases are superficial, they also have a high rate of recurrence within five years of initial diagnosis. This becomes more concerning as approximately 30% of recurrent bladder cancers are likely to become muscle-invasive (Lamm 1998). Together this stresses the challenge that bladder cancer is a high economic burden because of expenses due to treatment, complications, and long-term screening for recurrence (Bischoff and Clark 2009). Early detection is also a challenge because there are few known early disease symptoms for bladder cancer. The few early symptoms that a subset of patients experience include hematuria, frequent urination, and dysuria; all of these may be indicators of other pathologies besides cancers (Droller 1998). Diagnosing bladder cancer also relies upon cystoscopy, which is known to be unreliable in detecting flat carcinoma *in situ* (CIS) lesions (Droller 1998). This is of great significance as it is the CIS subtype that is most likely to progress to muscle-invasive disease.

1.1.2 Current Bladder Cancer Treatments

The treatment for most bladder cancers typically involves of transurethral resection of the bladder tumor (TURBT) followed by intravesical therapy with *Bacillus Calmette-Guerin* (BCG) (Jacobs, B.L., Lee, C.T., Montie 2010). For invasive bladder cancers, radical cystectomy is recommended though around 50% of patients will exhibit metastasis following this treatment (Bischoff and Clark 2009). More effective treatments

are desired as up to 40% of BCG treated cancers exhibit recurrence with a second BCG treatment providing a 35% chance of lasting success (Jacobs, B.L., Lee, C.T., Montie 2010). Clearly, there is a need for more effective bladder cancer screening in hopes of diagnosing bladder cancers at earlier, more treatable stages. This has the potential to significantly reduce bladder cancer mortality in the future.

1.2 Breast Cancer

Breast cancer is the second leading cause of cancer-related deaths among women and constitutes 1 in 3 cancers diagnosed among United States women (Desantis et al. 2011). Due to the high prevalence of breast cancer, there is a need to develop better prognostic as well as diagnostic markers of breast cancer that will aid in the treatment and diagnosis of the disease. Risk factors for breast cancer include those that can be modified as well as those that cannot be changed. Diet, lifestyle factors (i.e. exercise), and estrogen exposure are factors that may be controlled or changed in response to risk concerns. Among the risk factors that cannot be altered are age, race, genetic susceptibility, sex, familial cancer diagnoses, and history of other benign breast lesions. These risk factors also include the timing of the various stages of sexual development including the age at which a women undergoes menarche, has a first successful pregnancy (including the duration of breast-feeding), and the age at which a woman undergoes menopause (Kamińska et al. 2015).

1.2.1 Diagnosis of Breast Cancer

Successful treatment of breast cancer depends on several factors, perhaps the most important of which is early diagnosis. One contributing factor to early detection involves routine breast cancer screening which typically consists of mammography as well as

clinical and self-breast examination. While such screening has been effective in identifying cases of breast cancer one major concern remains that generally by the time that a patient has a palpable tumor, as identified by breast examinations, most cancers have already progressed to a more advanced stage. Once screening identifies a patient of concern for breast cancer more diagnostic testing is done. This can involve utilizing additional imaging techniques (MRI or molecular breast imaging), sampling of breast tissue (biopsy), and testing for known tumor markers (Anderson et al. 2015; Nounou et al. 2015).

1.2.2 *Prognostic Markers for Breast Cancer*

Following initial diagnosis, it is imperative that each cancer is well-characterized for type and grade. Breast cancer is divided into either ductal or lobular subtypes, each of which may exhibit noninvasive or invasive phenotypes. Invasive ductal carcinoma constitutes 55% of breast cancers at the time of diagnosis (Makki 2015). Additionally, breast cancer is further subdivided using various molecular characteristics. The common molecularly classified subtypes include: luminal A, luminal B, HER2 positive, and basal-like. The most common of these subtypes is luminal A, which makes up about 50% of all invasive breast tumors. Generally luminal A cancers express estrogen receptor (ERα) and the progesterone receptor (PR) and do not express HER2. Making up around 20% of invasive breast cancers are those of the luminal B subtype which do express ERα and PR but which exhibit HER2 expression to various degrees. Cancers of this subtype tend to have a range of responses to endocrine based treatments. About 15% of invasive breast cancers are of the subtype characterized by the overexpression of HER2 and a lack of expression of ERα or PR. For breast cancers highly expressing HER2, there is a greater

probability of the cancer being higher in grade and having undergone metastasis to the lymph nodes. Finally, 15% of invasive breast cancers may be categorized as basal-like in exhibiting gene expression similar to basal epithelial cells. These have also become known as triple-negative breast cancers as they do not express ERα, PR, or HER2 while they do usually express the epidermal growth factor receptor (EGFR) and cytokeratins 5 and 6. Characterization of these molecular subtypes is essential as it indicates which subtypes are likely to have a poorer prognosis and which will be either resistant or responsive to the various available therapies. This in turn will aid in deciding on which course(s) of treatment will be most advantageous for each breast cancer patient (Makki 2015).

1.2.3 *Current Breast Cancer Treatments*

Following diagnosis and characterization of breast cancer cases, a course of treatment must be decided upon. Generally treatment options include surgery and/or a combination of local or systemic treatments including chemotherapeutics, radiation, or endocrine therapies (Nounou et al. 2015). The age of the patient may also play a role in deciding treatment course as younger patients generally have unique concerns from those of older patients. Among these concerns are decreased fertility, longer survivorship and need for screening, and the potential impact that treatment may have on the patient's ability to work and care for their families. Complicating these issues is the fact that, as younger women are not encouraged to undergo routine breast screening, it is more likely that younger patients with breast cancers are diagnosed with cancers advanced to higher stages (Partridge et al. 2012; Ademuyiwa et al. 2015). In metastatic breast cancers, generally a two-tiered treatment plan may be considered. Initial treatment may consist of

a combination of endocrine therapies whereas other strategies may be needed if these are unsuccessful. (Reinert and Barrios 2015).

1.3 Arsenic and Cadmium as Environmental Carcinogens

This laboratory is interested in the identification of biomarkers that indicate potential human exposure to environmental agents, particularly heavy metals. Arsenic, a metalloid, and cadmium (Cd^{2+}), a heavy metal, are known to be carcinogenic and previous studies have suggested a link between arsenic and Cd^{2+} exposure and breast cancer risk (Soh et al. 2011). In fact, arsenic and Cd^{2+} are two of the four metals known to be carcinogenic in humans, the other two metals being chromium and nickel (Ernst and Theriault 1984). Both arsenic and Cd^{2+} have been officially recognized as human carcinogens according to the International Agency for Research on Cancer (IARC) (Navarro Silvera and Rohan 2007).

1.3.1 Arsenic Metabolism

As an environmental carcinogen, arsenic is found naturally in the soil and water of certain geographic areas. It can also be found as airborne particles when associated with industrial areas (Arita and Costa 2009). Arsenic exposure also occurs through the diet when eating seafood, mushrooms, poultry, and rice grown in contaminated areas (Jomova et al. 2011). Humans are generally exposed to arsenic through contaminated drinking water or occupational exposure in some industries (Navarro Silvera and Rohan 2007). Generally arsenic is found in either organic or inorganic arsenic (iAs) forms and it is the inorganic form that has generally been shown to exhibit toxicity (Jomova et al. 2011). The body metabolizes iAs through oxidation-reduction reactions and methylation. Methylation becomes important as it can actually increase toxicity. Arsenic is also known

to bind to thiol groups or to glutathione which may also aid in detoxification when binding to a protein, effectively preventing further toxic reactions (Carter, Aposhian, and Gandolfi 2003; Luster and Simeonova 2004).

Most commonly, arsenic is ingested as a trivalent inorganic species. Arsenic can be secreted in urine but some species have been known to accumulate in the body for as long as several months before being cleared. Inorganic arsenic has two primary forms: arsenite (As^{3+}) or arsenate (As^{5+}). Glutathione (GSH) is responsible for the conversion of As^{5+} into As^{3+} after which methylation can occur to generate organic arsenic forms (Jomova et al. 2011). During metabolism both forms can be either di- or tri-methylated. Arsenite can be bound to three thiol groups by GSH or converted to monomethyl arsenic (MMA) or dimethyl arsenic (DMA) by arsenic methyltransferases (Figure 1).

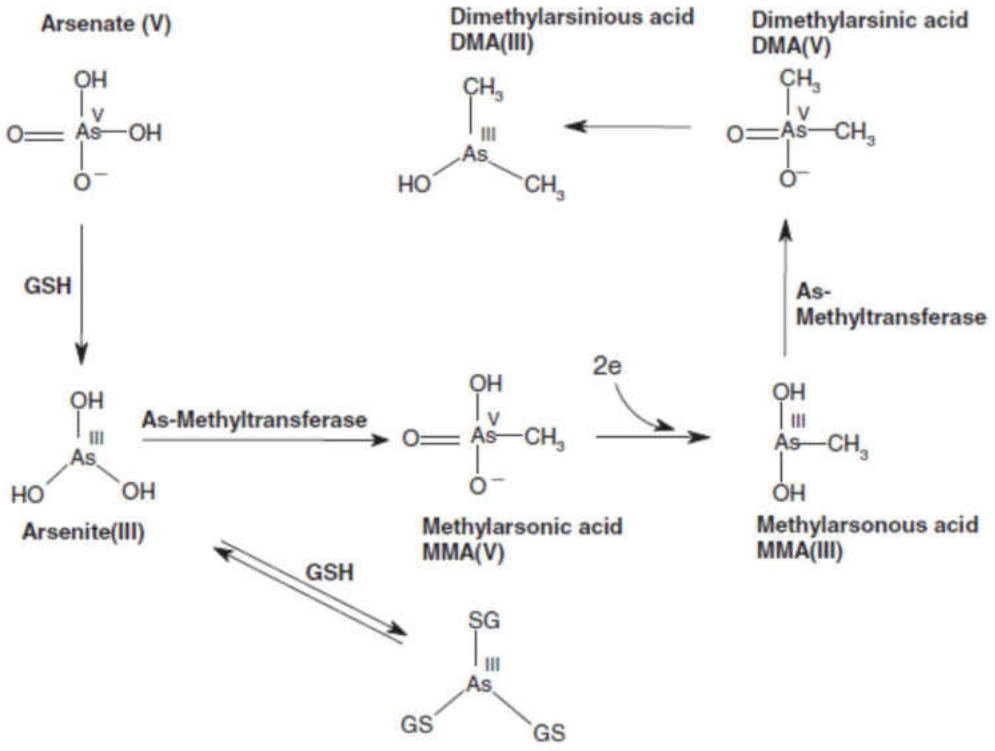

Figure 1 – The Metabolism of Inorganic Arsenic. Reproduced from Jomova et al. 2011 with permission from John Wiley and Sons.

1.3.2 Arsenic Toxicity and Carcinogenesis

With exposure to even low levels of arsenic, risk of several forms of cancer have been shown. These include cancers of the skin, bladder, liver, kidney, and lung (Arita and Costa 2009). Several sources have demonstrated that contaminated drinking water can lead to cancer, including specifically bladder cancer (Smith et al. 1992; Steinmaus et al. 2000). Arsenic is capable of causing carcinogenic changes through several mechanisms, a couple of which are known to include changes in cell differentiation and growth. In addition, iAs exposure has been demonstrated to induce chromosomal abnormalities (Navarro Silvera and Rohan 2007). Other potential mechanisms include interference with DNA repair, alteration of DNA methylation patterns, direct cytotoxicity, the induction of oxidative stress, and influence on signaling pathways (Pershagen 1981; Kitchin and Wallace 2008; Arita and Costa 2009).

1.3.3 Arsenic and Bladder Cancer

In bladder cells, arsenic is able to increase cell proliferation through the stimulation of the mitogen-activated protein kinase (MAPK) and extracellular-signal related kinase (ERK) signaling pathways (Luster and Simeonova 2004). This may contribute to the uncontrolled growth which is definitive of cancer. Furthermore, arsenic exposure has been well-established as a link to bladder cancer occurrence through several epidemiological studies. Looking at several of these studies, there is still some debate as to the levels of iAs exposure that increase the probability of bladder cancer and even whether low doses are linked to bladder cancer at all. Taken together however, it appears that iAs exposures as low as100-150 μg/L may represent a baseline level for which a link

to bladder cancer incidence occurs, especially when combined with smoking (Letašiová et al. 2012; Cohen et al. 2013; Saint-Jacques et al. 2014).

1.3.4 Arsenic and Breast Cancer

The relationship between arsenic and breast cancer has yet to be fully elucidated but from what is known, it is a complex interaction. One study has demonstrated that *in utero* exposure to arsenic impacts mammary tissue development and increases the risk of developing breast cancer later in life (Parodi et al. 2015). On the other hand, arsenic trioxide has been used in some attempts to treat breast cancer, particularly as a means to re-establish sensitivity to endocrine therapy (Zhang et al. 2011) or paclitaxel (Bakhshaiesh et al. 2015) and to work with mammalian target of rapamycin (mTOR) inhibitors to increase anti-tumor activity (Guilbert et al. 2013). Arsenic has been shown to stimulate the epithelial to mesenchymal transition (EMT) in breast cells, with the possible generation of a cancer stem cell population within transformed cells (Xu, Erik J. Tokar, and Waalkes 2014).

Further complicating the relationship between arsenic and breast cancer is the fact that arsenic is known to act as a metalloestrogen to disrupt normal endocrine signaling, with serious repercussions for breast cancers. It appears that arsenic can have both ERα-dependent and –independent mechanisms of action, either of which may induce or impact breast cancers (Davey et al. 2007; Xu, Erik J. Tokar, and Waalkes 2014). One study in MCF-10A cells has demonstrated that arsenic exposure can transform ERα-negative breast epithelium into a cell line exhibiting the common features of triple-negative breast cancers, which usually exhibit poor prognosis and are resistant to chemotherapeutic treatment (Xu, Erik J. Tokar, and Waalkes 2014).

1.3.5 Cadmium Metabolism

Exposure to Cd^{2+} generally results from cigarette smoking, occupational exposure (including metal industries), or through the diet (Navarro Silvera and Rohan 2007; Arita and Costa 2009). Of particular concern in the case of Cd^{2+} exposure is that the human body is not equipped to metabolize Cd^{2+}, therefore it accumulates in the body and it is not easily secreted (Arita and Costa 2009; Martinez-Zamudio and Ha 2011). Cadmium can be retained in the body for longer than 20 years before it is secreted. Generally detoxification occurs via binding to proteins that contain thiol groups (such as GSH), which leads to the production of oxidative stress and can eventually alter gene expression patterns, arresting the cell cycle, inducing differentiation and immortalization, or triggering apoptosis (Martelli et al. 2006). One of the more well understood proteins known to aid in the detoxification of Cd^{2+} are those in the metallothionein superfamily. Metallothioneins contain multiple cysteine amino acids which give them a very high affinity for certain metals, including Cd^{2+}. While binding to metallothionein, Cd^{2+} is prevented from undergoing further reactions, resulting in detoxification (Klaassen, Liu, and Choudhuri 1999; Klaassen, Liu, and Diwan 2009).

1.3.6 Cadmium Toxicity and Carcinogenesis

Cadmium is believed to stimulate carcinogenesis through various genotoxic means: apoptosis inhibition, single-stranded DNA breaks, DNA repair inhibition, mismatch repair inactivation, stimulation of oxidative stress, interference with cell-cell connections, and proto-oncogene activation (Navarro Silvera and Rohan 2007; Arita and Costa 2009; Feki-Tounsi and Hamza-Chaffai 2014). Of obvious interest when considering carcinogenic mechanisms is that Cd^{2+} can inactivate the tumor suppressor

protein p53, through a mechanism that appears to involve interference with the zinc-binding sites which usually activate p53 (Hartwig 2013). Another study noted differences in the p53 response to Cd^{2+} depending on the concentration; lower doses of Cd^{2+} appeared to activate p53 (possibly leading to apoptosis) through the generation of reactive oxygen species (ROS) and stabilization of p53 structure. On the other hand, higher doses of Cd^{2+} appeared to inhibit p53 activity by inducing conformational changes which interfere with the ability of p53 bind to zinc preventing p53 activation (Méplan, Mann, and Chem 1999). Cadmium exposure has also been linked to other diseases including kidney and cardiovascular disease as well as effects on lung and mammary tissue (Satarug et al. 2010).

1.3.7 Cadmium and Bladder Cancer

Epidemiological studies have indicated that there is a link between Cd^{2+} exposure and bladder cancer risk (Feki-Tounsi and Hamza-Chaffai 2014). In Belgium, one study demonstrated a connection between higher blood Cd^{2+} levels and increased risk of bladder cancer. The odds ratio (OR) for Cd^{2+} exposure was 8.3 with a 95% confidence interval (CI) once adjusted for age, gender, and occupational exposures to either aromatic amines or polycyclic aromatic hydrocarbons. When also controlled for smoking, the OR for Cd^{2+} remained significant at 5.7 (Kellen et al. 2007). One study evaluated the interactions between arsenic and Cd^{2+} in relation to bladder cancers using exposed Tunisian men. The results suggested that there was an increased blood Cd^{2+} concentrations in bladder cancer patients, especially smokers where blood Cd^{2+} levels were nearly doubled compared to non-smokers once controlled for other confounding factors. Overall, data showed that the OR for blood Cd^{2+} levels was 4.10 (95% CI)

compared to participants also exhibiting increased blood As^{3+} levels which exhibited a 2.10 OR (Feki-Tounsi et al. 2013). At least one other study compared urine Cd^{2+} levels between controls and patients with transitional cell carcinoma of the bladder. Results indicated a correlation between increased Cd^{2+} concentrations and the presence of transitional cell carcinoma. This study determined the effect of Cd^{2+} to have an OR of 7.11 for urinary Cd^{2+} when controlled for total protein (95% CI). It is also interesting to note that nearly all of the Cd^{2+} found in the urine samples of this study were bound to metallothionein (Wolf, Strenziok, and Kyriakopoulos 2009).

1.3.8 Cadmium and Breast Cancer

High urinary Cd^{2+} levels have been linked to an increased risk for breast cancers, in part due to the ability of Cd^{2+} to function as a metalloestrogen. A meta-analysis of case-control and cross sectional studies found a combined OR of 2.24 for Cd^{2+} levels in breast cancer cases comparing participants with the highest Cd^{2+} levels to those with the lowest (Larsson, Orsini, and Wolk 2015). As a metalloestrogen, Cd^{2+} is known to bind to and activate ERα, resulting in the activation of several signal transduction pathways which could contribute to the unregulated growth of mammary cells (Byrne et al. 2013). This ERα activation would potentially have further repercussions in breast cancers, affecting the ability of the tumor to respond to some treatments, especially those that are endocrine or hormone based.

1.4 Anterior Gradient 2

1.4.1 AGR2 Function

Originally identified in *Xenopus laevis*, anterior gradient 2 was found to be responsible for differentiation of the cement gland and shown to play a role in ectodermal

patterning (Aberger et al. 1998). The human analog of the anterior gradient 2 (AGR2) gene is of great interest due to the roles it performs in the endoplasmic reticulum stress response and as a proto-oncogene in various human cancers. One primary known function of AGR2 is that it is a member of the protein disulfide isomerase (PDI) family of chaperone proteins (Persson et al. 2005; Park et al. 2009; Higa et al. 2011; Shishkin et al. 2013).

Primarily, AGR2 is known to function within the endoplasmic reticulum, though there is evidence to suggest that it is secreted in gastrointestinal mucus (Park et al. 2009; Bergström et al. 2014). Anterior gradient 2 is normally expressed in mucus-secreting cells such as that of the lung, trachea, stomach, colon, prostate, and small intestine where it is known to play a role in mucin production and secretion (Missiaglia et al. 2004). Additional functions of AGR2 are still somewhat unclear, beyond its role as a PDI as part of the cellular response regulating endoplasmic reticulum stress (Higa et al. 2011). One role for AGR2 that is of great interest for this project is that of a proto-oncogene in various cancers.

One very recent study has begun to clarify roles for extracellular or plasma membrane localized AGR2. This study found that growth, migration, and cell cycle progression were all increased in the MCF-7 cell line in response to the presence of extracellular AGR2. They were also able to demonstrate that ERα can signal for AGR2 to relocalize from the endoplasmic reticulum to the plasma membrane. The same study showed that AGR2 interacts extracellularly with ERα and the insulin-like growth factor 1 (IGF-1) receptor and that these interactions influence cell growth, migratory ability, progression through the cell cycle, and EMT (Li et al. 2016). Another recent study

revealed that extracellular AGR2 can influence extracellular matrix function, leading to changes in the tumor microenvironment. Here AGR2 was also shown to disrupt contacts between cells by inducing the loss of E-cadherin (Fessart et al. 2016).

1.4.2 AGR2 as a Protein Disulfide Isomerase

Human AGR2 was identified as a member of the PDI family in 2005. As a member of this family, the AGR2 gene is known to have some of the common characteristics of PDIs, including a CXXC, or thioredoxin, motif which plays a role in oxidation and reduction reactions, enabling AGR2 to interact with misfolded proteins by forming disulfide bridges. Protein disulfide isomerases are able to oxidize, reduce, or isomerize these disulfide bonds to correct improperly folded domains in client proteins (Persson et al. 2005). Another common property of PDIs is a localization to the endoplasmic reticulum. In AGR2 endoplasmic reticulum localization is accomplished by the presence of a KTEL retention sequence, which is similar to the more well-understood and frequently seen KDEL sequence (Fourtouna et al. 2009; Park et al. 2009).

1.4.3 AGR2 Protein Interactions and Effects

While performing it's normal function as a PDI, AGR2 is known to interact with mucin 2 (MUC2), preparing it for secretion and maintaining endoplasmic reticulum homeostasis (Park et al. 2009; Bergström et al. 2014). Anterior gradient 2 is also known to bind and act as a molecular chaperone for reptin (Maslon et al. 2010; Chevet et al. 2013). Reptin functions as a tumor repressor and is known to impact the progression of cancer cells to metastasis (Kim et al. 2006). While most of the exact mechanisms have yet to be studied, AGR2 has been demonstrated to impact the expression of several proteins of particular interest due to their known roles implicated in tumorigenesis or

cancer progression. Most of these cancer-associated roles seem to correspond to extracellular or plasma membrane-associated AGR2. Perhaps the most obvious link to cancer is the ability of AGR2 to silence p53 expression, interfering with the cells ability to respond to DNA damage and initiate repair pathways (Pohler et al. 2004). One study has suggested that Cyclin D1 may be activated downstream of AGR2 resulting in increased cell growth and progression through the cell cycle (Vanderlaag et al. 2010).

Extracellular AGR2 has been shown to bind C4.4A and dystroglycan, suggesting a possible role for AGR2 in metastasis (Fletcher et al. 2003). One study demonstrated that AGR2 can activate YAP1 via dephosphorylation resulting in the activation of the hippo pathway and the induction of AREG expression. In turn, AREG has been shown to have a role in tumorigenesis and the regulation of cell growth (Dong et al. 2011). In pancreatic cancer, AGR2 has been shown to be an indicator of poor prognosis and AGR2 upregulation can increase metastasis through the post-transcriptional regulation of Cathepsin B and D expression (Ramachandran et al. 2008; Dumartin et al. 2011; Brychtova et al. 2014). It has also been reported that AGR2 has the ability to enable cancer cells to escape normal cell death mechanisms through signaling mechanisms which increase survivin expression (Vanderlaag et al. 2010). Additionally, AGR2 appears to interact with ERα, which has implications specifically in hormone-responsive cancers (Vanderlaag et al. 2010).

1.4.4 AGR2 Gene Regulation

The regulation of AGR2 is not completely understood but there are a few mechanisms known to regulate AGR2 expression. Most notably, the inositol requiring 1 (IRE1) and activating transcription factor 6 (ATF6) pathways of the unfolded protein

response are known to induce AGR2 expression (Higa et al. 2011). In response to extracellular stimuli, the ERK pathway has been shown to induce AGR2 expression (Zweitzig et al. 2007). There have also been a few studies which suggested the possibility that As^{3+} could induce AGR2 expression. These related studies have demonstrated that *in utero* exposure of mice to iAs resulted in offspring exhibiting increased ERα expression and increased expression of related genes, including AGR2 (Liu et al. 2007; Shen et al. 2007; Liu et al. 2008). In specific relation to cancers, AGR2 is known to be induced by ERα and has been shown to be repressed by erb-b2 receptor tyrosine kinase 3 (ErbB3) in prostate cancers (Vanderlaag et al. 2010; Zhang et al. 2010; Verma et al. 2012; Salmans, Zhao, and Andersen 2013). One more recent study was able to demonstrate that IGF-1 can induce AGR2 expression using an estrogen-response element (ERE) and an activator protein 1 (AP-1) site on the AGR2 promoter. This mechanism was shown to involve the ERK, protein kinase B (AKT), and ERα signaling pathways. The IGF-1-mediated induction of AGR2 occurred either with or without estrogen but was demonstrated to require ERα (Li et al. 2015).

1.4.5 AGR2 in Cancers

The anterior gradient homolog 2 protein is known to be expressed in a wide variety of cancers including carcinomas of the ovaries, colon, thyroid, pancreas, breast, prostate and lung (Liu et al. 2005; Zhang et al. 2005; Bu et al. 2011; Darb-Esfahani et al. 2012; Pizzi et al. 2012; Kani et al. 2013; Di Maro et al. 2014; Riener et al. 2014). The AGR2 protein is also known to be involved in various tumor associated pathways which include those involved in tumor growth, cellular transformation and metastasis (Liu et al. 2005; Wang, Hao, and Anson W Lowe 2008). Further implications for an impact of

AGR2 on the progression of cancer include the previously discussed interactions it has with Cathepsins B and D, C4.4a, dystroglycan, yes-associated protein 1 (YAP1), and amphiregulin (AREG) (Fletcher et al. 2003; Wang, Hao, and Anson W Lowe 2008; Dong et al. 2011; Dumartin et al. 2011).

Regulation of the epithelial to mesenchymal transition (EMT) is another possible role of AGR2 (Bu et al. 2011; Ma et al. 2015; Mizuuchi et al. 2015). This is of significant interest as cells with the ability to undergo EMT are characteristic of metastatic cancers. A connection between AGR2 and EMT seems to have been originally suggested in Bu et al. 2011, a study which determined that AGR2 is upregulated in prostate cancers. Concurrently it was observed that in AGR2 overexpression and knockdown studies, a significant effect occurred in the ability of the cells to proliferate and metastasize. These changes exhibited characteristics similar to what is seen in the actions of some transcription factors known to have roles in stimulating EMT during both development and in various cancers (Bu et al. 2011). Another study demonstrated that AGR2 expression can be regulated by known EMT inducers in a subset of prostate cancers (Mizuuchi et al. 2015). An AGR2-involving EMT pathway was also demonstrated to exist in glioblastoma cases (Xu et al. 2015).

1.4.6 AGR2 and Bladder Cancer

Studies have suggested that while the bladder normally expresses AGR2, it does not usually secrete AGR2 in the urine or express AGR2 on the cell surface. This suggests that AGR2 typically remains localized to the endoplasmic reticulum in normal bladder epithelium. On the other hand, bladder cancers have been shown to exhibit lower cellular AGR2 expression in general and bladder cancer patients tended to exhibit detectable

secreted AGR2 in urine specimens. This suggests that overall AGR2 expression may be relatively unchanged, rather it is the localization of AGR2 that is important for indicating the presence of bladder cancer. It appears that rather than being retained in the endoplasmic reticulum, AGR2 becomes secreted in the presence of bladder cancer. The presence of secreted AGR2 in the blood or urine is therefore a potential biomarker for bladder cancer among other cancers (Ho et al. 2016).

1.4.7 AGR2 in Breast Cancer

In breast cancer, AGR2 is known to be estrogen receptor responsive and is overexpressed in estrogen receptor positive (ERα-positive) breast cancers (Thompson and Weigel 1998; Fletcher et al. 2003; Pohler et al. 2004; Innes et al. 2006; Salmans, Zhao, and Andersen 2013). While AGR2 expression has been demonstrated to have significant prognostic meaning in ERα-positive breast cancers, less is known about the effect of AGR2 in ERα-negative breast cancers. It is of interest to note that, though not well understood, AGR2 has been shown to act through ERα-independent mechanisms (Zweitzig et al. 2007). It has been shown that AGR2 may play a role in the metastasis of breast cancer and is an indicator of poor prognosis (Fletcher et al. 2003; Fritzsche et al. 2006; Innes et al. 2006; Barraclough et al. 2009; Lacambra et al. 2015). Furthermore, AGR2 is known to increase cell proliferation and survival in breast cancers through interactions with cyclin D1, ERα, and survivin (Vanderlaag et al. 2010). Research has also linked AGR2 expression to Tamoxifen resistance in breast cancers (Hrstka et al. 2010; Hengel et al. 2011; Wright et al. 2014).

1.4.8 AGR2 and the Unfolded Protein Response

It is known that AGR2 plays a role in the cellular response to endoplasmic reticulum stress. The pathway responsible for initiating AGR2 in response to stress is the unfolded protein response. In the presence of cellular stress such as misfolded proteins, cells can initiate signaling through the activating transcription factor (ATF6), double stranded RNA-activated protein kinase (PRK)-like endoplasmic reticulum kinase (PERK), and inositol requiring 1 (IRE1) transmembrane proteins. The downstream signaling pathways of ATF6 and IRE1 are known to initiate AGR2 transcription and translation. AGR2, in turn binds misfolded client proteins via disulfide bonds (Higa et al. 2011).

1.5 Experimental Models

1.5.1 UROtsa

UROtsa is a model of transitional cell carcinoma arising from SV40 large T antigen-immortalized-human urothelial cells. The UROtsa cell line was initially cultured from the urothelial lining of a 12-year old female. This new cell line was therefore immortalized but did not display characteristics consistent with tumor cells as they did not grow colonies when cultured on soft agar plates or form tumors upon injection into nude mice (Petzoldt et al. 1995). This lab has further evaluated the UROtsa cell line and determined that it is a good model for human urothelium and useful for the evaluation of the stress response and responses to environmental toxicants, including As^{3+} or Cd^{2+}. In this study UROtsa cells were cultured in serum-free media and were demonstrated to form cell layers with features consistent with *in situ* urothelium, particularly those of the intermediate layers of transitional epithelium (Rossi et al. 2001). Additionally, the

UROtsa cell line was transformed by exposure to 1 μM sodium arsenite ($NaAsO_2$) or 1 μM cadmium chloride ($CdCl_2$) so that six As^{3+} and seven Cd^{2+}-transformed cell lines were created. These cell lines were also injected into nude mice and allowed to form tumors. Together, the cell lines and tumors have formed a model for arsenic and Cd^{2+}-induced bladder cancers, which allows for the study of and comparison between the *in vitro* cultured transformed cell lines and their corresponding heterotransplant tumors, a more *in vivo* approach (Sens et al. 2004). Upon microarray analysis comparing the transformed cell lines to the non-transformed UROtsa, several differentially expressed genes were identified and may be investigated as potential biomarkers for As^{3+} and Cd^{2+}-induced bladder cancers. (Garrett et al. 2014).

1.5.2 MCF-10A

The MCF-10A cell line is a human breast epithelial cell line, obtained from a 36-year old Caucasian female with fibrocystic disease. MCF-10A is known to have undergone spontaneous immortalization and is not tumorigenic when injected into nude mice. Previously, the MCF-10A cell line was obtained by this laboratory and transformed by exposure to 1 μM $NaAsO_2$ or 1 μM $CdCl_2$. These As^{3+} and Cd^{2+}-transformed cell lines were evaluated for an ability to grow in soft agar, indicating anchorage independent growth. Further characterization has demonstrated that the MCF-10A parent cell line and corresponding As^{3+} and Cd^{2+}-transformed cell lines are a good model of metal-induced breast cancers (Soh et al. 2011).

1.6 Intent and Goals of Study

This study was intended to answer several questions aimed at improving understanding regarding the role(s) of AGR2 in cancers. The two main objectives were to

demonstrate whether AGR2 has a role in bladder cancers and in breast cancers. This study also sought to gain a better understanding about the function of AGR2 in these cancers and to elucidate a possible mechanism by which AGR2 expression is regulated in cancers. These objectives stem from the hypothesis that the proto-oncogene AGR2 is a useful biomarker for breast and bladder cancers resulting from exposures to As^{3+} and Cd^{2+}. Anterior gradient 2 is expressed in the normal bladder urothelium and it has been shown that the expression of AGR2 decreases within the cell while AGR2 secretion increases as the grade and stage of urothelial cancers increases (Ho et al. 2016). Immunohistochemical analysis was utilized to determine the expression of AGR2 in human bladder cancer specimens and to evaluate whether the expression of AGR2 could be used as a prognostic or diagnostic marker for bladder cancer. This laboratory has developed an *in-vitro* model of bladder cancer by transforming the normal urothelial cell line UROtsa with As^{3+} and Cd^{2+}. A microarray analysis of the transformed cells showed that transformation of the UROtsa cells with As^{3+} increased the expression of the proto-oncogene AGR2 and this study attempted to validate the microarray results using real-time PCR analysis and western blotting. The increased AGR2 expression seen in transformed UROtsa cell lines could be attributable to the differences between *in vitro* cell culture models and *in vivo* tissue or animal models. The expression of AGR2 in tumor heterotransplants derived from the As^{3+} and Cd^{2+}-transformed UROtsa cell lines was determined in order to evaluate whether the effect of As^{3+} or Cd^{2+} would remain or increase in an *in vivo* model. This led to the question of whether short term As^{3+} or Cd^{2+} exposure could induce AGR2 expression in UROtsa cells.

Previously this laboratory has also shown that chronic exposure of the normal breast epithelial cell line MCF-10A to As^{3+} or Cd^{2+} results in the transformation of these cells (Soh et al. 2011). This prompted investigation into whether AGR2 expression was differentially expressed in the MCF-10A model of metal induced breast cancers using real-time PCR analysis and western blotting. Similar to the previous evaluation of AGR2 in the bladder, it was next determined whether short term exposure to As^{3+} or Cd^{2+} could induce the expression of AGR2 in the parent MCF-10A cells. Previous studies have suggested that overexpression of AGR2 can increase the growth and migratory potential of breast cancer cells, therefore this study sought to determine whether the overexpression of AGR2 in the MCF-10A cells would increase the growth and migratory potential of these cells. For this purpose, the parent MCF-10A cells were transfected with the AGR2 gene and the growth rate and migratory potential of the parent, As^{3+}-and Cd^{2+}-transformed MCF-10 cells and the AGR2 transfected cells were determined using the MTT and the wound scratch assays.

Other studies have shown that expression of AGR2 is associated with the estrogen receptor alpha (ERα) status of the breast tumors, therefore was asked whether ERα expression is present in the MCF-10A model using real-time PCR analysis. Since methylation and histone modification are two of the mechanisms that are involved in the regulation of gene expression, this study determined whether either of these mechanisms could be responsible for the regulation of AGR2 in MCF-10A cells. To address this question, MCF-10A cells were treated with the demethylating agent 5'-azacytidine (5-AZC) or the histone deacetylase (HDAC) inhibitor, Entinostat (MS-275) after which real-time PCR analysis was used to determine AGR2 expression. It is known that cancer cells

can secrete AGR2 and therefore this study attempted to determine whether AGR2 is secreted by MCF-10A cells. Immunohistochemical localization of AGR2 in a variety of different breast cancers was also determined to evaluate whether the expression of AGR2 correlated to particular grades or subtypes of breast cancers.

CHAPTER 2

METHODS

2.1 Cell Culture

UROtsa cells were obtained from from the American Type Culture Collection (ATCC) (Rockville, MD) and were grown in Dulbecco's Modified Eagles Medium (DMEM) (Sigma-Aldrich, St. Louis, MO; D5523) supplemented with 5% (v/v) FBS (Gibco/Invitrogen, Grand Island, NY; 16000-044). Cells were supplied with fresh media every 3 days or upon confluency. Subculture was also completed upon confluency using 0.25% Trypsin-EDTA (Gibco/Life Technologies, Carlsbad, CA; 25200-072) and reseeding at a split ratio of 1:4. J82 (HTB-1), RT4 (HTB-2), and HT-1376 (CRL1472) cell lines were obtained from ATCC and cultured in DMEM (Sigma-Aldrich, St. Louis, MO; D5523) with 10% (v/v) FBS (Gibco/Invitrogen, Grand Island, NY; 16000-044), 5 mg/ml glucose (Fisher Scientific, Pittsburgh, PA; D16-500), and 1x nonessential amino acids (Gibco/Invitrogen, Grand Island, NY; 11140). Cells were given fresh media every 2-3 days or upon confluency and were subcultured at a split ratio of 1:3 upon confluency using 0.25% Trypsin-EDTA (Gibco/Life Technologies, Carlsbad, CA; 25200-072).

MCF-10A cells were obtained from ATCC and were grown in 1:1 DMEM (Sigma-Aldrich, St. Louis, MO; D5523): Ham's F12 Nutrient Mixture (Sigma-Aldrich, St. Louis, MO; N6760). Culture media was supplemented with 5% (v/v) fetal bovine serum (FBS) (Gibco/Invitrogen, Grand Island, NY; 16000-044), 20 ng/ml epidermal growth factor (EGF) (Gibco/Life Technologies, Carlsbad, CA;

PHG0311), 0.5 μg/ml hydrocortisone (Sigma-Aldrich, St. Louis, MO; HO135), 10 μg/ml insulin (Sigma-Aldrich, St. Louis, MO; I2643), and 0.1 μg/ml cholera toxin (Sigma-Aldrich, St. Louis, CA; C8052). Cells were supplied with fresh media every 3 days or upon confluency. Subculture was also completed upon confluency using 0.25% Trypsin-EDTA (Gibco/Life Technologies, Carlsbad, CA; 25200-072) and reseeding at a split ratio of 1:10. MDAMB-231, Hs578T, T47D, and MCF-7 cells were obtained from ATCC and cultured using G-5 media consisting of DMEM (Sigma-Aldrich, St. Louis, MO; D5523) with 5% (v/v) FBS (Gibco/Invitrogen, Grand Island, NY; 16000-044) and 5 mg/ml glucose (Fisher Scientific, Pittsburgh, PA; D16-500). Cells were supplied with fresh media every 2 days or upon confluency. Subculture was also competed upon confluency using 0.25% Trypsin-EDTA (Gibco/Life Technologies, Carlsbad, CA; 25200-072) and reseeding at a split ratio of 1:10.

2.2 Transformation of UROtsa Cells with As^{3+} and Cd^{2+}

In order to evaluate the impact of As^{3+} and Cd^{2+} exposure on bladder cancers, a model of metal-induced bladder cancers was made using the UROtsa bladder epithelial cell line. In order to create this model, UROtsa cells were transformed by feeding cells with media containing either 1 μM $NaAsO_2$ (Sigma-Aldrich, St. Louis, MO) or 1 μM $CaCl_2$ (Sigma-Aldrich, St. Louis, MO). This exposure was continued and cells were evaluated every 5 passages for the ability to form colonies in soft agar (Sens et al. 2004; Cao et al. 2010; Somji et al. 2010). Once transformed with either metal, microarray analysis was previously competed using the GeneChip human Genome U133 plus 2.0 arrays (Affymetrix, Santa Clara, CA) and was analyzed for global gene expression by

Genome Explorations (Menphis, TN) in order to evaluate differential gene expression patterns in response to either As^{3+} or Cd^{2+} (Talaat et al. 2011).

Previously, transformed UROtsa cell lines were used to generate heterotransplant tumors. Using the transformed cell lines, 1 $x10^6$ cells were injected either subcutaneously or intraperitoneally into nude mice. As formerly described, tumors were allowed to grow for 10 weeks following subcutaneous injection or 53 days following intraperitoneal injection, at which time mice were sacrificed and the tumors collected for analysis (Cao et al. 2010; Somji et al. 2010). The UROtsa cell lines were also used to derive spheroids as previously described (Slusser-Nore et al. 2016). Briefly, the transformed UROtsa cell lines were cultured in ultra-low attachment flasks and supplied with serum-free medium for 8 days. UROtsa spheroids were then harvested and processed for RNA and protein.

2.3 Exposure of UROtsa Cells to As^{3+} and Cd^{2+}

In order to determine whether AGR2 is induced by either As^{3+} or Cd^{2+}, time course exposures were done using UROtsa cells. To determine the effect of As^{3+}, UROtsa cells were exposed to 2, 4, or 6 μM $NaAsO_2$ (Sigma-Aldrich, St. Louis, MO) for 72 hours. For Cd^{2+}, UROtsa cells were exposed to 1, 2, or 4 μM $CdCl_2$ (Sigma-Aldrich, St. Louis, MO) for up to 72 hours. For both As^{3+} and Cd^{2+} exposures, cells were harvested at 12, 24, 48, and 72 hours and processed to obtain RNA and protein.

2.4 Transformation of MCF-10A Cells with As^{3+} and Cd^{2+}

In order to evaluate the impact of As^{3+} and Cd^{2+} on breast cancers, a model of metal-induced breast cancers was made using the MCF-10A breast epithelial cell line. In order to create this model, MCF-10A cells were transformed by feeding cells with media containing either 1 μM $NaAsO_2$ (Sigma-Aldrich, St. Louis, MO) or 1 μM $CaCl_2$ (Sigma-

Aldrich, St. Louis, MO). This exposure was continued and cells were evaluated every 5 passages for the ability to form colonies in soft agar (Soh et al. 2011). Once transformed with either metal, microarray analysis was competed using GeneChip human Genome U133 plus 2.0 arrays (Affymetrix, Santa Clara, CA) and was analyzed for global gene expression by Genome Explorations (Memphis, TN) in order to evaluate differential gene expression patterns in response to either As^{3+} or Cd^{2+}.

2.5 Exposure of MCF-10A Cells to As^{3+} and Cd^{2+}

In order to determine whether AGR2 is induced by either As^{3+} or Cd^{2+}, time course exposures were done using MCF-10A cells. To determine the effect of As^{3+}, MCF-10A cells were exposed to 1, 8, or 16 μM $NaAsO_2$ (Sigma-Aldrich, St. Louis, MO). For Cd^{2+}, MCF-10A cells were exposed to 2, 4, or 8 μM $CdCl_2$ (Sigma-Aldrich, St. Louis, MO) for up to 48 hours. For both As^{3+} and Cd^{2+} exposures, cells were harvested at 12, 24, 36, and 48 hours and processed to obtain RNA and protein.

2.6 AGR2 Transfection of MCF-10A Cells

A construct containing AGR2 was made using the 6.2 V5-DEST vector and obtained from Invitrogen (Carlsbad, CA). Amplification of the construct was accomplished by transforming the plasmid into E. coli cells (OneShot-OmniMax 2-T1R; Invitrogen/Life Technologies, Carlsbad, CA; C8540-03). Successfully transformed colonies were selected using LB (Fisher, Pittsburgh, PA; BP1427-500) agar (Fisher, Pittsburgh, PA; BP1423-500) plates with 100 μg/ml ampicillin. Transformed bacterial colonies were inoculated into liquid LB and bacterial stocks were amplified and pelleted. Plasmid preparation was done using the Endo-Free Maxi Prep Kit (Qiagen, Germantown, MD; 12362). Prior to transfection, the AGR2 construct was linearized using BspHI (New

England BioLabs, Ipswich, MA; R0517S) and purified using the GeneClean Kit (MPBio, Santa Ana, CA; 111102-400). Stable transfection of 2 μg blank vector or 2 μg AGR2 vector was accomplished via electroporation using the Amaxa Cell Line Nucleofector Kit L (Lonza, Allendale, NJ; VCA-1005). Colonies were selected using 20 μg/μl blasticidin S HCl (BSD) (Gibco/Life Technologies, Carlsbad, CA; A11139-03).

2.7 Cell Viability and Doubling Times

In order to determine the effects of AGR2 expression on MCF-10A cell growth, 3-(4,5-dimethylthiazol-2-yl)-2,5-diphenyltetrazolium bromide (MTT) reduction and wound healing assays were used. The MCF-10A model was used for these assays, including As^{3+} and Cd^{2+}-transformed cell lines as well as MCF-10A cells transfected with either blank 6.2 V5-DEST vector or a 6.2 V5 vector containing the coding regions of the AGR2 gene. For proliferation, MTT assays were performed. Cells were seeded in 6-well plates and allowed to grow for up to 6 days. Plates of cells were taken daily and exposed to 100 mg/ml MTT (Sigma-Aldrich, St. Louis, MO; M5655) for 3.5 hours. Cells were then rinsed twice with phosphate buffered saline and then with 1 ml acidic propanol. Optical density was evaluated at 570 nm and data were used to calculate doubling times for each cell line.

2.8 Wound/Scratch Assays

Cells were grown to confluency in 6-well plates and a scratch was made created using a 100 μl pipette tip. The wells were washed twice with phosphate buffered saline and fresh media was added to the cells. Images were taken right after the addition of media (0 hours) and after 4, 8, and 12 hours in order to evaluate the levels of cell migration into the wound. Percent wound closures were determined.

2.9 RNA Isolation and Real-time RT-PCR

Cells were harvested using a cell scraper and pelleted via centrifugation. Total RNA isolation was performed using TRI REAGENT (Molecular Research Center, Inc. Cincinnati, OH; TR 118) according to supplied protocol and as previously outlined by this laboratory (Somji et al., 2006). RNA was converted to cDNA using the iScript cDNA Synthesis Kit (Bio-Rad Laboratories, Hercules, CA; 170-8890). Real-time PCRs were run using iTaq Universal SYBR Green Superrmix (Bio-Rad Laboratories, Hercules, CA; 172-5124) or IQ SYBR Green Supermix (Bio-Rad Laboratories, Hercules, CA; 1708882). For Anterior Gradient 2 (AGR2) and Estrogen Receptor 1 (ESR1 or ERα), QuantiTect Primer Assays (Qiagen) were obtained for the determination of mRNA expression. These primer assays were Hs_AGR2_1_SG and Hs_ESR1_1_SG respectively. Identical cycling parameters were used for AGR2 and ESR1 primers. Cycling was done with denaturation at 95℃ for 15 sec, annealing at 62℃ for 45 sec, and extension at 72℃ for 30 sec. To aid in validation of construct expression, primers were designed for the V5 tag of the 6.2 V5 DEST vector and obtained from Invitrogen (Grand Island, NY). Primer sequences for the V5 tag were sense, TTCGAAGGTAAGCCTATCCCT, and antisense, AGTCATTACTAACCGGTACGC. Cycling parameters for V5 primers were denaturation at 95℃ for 15 sec, annealing at 55℃ for 45 sec, and extension at 72℃ for 30 sec.

2.10 Protein Extraction and Quantitation

Whole cell lysates were prepared using 1x SDS (Life Technologies, Carlsbad, CA; 15525-017) Lysis Buffer and briefly sonicated to obtain cellular protein samples.

Quantification of protein levels in each sample was done using the BCA assay kit obtained from Thermo-Fisher Scientific (Waltham, MA; 23228 and 1859678).

2.11 Collection and Preparation of Spent Media

MCF-10A cells were cultured for 24 hours in serum free media in a T75 flask prior to confluency. Spent media was collected and the cell monolayer was harvested using a cell scraper. Spent media was prepared using Amicon® Ultra-15 centrifugal filters with Ultracell® 3 membranes (EMD Millipore, Billerica, MA;UFC900308). Media was centrifuged for 1 hour at 4℃ and 3700 relative centrifugal force (RCF) to concentrate media samples. Total protein concentrations were then determined using the BCA assay reagents (Thermo-Fisher Scientific, Waltham, MA; 23228 and 1859678).

2.12 Western Blot Analysis

Protein expression levels were determined using 10 or 20 µg of total cellular protein on 4-20% Mini-PROTEAN TGX Stain-Free Gels (Bio-Rad Laboratories, Hercules, CA; 456-8094). AGR2 protein levels were detected using a rabbit monoclonal antibody to AGR2 (Abcam, Cambridge, MA; ab76473) at a 1:5,000 dilution and secondarily anti-rabbit IgG, HRP-Linked antibody (Cell Signaling, Boston, MA; 7074S) at a 1:2,400 dilution. Beta Actin protein levels were detected using a mouse monoclonal antibody to Beta-Actin (Abcam, Cambridge, MA; ab8226) at a 1:1,000 dilution and secondarily anti-mouse IgG, HRP-Linked antibody (Cell Signaling, Boston, MA; 7076S) at a 1:2,400 dilution. Biotinylated markers were detected using anti-biotin-linked antibody (Cell Signaling, Boston, MA; 7075S) at a 1:1,200 dilution. Antibody visualization was accomplished using Clarity Western ECL Blotting Substrate (Bio-Rad Laboratories, Hercules, CA; 170-5061).

Table 1 – Western Antibody Sources

Antibody Target	Company	Catalog Number
AGR2	Abcam	ab76473
Biotin secondary	Cell Signaling	7075S
Mouse secondary	Cell Signaling	7076S
Rabbit secondary	Cell Signaling	7074S
β-Actin	Abcam	ab8226

2.13 Immunofluorescent Staining of MCF-10A Cell Lines

MCF-10A cells were cultured on 12 mm glass coverslips in 24-well plates until confluent. Cells were then rinsed twice with DMEM:F12 media containing no phenol red and fixed in 3.7% paraformaldehyde (Polysciences, Warrington, PA; 18814-10) for 20 min. 0.1 M NH_4Cl (Sigma, St. Louis, MO; A-5666) was used for 15 min to quench free aldehyde groups and cells were permeabilized for 30 min using 0.3% Triton-X100 (Fisher Scientific, Pittsburg, PA; BP151-100). Cells were incubated for 1 hour in AGR2 primary antibody (Abcam, Cambridge, MA; ab76473) at a 1:600 dilution. Alexa Fluor®488 goat anti-rabbit IgG secondary antibody (Life Technologies, Carlsbad, CA; A11008) was used for 1 hour at a 1:1,000 dilution. Stained coverslips were then mounted in ProLong® Diamond Antifade Mountant with DAPI (Life Technologies, Carlsbad, CA; P36971). Anterior gradient 2 immunofluorescence was visualized using a Leica DM5500 Q TCS SPE confocal microscope. Z-slice images were captured and processed using LAS-X software.

2.14 Immunohistochemical Analysis of Tumors and Tumor Specimens

UROtsa heterotransplant tumors were formalin-fixed and embedded in paraffin prior to immunohistochemical analysis. Formalin-fixed paraffin-embedded breast and bladder cancer specimens were also used for immunohistochemical analysis. Specimens from archival paraffin blocks were 10 years post diagnosis and scheduled for disposal as

medical waste. These archival specimens contained no patient identifiers and are in the exempt category for human research. Sections of transplanted tumors were cut into 3-5 μm thick slices for use in immunohistochemical protocols. The primary antibody used was AGR2 (Abcam, Cambridge, MA; ab76473) at a 1:500 dilution for 30 minutes. Immunohistochemical staining was performed on Leica Bond-Max Automated IHC Staining System (Leica, Bannockburn, IL). Paraffin sections were processed starting with deparaffinization and ending with counterstaining by hematoxylin according to the manufacturer's recommended program with modification. Bond Polymer Refine Detection (Leica, DS9800) was used as the main reagent in the automatic staining process. Briefly, the major steps include deparaffinization, antigen retrieval in Bond Epitope Retrieval Solution 1 (Leica, Catalog No AR9961) for 20 min, peroxide block for 5 min, incubation with primary antibodies for 30 min at room temperature, incubation with Post Primary for 10 min, incubation with polymer for 10 min, visualization with 3,3'-diaminobenzidine (DAB) for 10 min, and counterstaining with hematoxylin for 5 min. Slides were rinsed in distilled water, dehydrated in graded ethanol, cleared in xylene, and coverslipped. The presence and degree of immunoreactivity in the specimens was judged by two pathologists. The scale used was 0 to +3 with 0 indicating no staining, +1 staining of mild intensity, +2 staining of moderate intensity, and +3 staining of strong intensity. All immunohistochemical preparation, staining, and analysis were performed by Dr. Xudong Zhou.

2.15 Treatment of MCF-10A Cells with 5-Azacytidine and MS-275

MCF-10A cells were fed with media containing 1, 3, or 10 μM Entinostat (MS-275) (ALEXIS Biochemicals, Lausen, Switzerland) or 1, or 3 μM 5'-azacytidine (5-AZC)

(Sigma-Aldrich, St. Louis, MO) for 72 hours. Following exposure, cells were harvested to obtain cell pellets which were processed to obtain RNA and protein as described above.

2.16 Statistical Analysis

Statistical analysis was conducted using GraphPad Prism® 5.0 software. Real-time PCR and western I.O.D. analysis was analyzed in triplicate and evaluated using an unpaired T-test when comparing two samples. When comparing multiple samples either one-way analysis of variance (ANOVA) with a post-hoc Tukey multiple comparison test or two-way ANOVA with Bonferroni post-hoc tests were used for statistical analysis. Asterisks are used to denote statistically significant differences compared to the control sample as follows: * ($p < 0.05$), ** ($p < 0.01$) and *** ($p < 0.001$).

CHAPTER 3

RESULTS

3.1 Expression of AGR2 in Bladder Cancers

Analysis of AGR2 expression in urothelial cancers by Ho and coworkers (2016) showed strong staining of AGR2 in normal urothelium, but in urothelial cancer AGR2 expression was lost, with only 25% of primary tumors observed to retain expression in a cohort of lymph node positive cases. The present study examined the immunohistochemical localization and expression of AGR2 in a small sample set: five specimens of benign urothelium; four cases of low grade urothelial cancer; five cases of high grade, non-invasive urothelial cancer; and, five cases of high grade, muscle invasive urothelial cancer. Immunohistochemical staining, imaging, and analysis were done by Xudong Zhou. All five specimens of normal urothelium showed moderate cytoplasmic staining of AGR2 throughout the urothelium, with lesser staining in the umbrella cells (black arrow) forming the outer layer of the bladder epithelium (Figure 2 A). This is not surprising as bladder epithelia have been shown to express AGR2 (Ho et al. 2016). The underlying smooth muscle cells showed no staining for AGR2. As illustrated for one specimen with moderate/heavy staining for AGR2, all four cases of low grade urothelial cancer stained positive for AGR2. The staining of the four specimens varied between moderate and strong and over 80% of the urothelial cancer cells in all specimens were positive for the expression of AGR2 (Figure 2 B). The expression of AGR2 in non-muscle invasive urothelium was variable with four cases showing moderate staining in 70

to 80% of the urothelial cells (one specimen illustrated as Figure 2 C) and two cases with moderate staining but with only 5% of the urothelial cells staining positive for AGR2 (one specimen illustrated as Figure 2 D). The expression of AGR2 was also variable in high grade, muscle invasive urothelial cancer. Three specimens of high grade, muscle invasive bladder carcinoma were negative for the expression of AGR2 (two specimens illustrated in Figure 2 E and F with 2 F having an internal control with staining for benign urothelium). The other two specimens showed weak to moderate staining for AGR2 in 30% of the cells (Figure 2 G) and the other moderate to strong staining in over 80% of the cells (Figure 2 H). These data demonstrate variability in AGR2 expression among high-grade and invasive urinary carcinomas. A summary of AGR2 staining in bladder cancers specimens is provided in Table 2. In this table, the intensity of AGR2 staining in benign epithelium (if present) was scored. Also evaluated were the intensity of AGR2 staining in tumor cells and the overall percentage of tumor cells stained for AGR2 for each slide evaluated. Overall, these results indicate that AGR2 expression can be lost in the presence of bladder cancers.

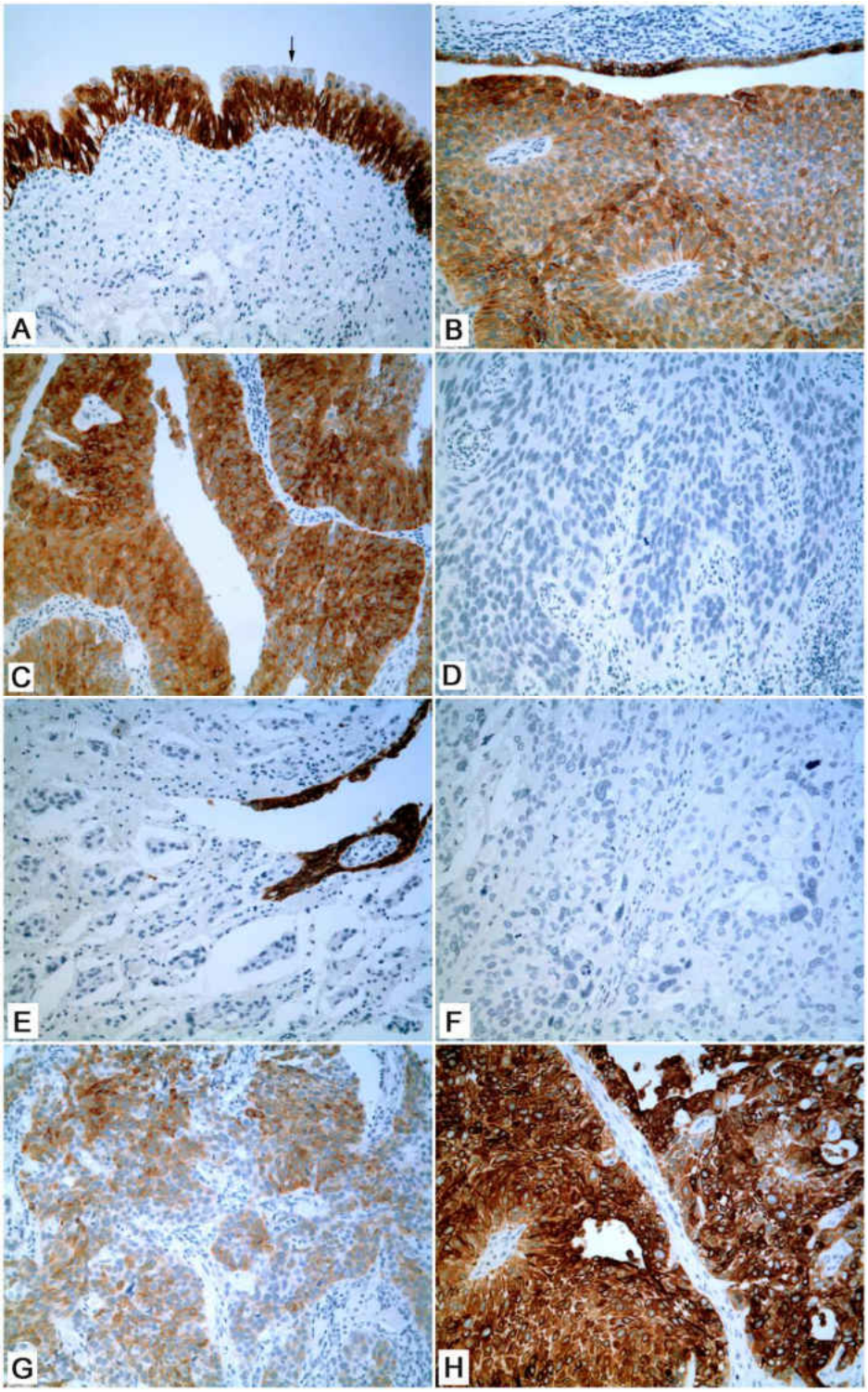

Figure 2 – AGR2 Staining in Urothelial Carcinomas. A: Normal bladder urothelium. **B:** Low grade non-invasive urothelial carcinoma of the ureter. **C:** High grade non-invasive urothelial carcinoma of the bladder. **D:** High grade non-invasive urothelial carcinoma with focal areas suspicious for invasion. **E-H:** High grade invasive urothelial carcinomas of the bladder.

Table 2 – Summary of AGR2 Staining in Specimens of Urothelial Carcinoma. Tumor type, AGR2 staining intensity, and percentage of cells positive for AGR2 staining for each tumor evaluated. LG – low grade, HG – high grade, LG ca. w/f HG – low grade carcinoma with focal high grade, NA – not applicable (no benign or tumor cells present), - denotes no staining observed

	AGR2		
Lesion	**Benign Epithelium**	**Intensity**	**Percentage**
Benign Urothelium	3+	NA	NA
Benign Urothelium	2+	NA	NA
LG carcinoma	3+	2-3+	80
LG carcinoma	NA	3+	80
LG ca. w/f HG	NA	2-3+	80
HG Noninvasive	NA	2-3+	5
HG Noninvasive	NA	2-3+	70
HG Noninvasive	NA	3+	80
HG Noninvasive	NA	3+	80
HG Invasive	3+	-	-
HG Invasive	NA	2-3+	30
HG Invasive	3+	-	-
HG Invasive	3+	-	-
HG Invasive	NA	-	-
HG Invasive	NA	3+	80
LG Benign Tissues	NA	3+	80

3.2 Expression of AGR2 in UROtsa Cells Transformed with As^{3+} or Cd^{2+}

As this laboratory is primarily interested in evaluating the effect that As^{3+} and Cd^{2+} have on various cancers, a model for As^{3+} and Cd^{2+}-induced urothelial cancers has previously been established using the UROtsa bladder epithelial cell line. Briefly, the UROtsa cell line was exposed to 1 μM $NaAsO_2$ or 1 μM $CdCl_2$, resulting in the formation of six As^{3+} and seven Cd^{2+}-transformed UROtsa cell lines. These UROtsa cell lines have been shown to be a good model for heavy metal induced urothelial carcinomas (Rossi et al. 2001). Gene expression changes in the transformed UROtsa cell lines were evaluated using microarray analysis and compared to that of the non-transformed UROtsa cell line. One of the genes determined to be upregulated in response to transformation with As^{3+}

was AGR2, which was induced 4.87 fold over parent (Garrett et al. 2014). Anterior gradient 2 expression in the bladder is of interest as it has been identified as a biomarker for advanced bladder cancers when secreted in the blood or urine (Ho et al. 2016). The next goal for this study was to evaluate AGR2 expression in the UROtsa model of heavy metal induced bladder cancers. Real-time PCR and western analysis were used to determine AGR2 expression in As^{3+} and Cd^{2+}-transformed UROtsa cell lines. The data showed that AGR2 is significantly upregulated in four of the As^{3+} and six of the Cd^{2+}-transformed UROtsa cell lines (Figure 3 A and D). Western analysis also confirmed an increase in AGR2 protein in the majority of the As^{3+} and Cd^{2+}-transformed cell lines (Figure 3 B-C and E-F). Complicating the analysis is that the western blotting for AGR2 exhibited evidence of post-translational modification, seen as two separate bands and/or as smeared bands. This requires using a generous area when integrating optical density for further analysis rather than a tight area around a single band, affecting the integrated optical density (I.O.D.) analysis of western blotting for AGR2 (Figure 3 B-C and E-F). This has been observed in other publications studying AGR2 and may indicate the O-glycosylation of secreted AGR2. At least one previous study demonstrated that the O-glycosylation of AGR2 may affect extracellular functions (Clarke, Rudland, and Barraclough 2015). This secondary or smeared band therefore makes it challenging to visualize the full impact of the changes to AGR2 protein expression which may account for some of the variability between mRNA and protein expression. Results indicate that AGR2 expression increases following transformation of UROtsa cells with As^{3+} or Cd^{2+}.

Transformed UROtsa cell lines were injected into nude mice and allowed to form heterotransplant tumors. These heterotransplant tumors were evaluated for AGR2

expression using real-time PCR. Only two of the As^{3+} heterotransplant tumors retained significantly increased AGR2 expression (Figure 4 A). Four of the Cd^{2+} heterotransplant tumors maintained significantly increased AGR2 expression (Figure 4 B). Immunohistochemical staining of As^{3+} and Cd^{2+} heterotransplant tumors was done to further evaluate AGR2 expression. Results showed that heterotransplant tumors arising from arsenic-transformed UROtsa cell lines #1, #3, and #6 exhibited AGR2 staining though all tumors had a small population of cells with moderate staining (Figure 5). In tumors derived from the Cd^{2+}-transformed UROtsa cell lines, AGR2 staining was strongest in cell lines #2, #5, and #6. Once again, all tumors exhibited a population with moderate AGR2 staining (Figure 6). A summary of the immunohistochemical staining is provided in Table 3. These results show that AGR2 expression is induced in urothelial cancers arising from As^{3+} and Cd^{2+}-transformed cells. In turn, this suggests that As^{3+} and Cd^{2+} are capable of inducing tumorigenesis in urothelial cells.

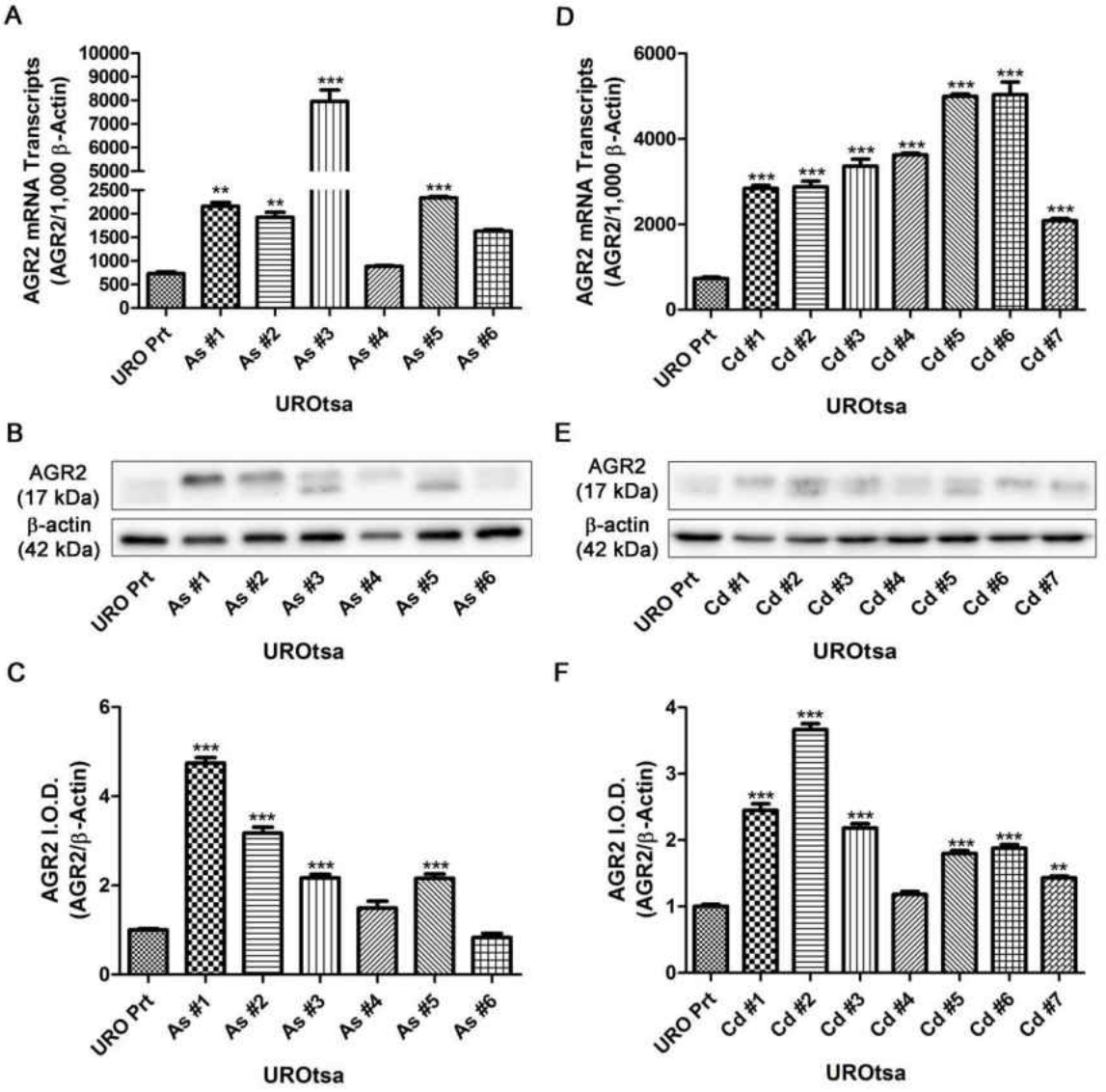

Figure 3 – AGR2 Expression in As^{3+} and Cd^{2+}-transformed UROtsa Cell Lines. A: Real-time PCR analysis of AGR2 expression in UROtsa cells transformed with As^{3+}. **B:** Western analysis of AGR2 in As^{3+}-transformed UROtsa cell lines. **C:** I.O.D. analysis of western data in **B**, plotted as AGR2/β-Actin. **D:** Real-time PCR analysis of AGR2 expression in UROtsa cells transformed Cd^{2+}. **E:** Western analysis of AGR2 in Cd^{2+}-transformed UROtsa cell lines. **F:** I.O.D. analysis of western data in **E**, plotted as AGR2/β-Actin. *** denotes ($p < 0.001$) and ** ($p < 0.01$) statistically significant difference from parent UROtsa cells. Real-time and western I.O.D. data is plotted as the mean ± SEM of triplicate determinations.

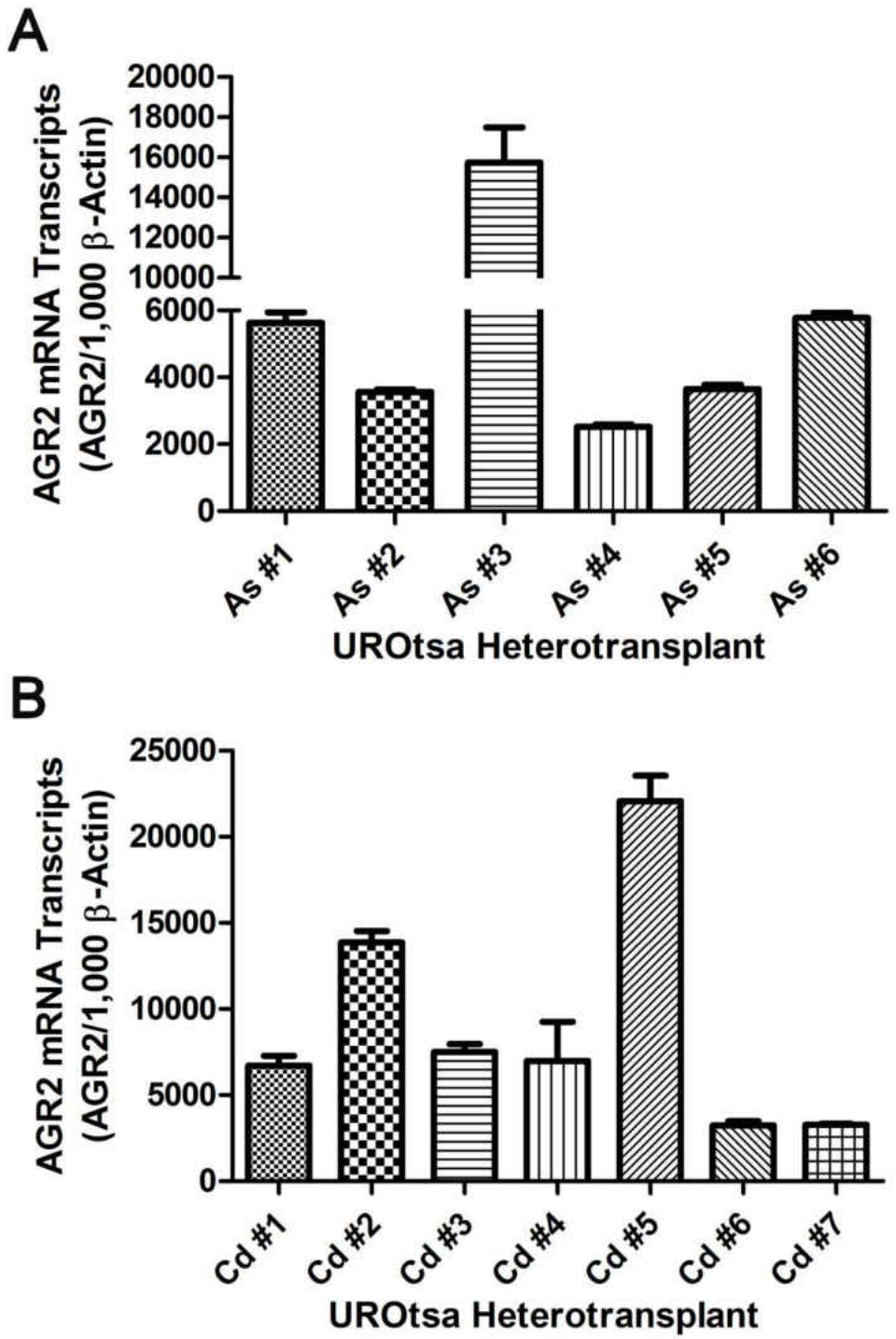

Figure 4 – AGR2 Expression in Heterotransplant Tumors from As^{3+} and Cd^{2+}-transformed UROtsa Cell Lines. A: Real-time PCR analysis of AGR2 expression in heterotransplant tumors arising from As^{3+}-transformed UROtsa cell lines injected into nude mice. **B:** Real-time PCR analysis of AGR2 expression in heterotransplant tumors arising from Cd^{2+}-transformed UROtsa cell lines injected into nude mice. Real-time data is plotted as the mean ± SEM of triplicate determinations.

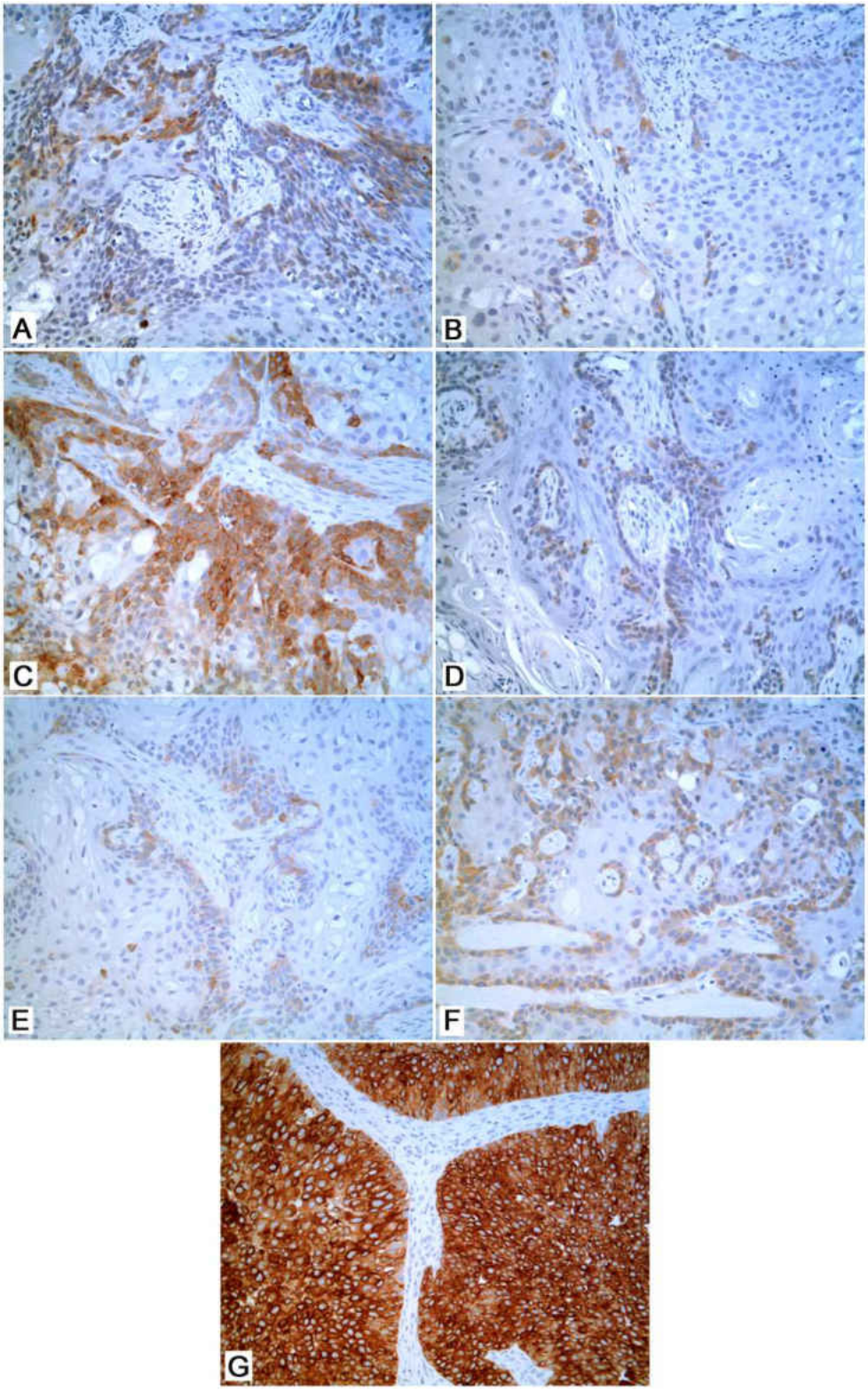

Figure 5 – AGR2 Staining in UROtsa As^{3+} Heterotransplants. A: UROtsa As #1 tumor. **B:** UROtsa As #2 tumor. **C.** UROtsa As #3 tumor. **D:** UROtsa As #4 tumor. **E:** UROtsa As #5 tumor. **F:** UROtsa As #6 tumor. **G:** Low grade bladder carcinoma.

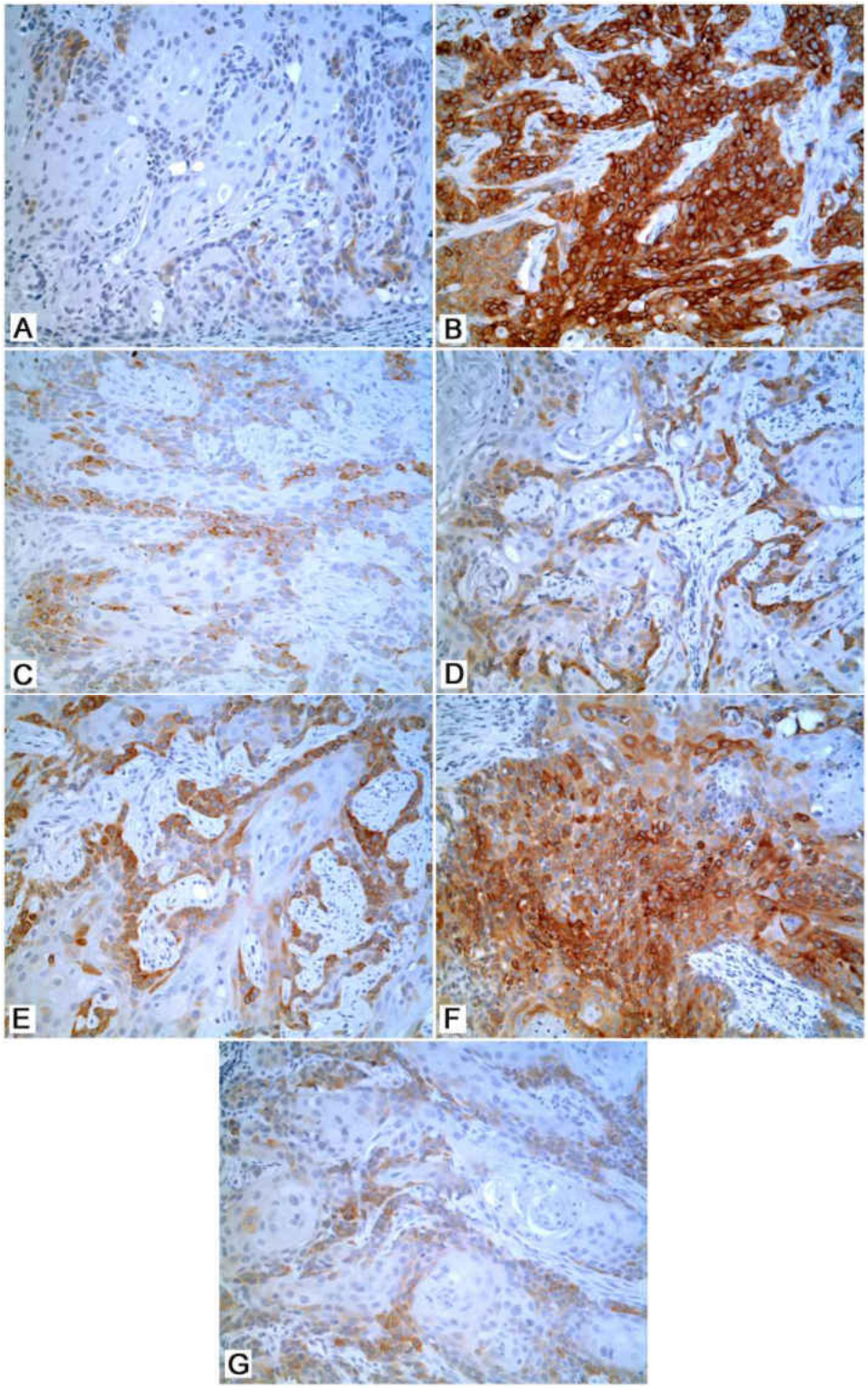

Figure 6 – AGR2 Staining in UROtsa Cd^{2+} Heterotransplants. A: UROtsa Cd #1 tumor. **B:** UROtsa Cd #2 tumor. **C:** UROtsa Cd #3 tumor. **D:** UROtsa Cd #4 tumor. **E:** UROtsa Cd #5 tumor. **F:** UROtsa Cd #6 tumor **G:** UROtsa Cd #7 tumor.

Table 3 – Summary of AGR2 Staining in UROtsa Heterotransplant Tumors. Intensity of AGR2 staining and percentage of cells positive for AGR2 staining.

	AGR2	
Group	**Intensity**	**Percentage**
UROtsa As #1	2+	10
UROtsa As #2	1-2+	<5
UROtsa As #3	2-3+	50
UROtsa As #4	1+	<5
UROtsa As #5	2+	5
UROtsa As #6	2+	20
UROtsa Cd #1	1-2+	<5
UROtsa Cd #2	3+	70
UROtsa Cd #3	2-3+	20
UROtsa Cd #4	2-3+	30
UROtsa Cd #5	2-3+	60
UROtsa Cd #6	3+	70
UROtsa Cd #7	2+	10
LG urothelial carcinoma	3+	80

3.3 Expression of AGR2 in UROtsa Cells Exposed to As^{3+} or Cd^{2+}

Next, this study sought to evaluate whether AGR2 expression can be induced by a short-term exposure to either As^{3+} or Cd^{2+}. UROtsa cells were exposed to 2, 4, or 6 μM $NaAsO_2$ or 1, 2, or 4 μM $CdCl_2$ for up to 72 hours. Expression of AGR2 increased within 48 hours in response to As^{3+} exposure (Figure 7 A). For the most part, significant induction of AGR2 in response to Cd^{2+} exposure was not seen. Notable increases in AGR2 expression did occur by 48 hours with 2 μM Cd^{2+} and at 72 hours with 1 μM Cd^{2+}. Significant decrease in AGR2 expression occurred at 48 hours with exposure to 4 μM Cd^{2+}. These decreases are likely attributable to the toxicity exhibited by the UROtsa cells at this concentration of Cd^{2+} (Figure 7 B). Results suggest that there is little to no significant effect of As^{3+} or Cd^{2+} exposure on the induction of AGR2 in UROtsa cells.

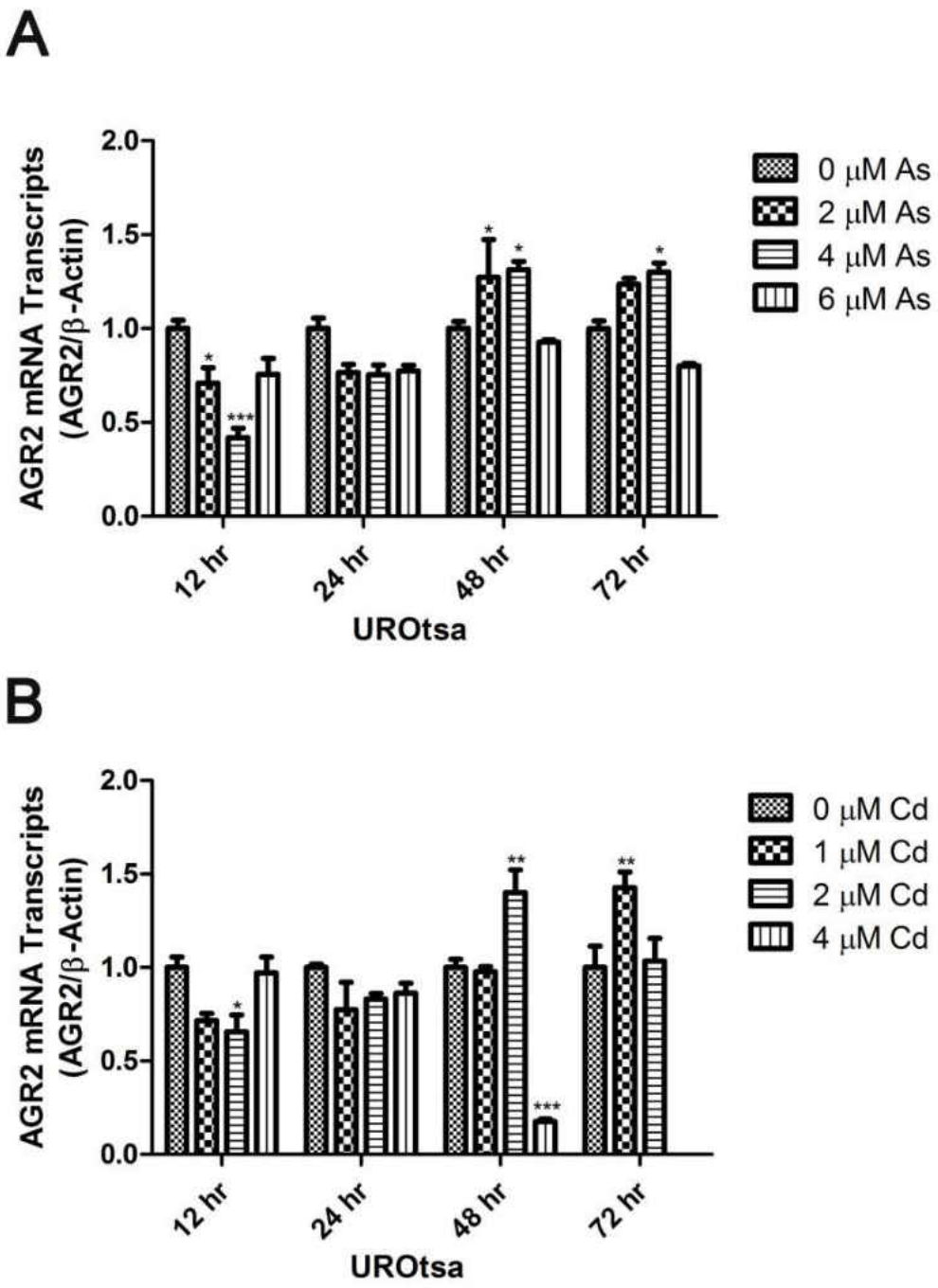

Figure 7 – AGR2 Expression in UROtsa Cells Exposed to As^{3+} or Cd^{2+}. A: Real-time PCR analysis of AGR2 expression in UROtsa cells exposed to 2, 4, or 6 μM As^{3+} for up to 72 hours. **B:** Real-time PCR analysis of AGR2 expression in UROtsa cells exposed to 1, 2, or 4 μM Cd^{2+} for up to 72 hours. *** denotes ($p < 0.001$), ** ($p < 0.01$), and * ($p < 0.05$) statistically significant difference from untreated UROtsa cells harvested with each time point. Real-time data is plotted as the mean ± SEM of triplicate determinations.

3.4 Expression of AGR2 mRNA in Cancer-Initiating-Cells (CICs) Isolated from the As^{3+} and Cd^{2+}-transformed UROtsa Cell Lines

This laboratory has extended the UROtsa model of As^{3+} and Cd^{2+}-induced bladder cancers to include spheroids isolated from the transformed cell lines by culturing the cell lines in serum-free media and in low attachment flasks. Previous studies by this group shown that these spheroids express high levels of aldehyde dehydrogenase 1 (ALDH1) and form subcutaneous tumor transplants identical to those of the As^{3+} and Cd^{2+}-transformed cells (Sandquist et al. 2016; Slusser-Nore et al. 2016). This fulfills the requirement that these spheroids represent cancer-initiating cells (CICs). The expression of AGR2 mRNA was determined on total RNA isolated from the spheroids isolated from the As^{3+} and Cd^{2+}-transformed cell lines and all the spheroids were shown to express AGR2 mRNA (Figure 8 A and B). Tumors generated from the CICs in the above two studies (Sandquist et al. 2016; Slusser-Nore et al. 2016) for two of the As^{3+}-transformed cell lines and two of the Cd^{2+}-transformed cell lines were examined for their expression of AGR2 protein using immunohistochemistry. The staining for AGR2 was similar to that found above for tumors generated directly from the cultured cell lines; cytoplasmic, focal, and associated with the more undifferentiated cells of the tumor (Figure 9). The results showed that between 20 to 30% of the tumor cells of all four tumor transplants stained moderately to strongly (+2 to +3) for the expression of AGR2 protein (Table 4).

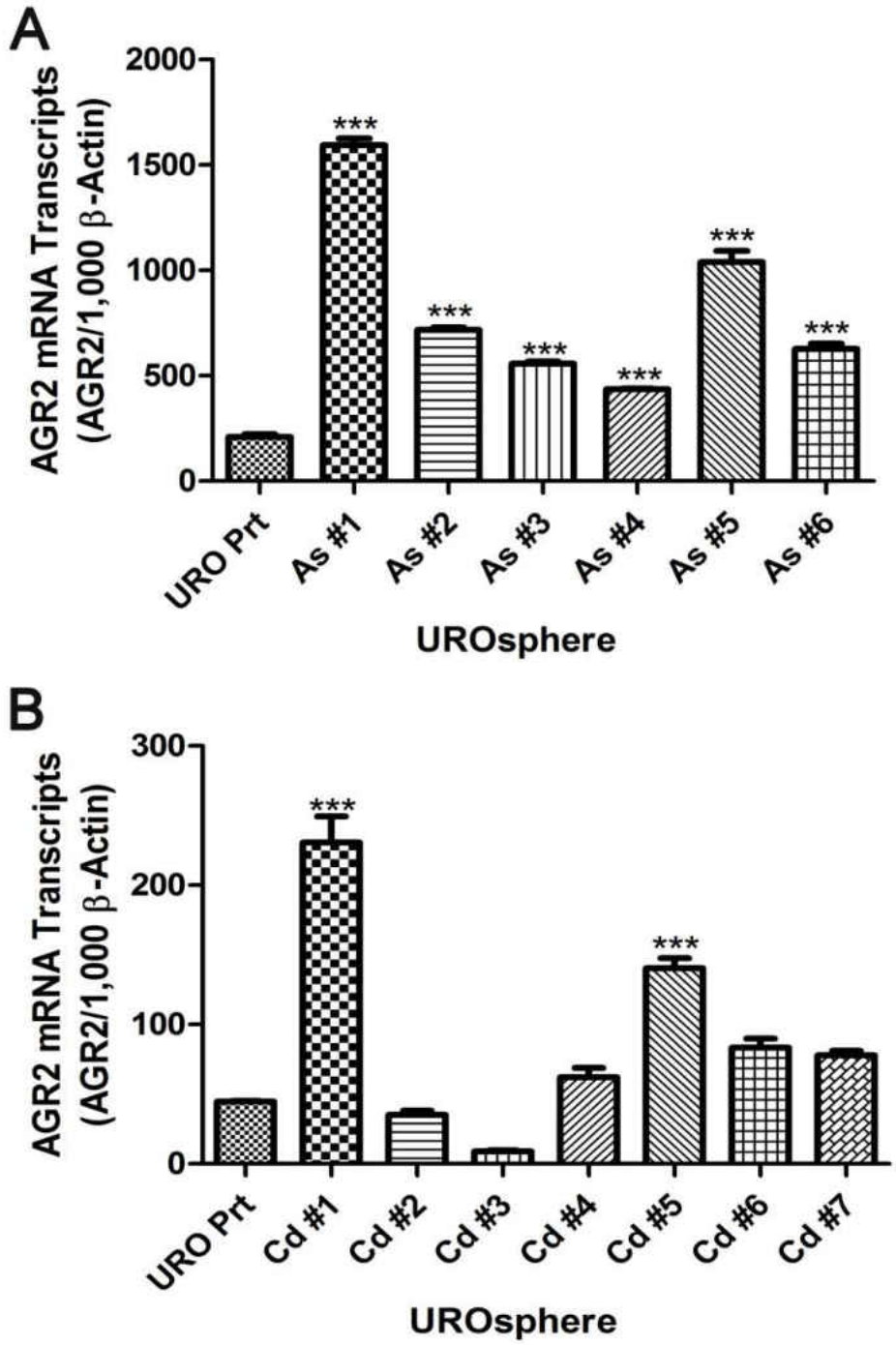

Figure 8 – AGR2 Expression in CICs Derived from As^{3+} and Cd^{2+}-transformed UROtsa Cell Lines. A: Real-time PCR analysis of AGR2 expression in spheroids derived from the As^{3+}-transformed UROtsa cell lines. **B:** Real-time PCR analysis of AGR2 expression in spheroids derived from the Cd^{2+}-transformed UROtsa cell lines. *** denotes a ($p < 0.001$), ** ($p < 0.01$), and * ($p < 0.05$) statistically significant difference from spheroids derived from the non-transformed parental UROtsa cell line. Real-time data is plotted as the mean ± SEM of triplicate determinations.

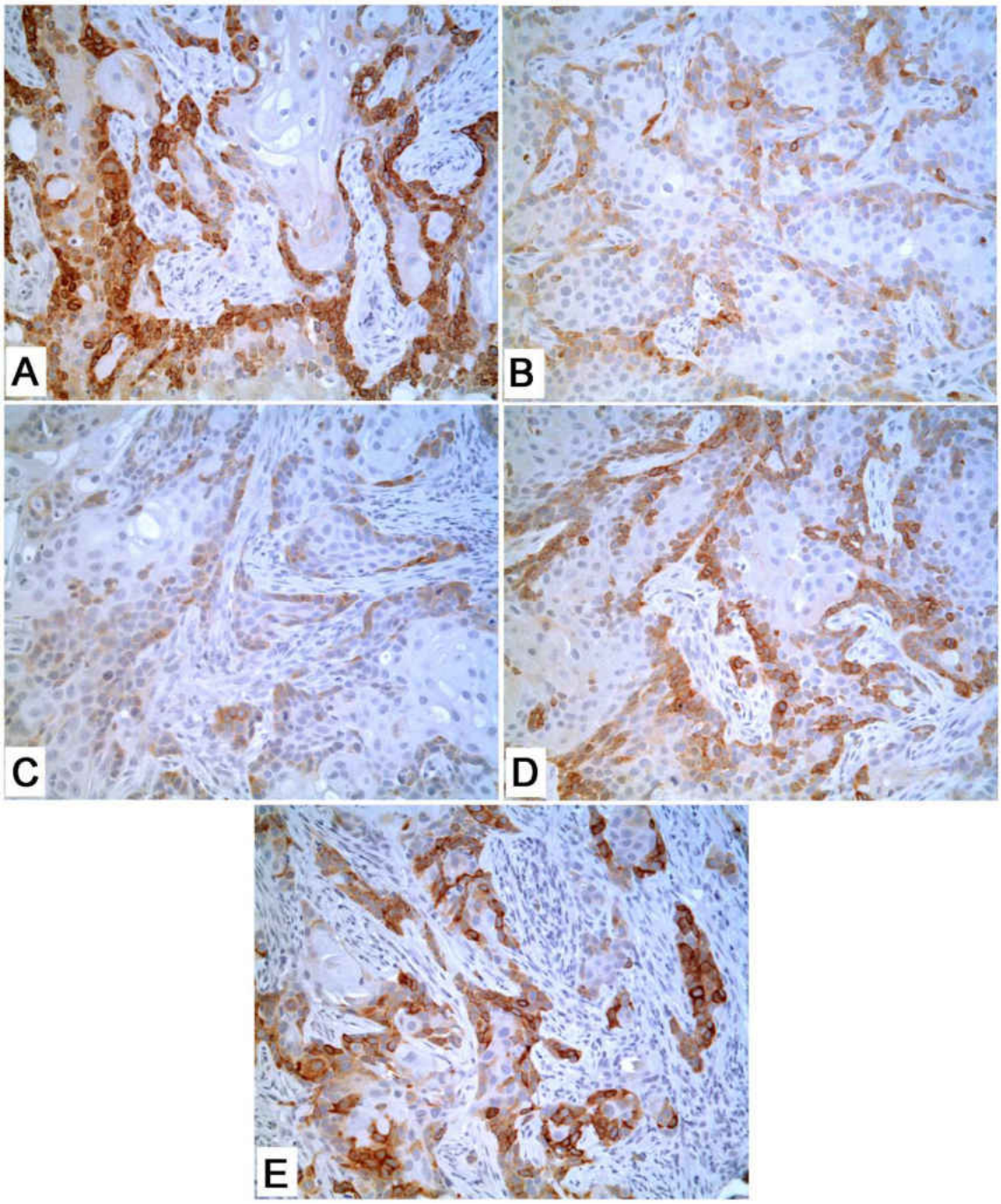

Figure 9 – AGR2 Staining in UROtsa-derived CICs. A: UROtsa As #1 spheroid derived tumor. **B:** UROtsa As #3 spheroid derived tumor. **C:** UROtsa As #6 spheroid derived tumor. **D:** UROtsa Cd #1 spheroid derived tumor. **E:** UROtsa Cd #4 spheroid derived tumor.

Table 4 – Summary of AGR2 Staining in Heterotransplant Tumors from UROtsa-derived CICs. Tumor type, AGR2 staining intensity, and percentage of cells positive for AGR2 staining for each tumor evaluated. LG – low grade.

		AGR2	
Group	**Tumor Type**	**Intensity**	**Percentage**
UROtsa As #1	Spheroid	3+	20
UROtsa As #3	Spheroid	2-3+	30
UROtsa As #6	Spheroid	2-3+	20
UROtsa Cd #1	Spheroid	2-3+	30
UROtsa Cd #4	Spheroid	3+	30
LG urothelial carcinoma	NA	3+	80

3.5 AGR2 Expression in Urothelial Carcinoma Cell Lines

After evaluating AGR2 expression in As^{3+} and Cd^{2+}-transformed UROtsa cell lines and corresponding heterotransplant tumors, this study next sought to evaluate AGR2 expression in three commercially-available urothelial carcinoma cell lines. Real-time PCR and western analysis were used to determine AGR2 expression in the J82 (HTB-1), RT4 (HTB-2), and HT-1376 (CRL1472) cell lines, which had been previously obtained from ATCC. The J82 cell line was obtained from a 58-year old Caucasian male with transitional cell carcinoma. The RT4 cell line was isolated from a transitional cell papilloma in a 63-year old Caucasian male. The HT-1376 cell line was isolated from a 58-year old Caucasian female with grade 3 urothelial carcinoma. Results showed that AGR2 mRNA is expressed in all three urothelial carcinoma cell lines but is most highly expressed in the RT4 and HT-1376 cell lines (Figure 10 A). Western analysis also showed that AGR2 is expressed in all three of the urothelial carcinoma cell lines and that it has the greatest expression in the RT4 cell line (Figure 10 B and C). These results demonstrate that AGR2 expression is present in bladder cancer cell lines.

Next, this study determined whether AGR2 expression remains elevated in tumors derived from the urothelial carcinoma cell lines. Tumors were generated for the urothelial

carcinoma cell lines by injecting each cell line subcutaneously or intraperitoneally into nude mice. Slides made from the isolated tumors were stained for AGR2 expression using immunohistochemical techniques. Results indicate positive AGR2 staining in subcutaneous and intraperitoneal tumors arising from the HT-1376 cell line (Figure 11 A and B). Tumors derived from subcutaneous or intraperitoneal injection of the J82 cell line did not exhibit staining for AGR2 (Figure 11 C and D). Strongly positive AGR2 staining was seen in subcutaneous tumors derived from the RT4 cell line (Figure 11 D and F). An intraperitoneal tumor derived from the RT4 cell line exhibited strong AGR2 staining in tumor cells (Figure 11 G). A further summary of these results is shown in Table 5. These results indicate that only the HT-1376 and RT4 derived tumors were able to maintain elevated AGR2 expression, which is consistent with these cell lines exhibiting the highest AGR2 expression.

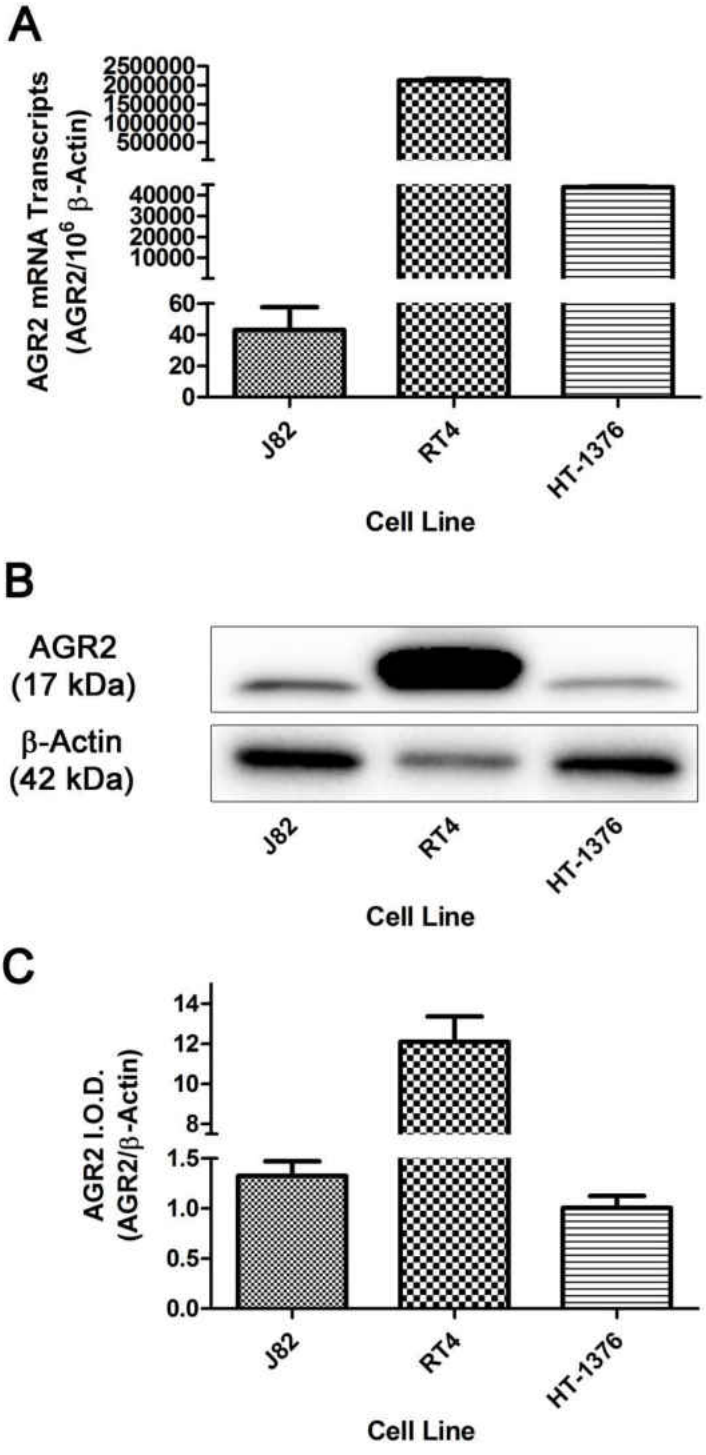

Figure 10 – AGR2 Expression in Urothelial Carcinoma Cell Lines. A: Real-time PCR analysis of AGR2 expression in urothelial carcinoma cell lines. Real-time data is plotted as the mean ± SEM of triplicate determinations. **B:** Western blot analysis of AGR2 in urothelial carcinoma cell lines. **C:** I.O.D. analysis of western blotting in **B**, plotted as AGR2/β-Actin.

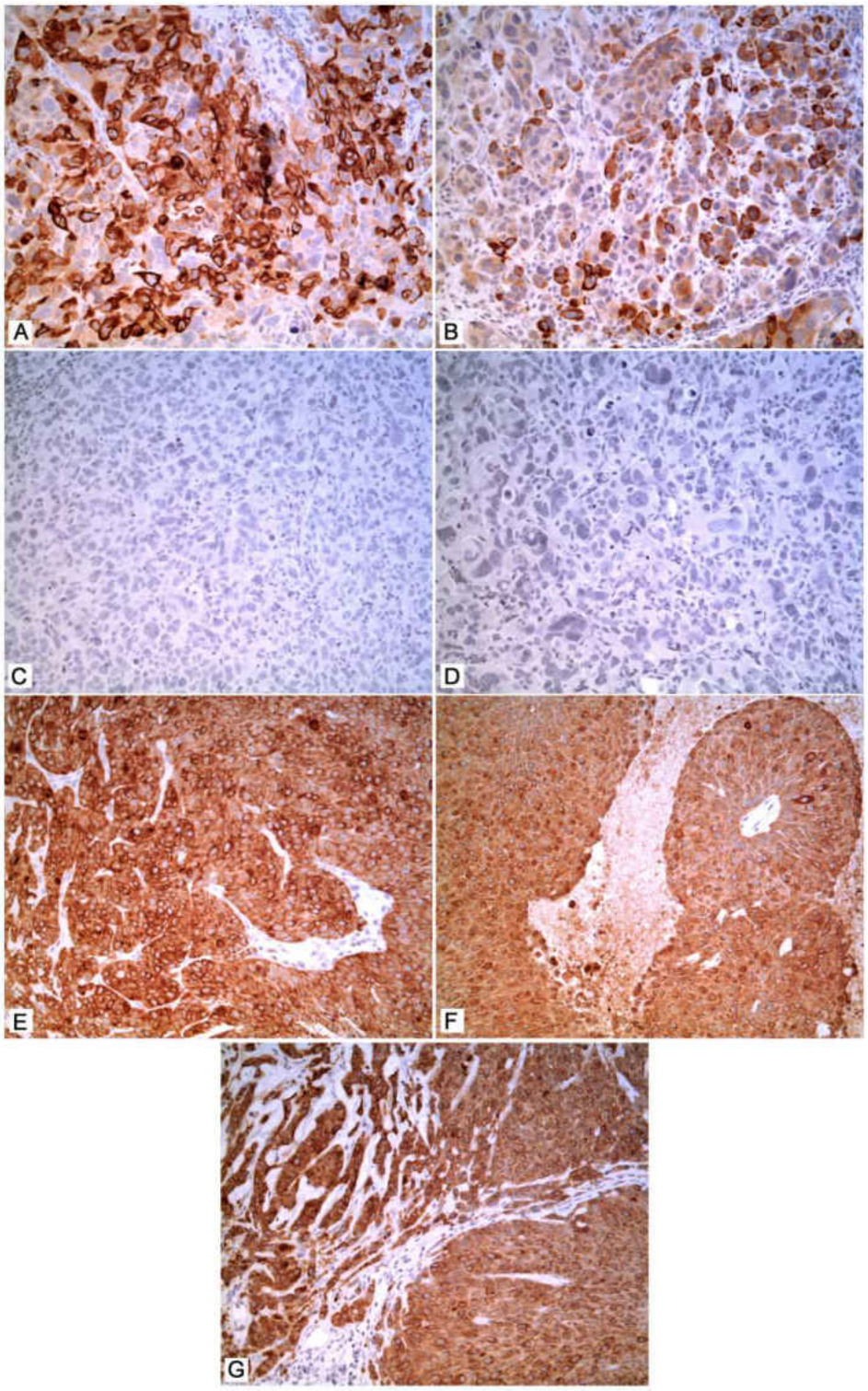

Figure 11 – AGR2 in Heterotransplants from Urothelial Carcinoma Cell Lines. A: Subcutaneous HT-1376 tumor. **B:** Intraperitoneal HT-1376 tumor. **C:** Subcutaneous J82 tumor. **D:** Intraperitoneal J82 tumor. **E:** Subcutaneous RT4 tumor. **F:** Subcutaneous RT4 tumor. **G:** Intraperitoneal RT4 tumor.

Table 5 – Summary of AGR2 Staining in Heterotransplants from Urothelial Carcinoma Cell Lines. Tumor type, AGR2 staining intensity, and percentage of cells positive for AGR2 staining for each tumor evaluated.

		AGR2	
Cell Line	**Tumor Type**	**Intensity**	**Percentage**
HT-1376	Subcutaneous	3+	30
HT-1376	Intraperitoneal	3+	40
J82	Subcutaneous	-	0
J82	Intraperitoneal	-	0
RT4	Subcutaneous	3+	100
RT4	Intraperitoneal	3+	100

3.6 Expression of AGR2 in MCF-10A Cells Transformed with As^{3+} or Cd^{2+}

In order to better understand the impact of As^{3+} and Cd^{2+} on breast cancers, a model for heavy metal-induced breast cancer has previously been established using the MCF-10A breast epithelial cell line (Soh et al. 2011). Previous microarray analysis and subsequent studies on how As^{3+} and Cd^{2+} affect the expression of AGR2 in the UROtsa model of heavy metal-induced bladder cancers prompted the question of whether similar effects might be seen in the MCF-10A model. In order to see if AGR2 may also serve as a biomarker for heavy metal-induced breast cancers, the expression of AGR2 was determined in the MCF-10A parent and the As^{3+} and Cd^{2+}-transformed cells using real-time PCR and western analysis. Real-time PCR analysis showed a significant increase in AGR2 expression in the As^{3+}-transformed MCF-10A cell line compared to non-transformed MCF-10A cells. A significant decrease in AGR2 expression was seen in the Cd^{2+}-transformed MCF-10A cell line (Figure 12 A). Western blotting of whole cell lysates was used to evaluate AGR2 protein expression in the transformed MCF-10A cell lines. The results also indicated a significant increase in AGR2 protein expression following As^{3+}-transformation and a significant decrease in AGR2 protein following Cd^{2+}-transformation compared to non-transformed MCF-10A cells (Figure 12 B and C).

These results indicate that AGR2 expression is increased in response to transformation with As^{3+} but not Cd^{2+} in MCF-10A cells.

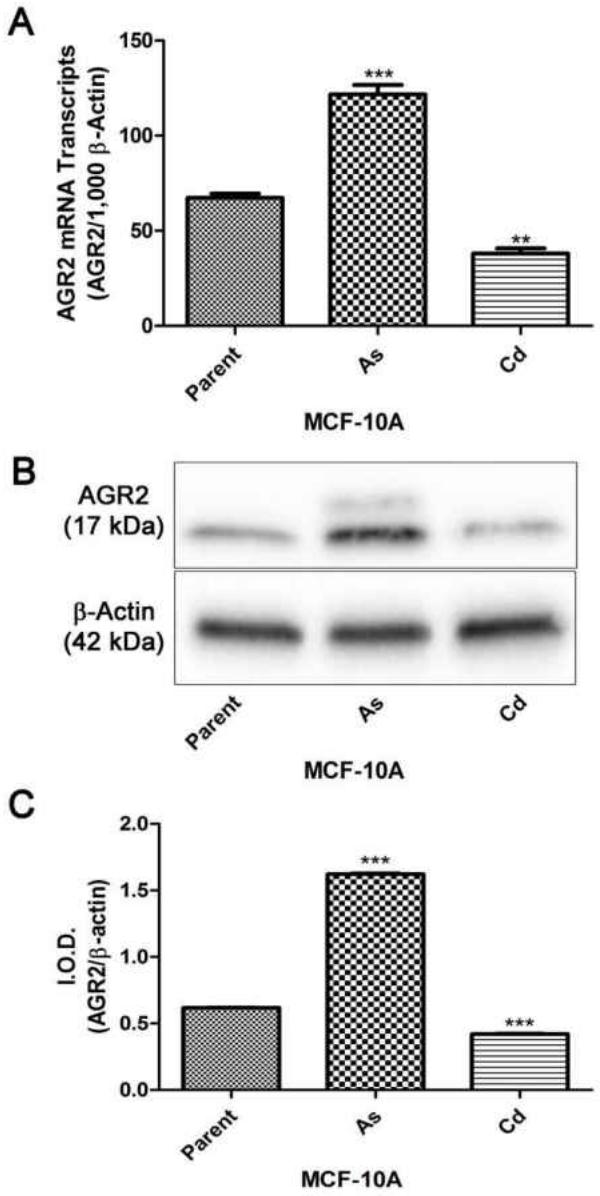

Figure 12 - Expression of AGR2 mRNA and Protein in As^{3+} and Cd^{2+}-transformed MCF-10A Cells. A: Real-time PCR analysis of AGR2 mRNA in As^{3+} and Cd^{2+}-transformed MCF-10A cells**. *****Denotes a statistically significant difference from MCF-10A parent cells ($p < 0.001$). Real-time data is plotted as the mean ± SEM of triplicate determinations. **B:** Western blot analysis of AGR2 and protein in As^{3+} and Cd^{2+}-transformed MCF-10A cells. **F:** I.O.D. analysis of western blotting in **C**, plotted as AGR2/β-Actin.

3.7 Expression of AGR2 in MCF-10A Cells Exposed to As^{3+} or Cd^{2+}

After having established that As^{3+}-transformation can result in increased AGR2 expression, this study next sought to determine whether AGR2 expression is induced by exposure to As^{3+} or Cd^{2+}. In order to evaluate the effect that As^{3+} exposure has on AGR2 expression, MCF-10A cells were exposed to 4, 8, or 16 μM $NaAsO_2$ for up to 48 hrs. Cells were harvested 12, 24, 36, and 48 hours following treatment and analyzed by real-time PCR and western analysis to determine AGR2 expression. Data indicate that AGR2 expression was significantly increased in response to As^{3+} exposure. By 36 hours, 2, 3.6, and 4.9 fold increases in AGR2 mRNA was seen at 4, 8, and 16 μM As^{3+} exposure respectively (Figure 13 A). Furthermore, western blotting followed by I.O.D. analysis indicated as much as a 7.5 fold increase in AGR2 protein expression after 36 hours exposure to 16 μM As^{3+} (Figure 13 B and C). Additionally, this study sought to establish whether Cd^{2+} is capable of inducing AGR2 expression. To accomplish this, MCF-10A cells were exposed to 2, 4, or 6 μM $CdCl_2$ for 12, 24, 36, or 48 hours and were analyzed using real-time PCR for AGR2 expression. The data obtained indicated that there was a transient increase in the expression of AGR2 at 12 hour of exposure with 4 μM Cd^{2+}, however the levels went down by 24 hours (Figure 14). These results demonstrate that As^{3+} is capable of inducing AGR2 expression in MCF-10A cells while AGR2 expression is not induced by Cd^{2+} exposure.

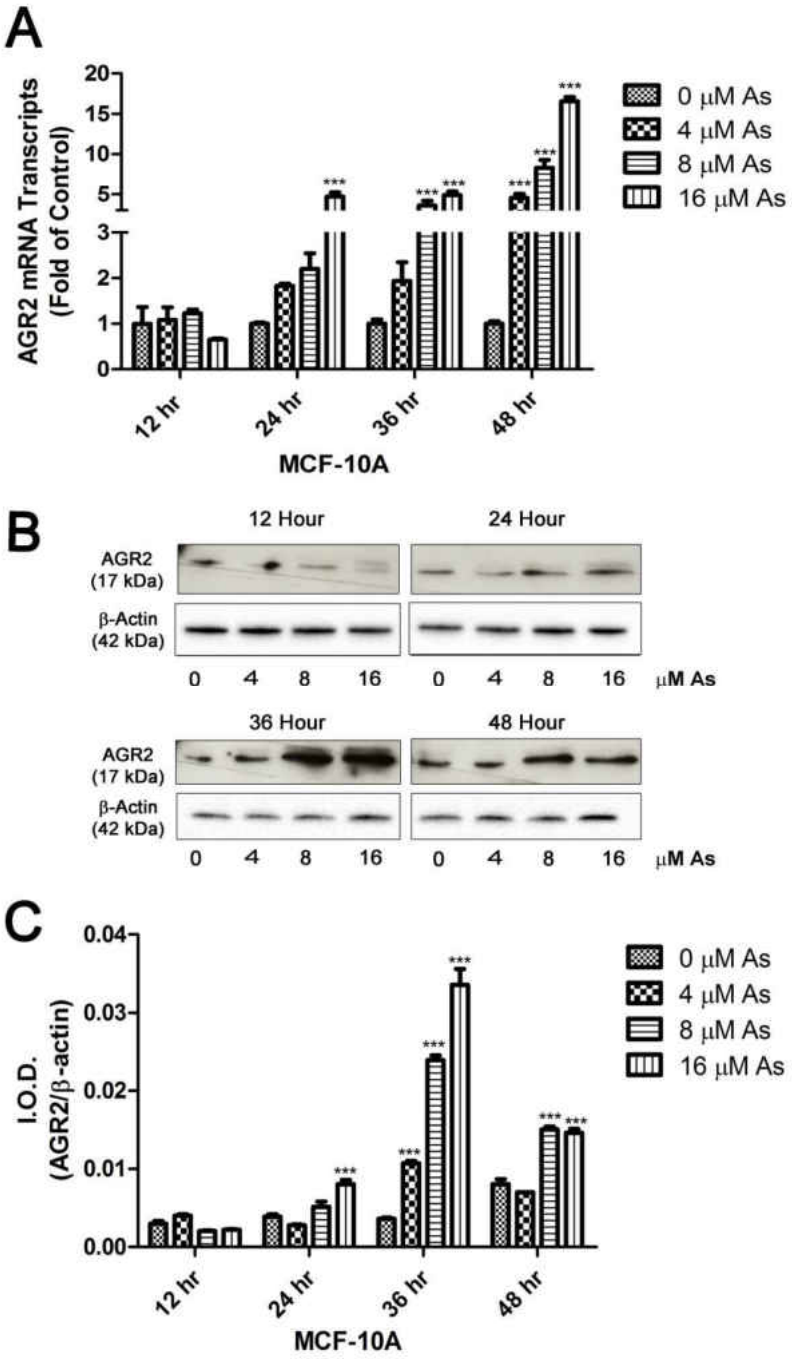

Figure 13 - Expression of AGR2 mRNA and Protein in As^{3+}-exposed MCF-10A Cells. MCF-10A cells were exposed to 4, 8, or 16 μM As^{3+} for 12, 24, 36, or 48 hrs and the expression level of AGR2 was determined. **A:** Real-time PCR analysis. Asterisks denote a statistically significant difference from 0 μM As^{3+} within each time point with * ($p < 0.05$), ** ($p < 0.01$) and *** ($p < 0.001$). Real-time data is plotted as the mean ± SEM of triplicate determinations. **B:** Western blot analysis of AGR2 expression in MCF-10A cells exposed to As^{3+}. **C:** I.O.D. analysis of western data in **B**, plotted as AGR2/β-Actin.

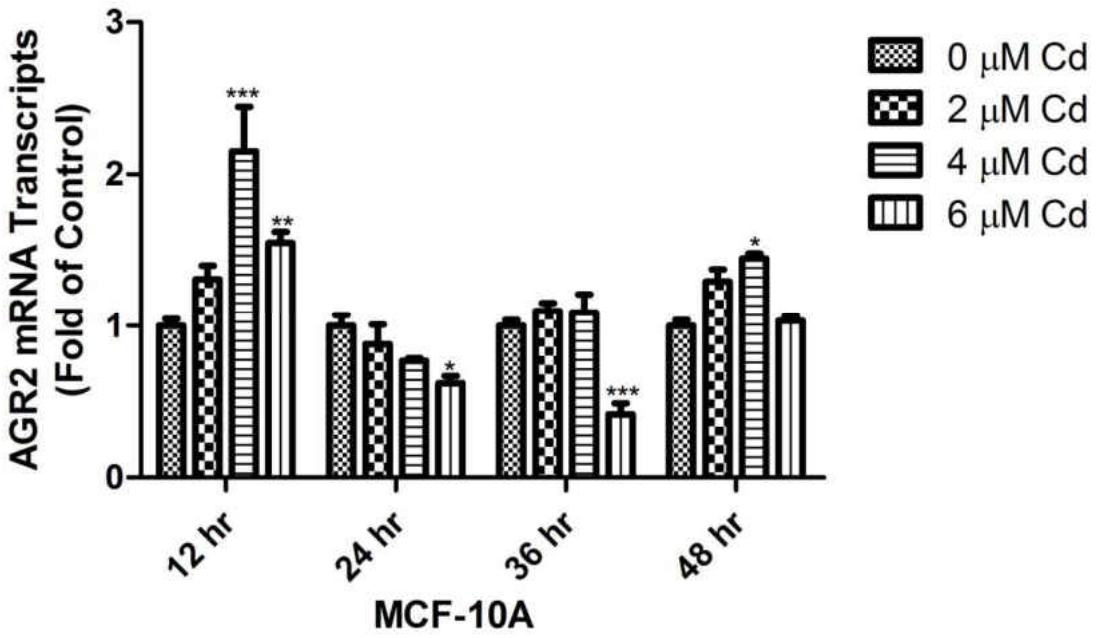

Figure 14 - Expression of AGR2 mRNA in Cd^{2+}-exposed MCF-10A Cells. Real-time PCR analysis of AGR2 transcripts in MCF-10A cells exposed to 2, 4, or 6 μM Cd^{2+} for 12, 24, 36, or 48 hrs. Asterisks denote a statistically significant difference from 0 μM Cd^{2+} within each time point with * ($p < 0.05$), ** ($p < 0.01$) and *** ($p < 0.001$). Real-time data is plotted as the mean ± SEM of triplicate determinations.

3.8 AGR2 Expression in Breast Cancer Cell Lines

Previous studies have demonstrated that AGR2 expression is correlated to breast cancers, specifically subtypes which commonly exhibit poor prognosis (Fritzsche et al. 2006; Barraclough et al. 2009; Lacambra et al. 2015) . Since the expression of AGR2 is correlated to the ERα status (Thompson and Weigel 1998; Innes et al. 2006; Salmans, Zhao, and Andersen 2013), this study sought to determine AGR2 expression in commercially available breast cancer cell lines that are widely used as *in-vitro* models of breast cancer. For this purpose, breast cancer cell lines known to have different ERα expression profiles were utilized. Real-time PCR and western analysis were used to determine AGR2 expression in two ERα-negative (MDAMB-231 and Hs578T) and two

ERα-positive (T47D and MCF-7) breast cancer cell lines. Results showed the greatest increase of AGR2 mRNA expression in the T47D breast cancer cell line, moderate increases in the MCF-7 and MDAMB cell lines, and essentially undetectable AGR2 expression in Hs578T cells (Figure 15 A). Western blotting analysis showed a similar trend for AGR2 protein expression, with the greatest expression in the T47D cell line. The MDAMB-231 and MCF-7 cell lines also exhibited increased AGR2 protein while AGR2 was not detectable in the Hs578T cell line using western blotting (Figure 15 B and C). These results suggest that AGR2 is highly expressed in a well-known ERα-positive breast cancer cell line and exhibits lower expression in ERα-negative breast cancer cell lines.

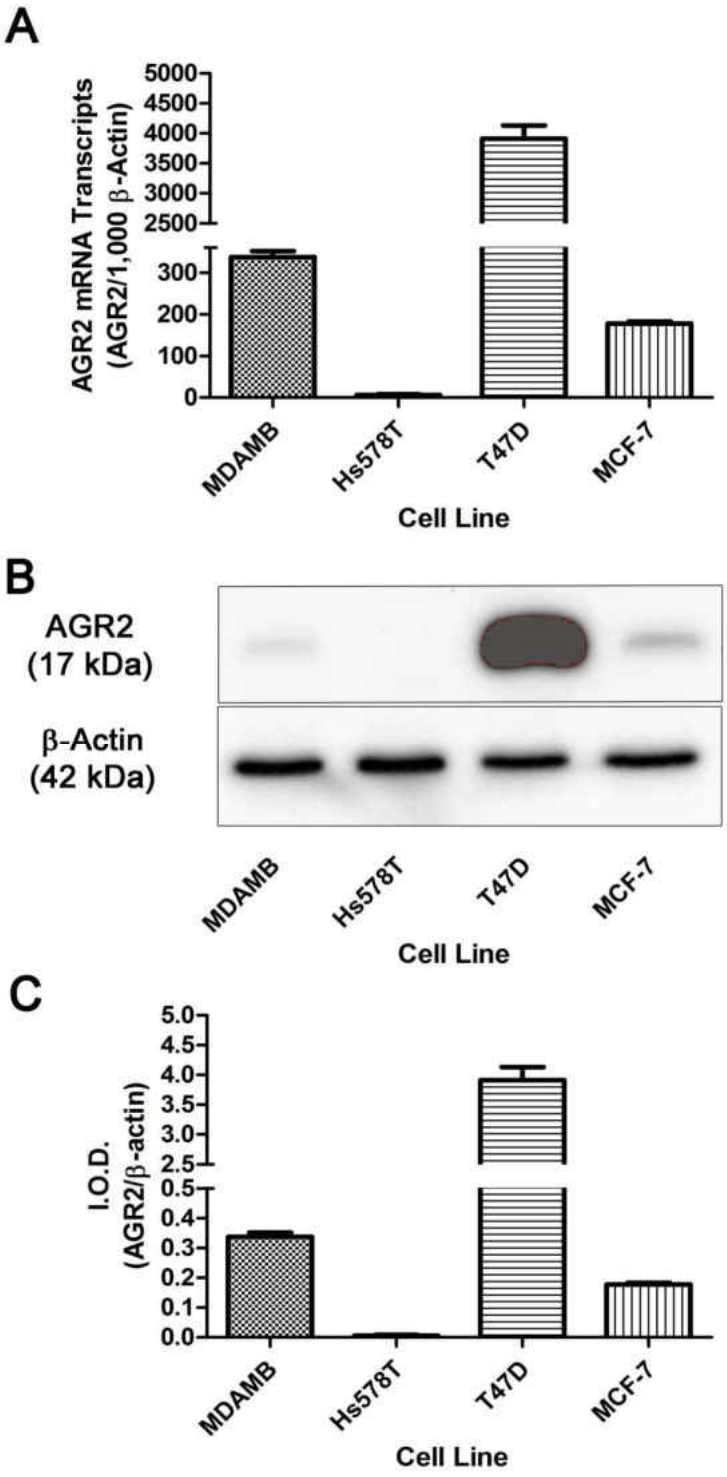

Figure 15 - Expression of AGR2 mRNA and Protein in Breast Cancer Cell Lines. A: Real-time PCR analysis of AGR2 expression in breast cancer cell lines. Real-time data is plotted as the mean ± SEM of triplicate determinations. **B:** Western blot analysis of AGR2 in breast cancer cell lines. **C:** Integrated optical density (I.O.D.) analysis of western blotting in **B**, plotted as AGR2/β-Actin.

3.9 Role of ERα in MCF-10A Cells

Anterior gradient 2 expression has been shown to be influenced by estrogen receptor (ERα) status in breast cancers (Thompson and Weigel 1998; Innes et al. 2006; Salmans, Zhao, and Andersen 2013). This study next sought to further investigate whether ERα has a role impacting AGR2 expression in the MCF-10A breast cell model. Normally MCF-10A cells are known to be ERα-negative, however the possibility for MCF-10A cells to begin expressing ERα has been demonstrated (Lane et al. 1999). With this in mind real-time PCR analysis was used to evaluate ERα (ESR1) expression in 2 ERα-negative (MDAMB-231 and Hs578T) and 2 ERα-positive (T47D and MCF-7) breast cancer cell lines as well as in parent and As^{3+} and Cd^{2+}-transformed MCF-10A cell lines. While ERα expression was confirmed in both ERα-positive breast cancer cell lines, high ERα-expression was not seen in any of the MCF-10A cell lines (Figure 16). These data suggest that the expression of AGR2 in MCF-10A cells is most likely due to ERα-independent mechanisms. This is especially true when evaluating the As^{3+} and Cd^{2+}-transformed MCF-10A cell lines. The non-transformed MCF-10A cell line did exhibit a low level of ERα expression, therefore the possibility of ERα influences on AGR2 expression and function cannot be dismissed entirely in non-transformed MCF-10A cells.

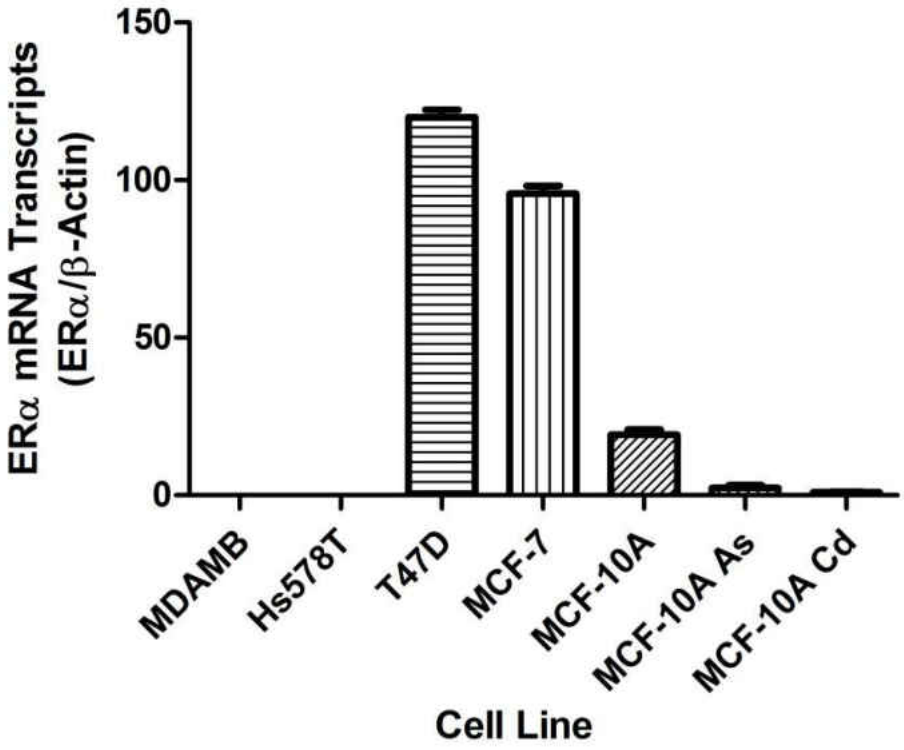

Figure 16 – ERα Expression in Breast Cancer and MCF-10A Cell Lines. Real-time PCR analysis of AGR2 transcripts in breast cancer cell lines (MDAMB, Hs578T, T47D, and MCF-7) as well as MCF-10A cell lines transformed with As^{3+} or Cd^{2+}. Real-time data is plotted as the mean ± SEM of triplicate determinations.

3.10 Effect of the Overexpression of AGR2 on MCF-10A Cell Proliferation

The next goal of this study was to investigate the functional impact that AGR2 expression has in breast tissue, especially as those functions may have significant impact on the outcome of AGR2-expressing breast cancers. An AGR2-overexpressing MCF-10A cell line was created which could be used to further elucidate the functions of AGR2 in breast epithelia. Real-time PCR and western analysis were used to confirm AGR2 overexpression (Figure 17). These data indicate that an AGR2-overexpressing MCF-10A cell line was generated and that this cell line will be useful for evaluating the functional role of AGR2 in breast epithelia.

As AGR2 expression has been known to affect cell proliferation and has been previously associated with metastasis (Liu et al. 2005; Ramachandran et al. 2008; Wang, Hao, and Anson W. Lowe 2008), the next goal of this project was to evaluate the growth and migration potential of MCF-10A cells transformed with As^{3+} or transfected with AGR2. In order to determine the effect of As^{3+} or Cd^{2+}-transformation on MCF-10A cell growth rates, MTT assays were utilized. The results obtained indicated a significant increase in proliferation for As^{3+}-transformed MCF-10A cells compared to the non-transformed MCF-10A cell line (Figure 18). Wound/scratch assays were performed on MCF-10A cell lines in order to determine the migration potential of the cells. Images were collected and analyzed from just after scratching (0 hr) and from 4, 8, and 12 hours later. Wound closure rates were then determined in order to evaluate migration into the wound. MCF-10A cells transformed with As^{3+} exhibited a 70.62% wound closure rate, significantly increased over parent MCF-10A cells (48.03%) or Cd^{2+}-transformed MCF-10A cells (57.37%) (Figure 19). These results demonstrate that As^{3+}-transformed cells had an increased growth rate and migration potential when compared to the parent MCF-10A cells and the Cd^{2+}-transformed cells, suggesting a more tumorigenic phenotype in As^{3+}-transformed MCF-10A cells. While it may seem tempting to correlate the changes in growth and migratory potential to the increased AGR2 expression exhibited by the As^{2+}-transformed MCF-10A cell line, there are any number of potential mechanisms to which these effects may be attributed. Further studies will be needed to determine which mechanism(s) may be involved.

We also wanted to determine if overexpression of AGR2 in MCF-10A cells would have an effect on their growth rate and migration potential. In order to determine

the growth rate, MTT assays were performed on the MCF-10A cells transfected with either the blank 6.2 V5-DEST vector or with an AGR2-containing construct. The data obtained shows that overexpression of AGR2 in MCF-10A cells can increase their growth rate when compared to cells transfected with the blank vector alone (Figure 20). This project also sought to determine whether overexpression of AGR2 would affect the migration potential of the MCF-10A cells transfected with AGR2 in a wound scratch assay. Results show that overexpression of AGR2 in MCF-10A cells results in an increase in the wound closure rate when compared to the blank vector (Figure 21). In conclusion, these data suggest that overexpression of AGR2 can affect the growth rate and migration potential of cells, hence its expression may have an effect on the metastatic potential of breast cancer cells. To further verify the effect of AGR2 on the proliferation and migration of MCF-10A cells, further experiments would need to be completed. These experiments might include the knock-down of AGR2 expression in the As^{3+}-transformed and AGR2-transfected MCF-10A cell lines.

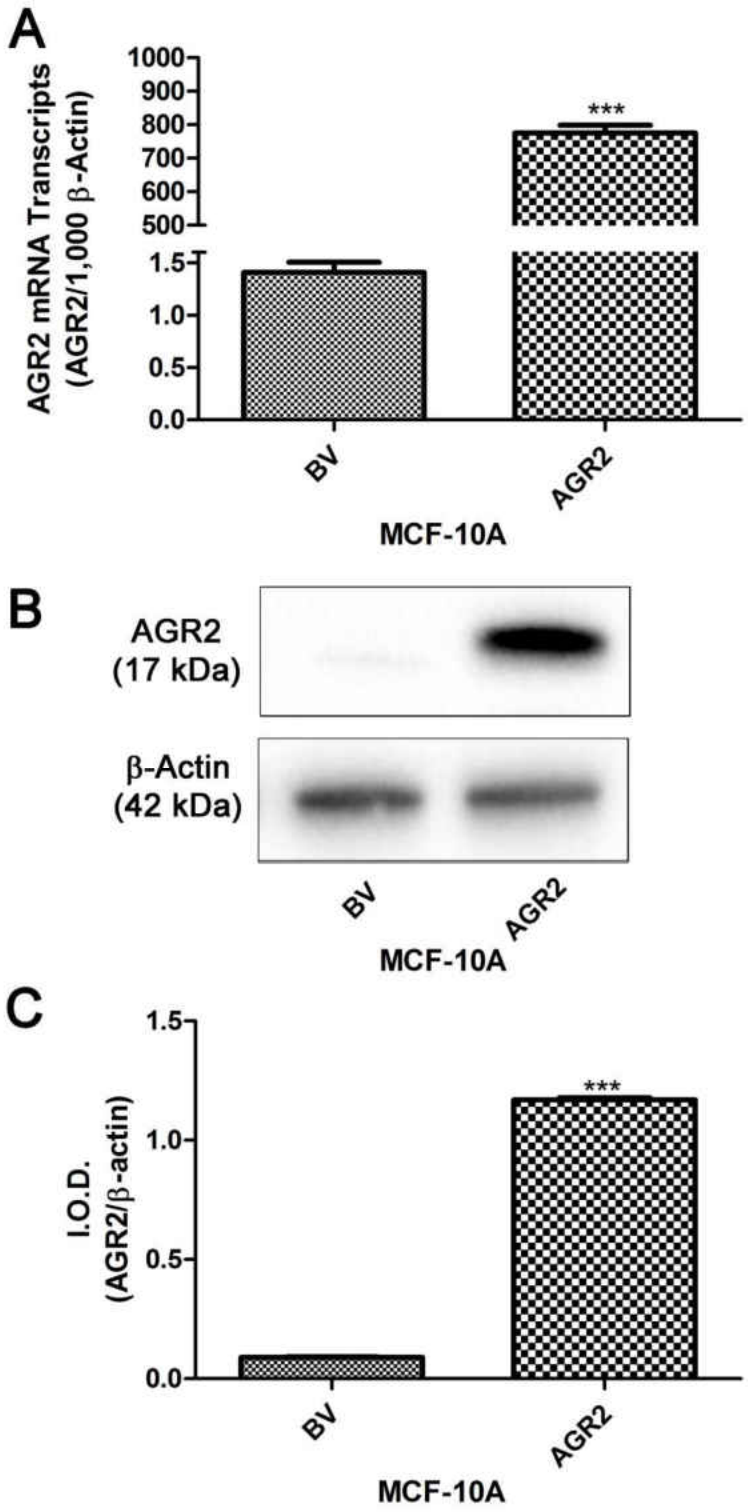

Figure 17 - Expression of AGR2 mRNA and Protein in MCF-10A Cells Transfected with AGR2. A: Real-time PCR analysis of AGR2 mRNA. **B:** Western analysis of AGR2 protein. **C:** I.O.D. analysis of Western data in **B**, plotted as AGR2/β-Actin.

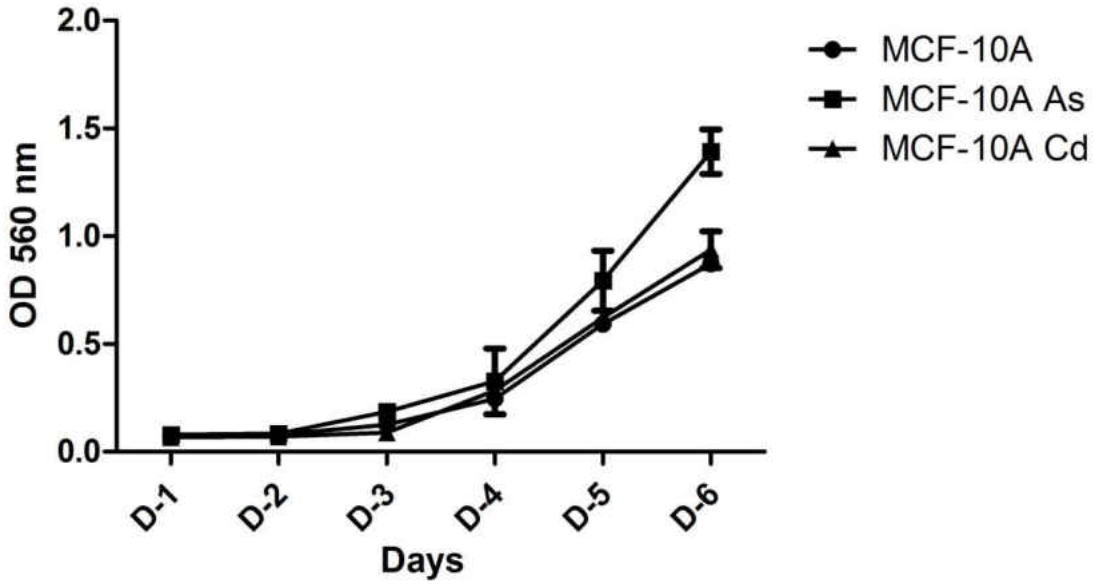

Figure 18 – Effect of As^{3+} and Cd^{2+}-transformation on the Growth Rate of MCF-10A Cells. The growth rates were determined by measuring the capacity of the cells to reduce MTT to formazan. The cells were allowed to grow for 6 days and the ability of the cells to reduce MTT was determined every day. All experiments were done in triplicates and shown is the mean ± SEM absorbance values.

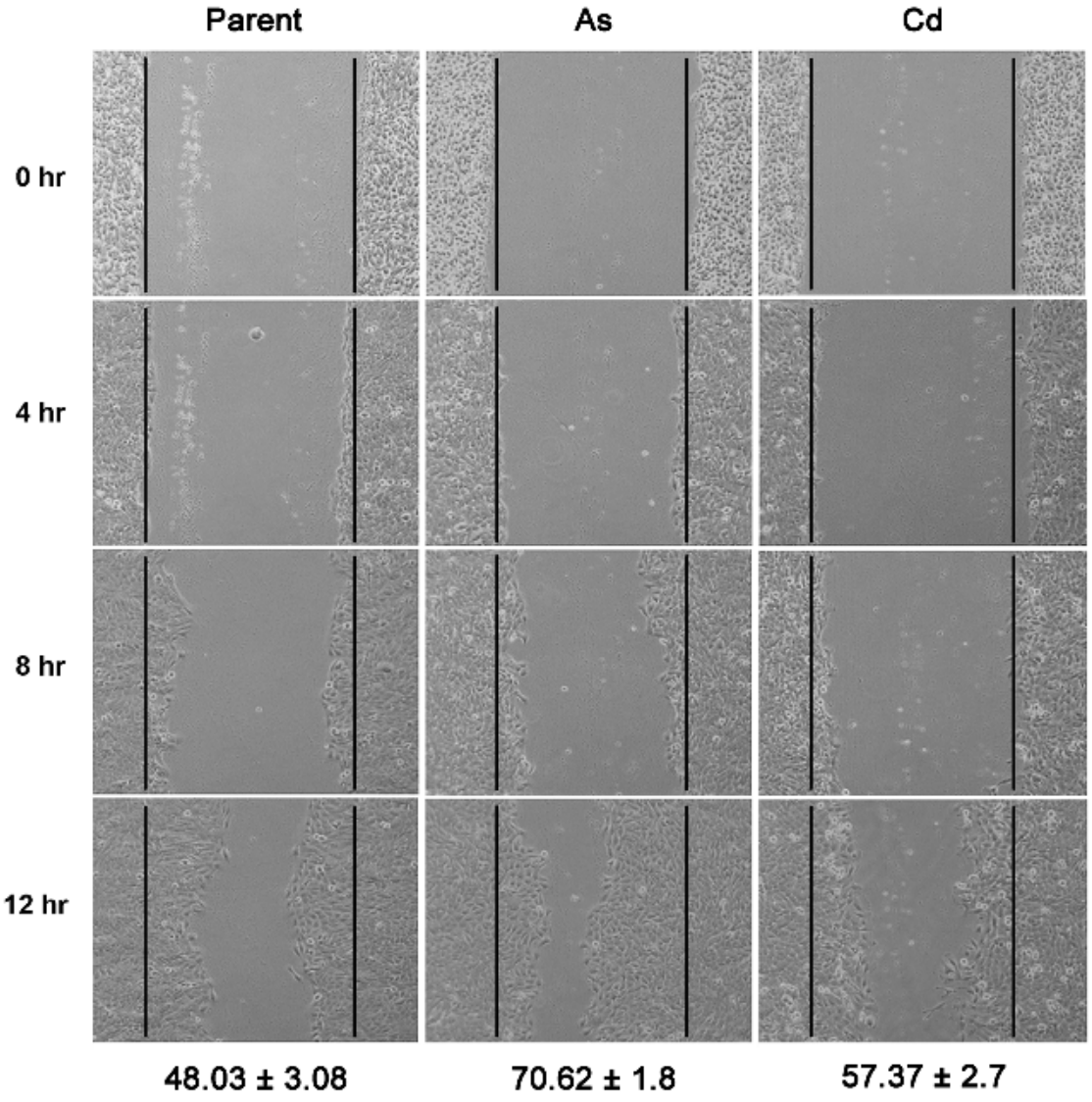

Figure 19 – Effect of As^{3+} and Cd^{2+}-transformation on the Migration of MCF-10A Cells. MCF-10A parent and transformed cell lines were subjected to wound scratch assay and migration of the cells was determined after 4, 8 and 12 hours. Percent wound closures were calculated and are presented beneath the 12 hour panels for each cell line.

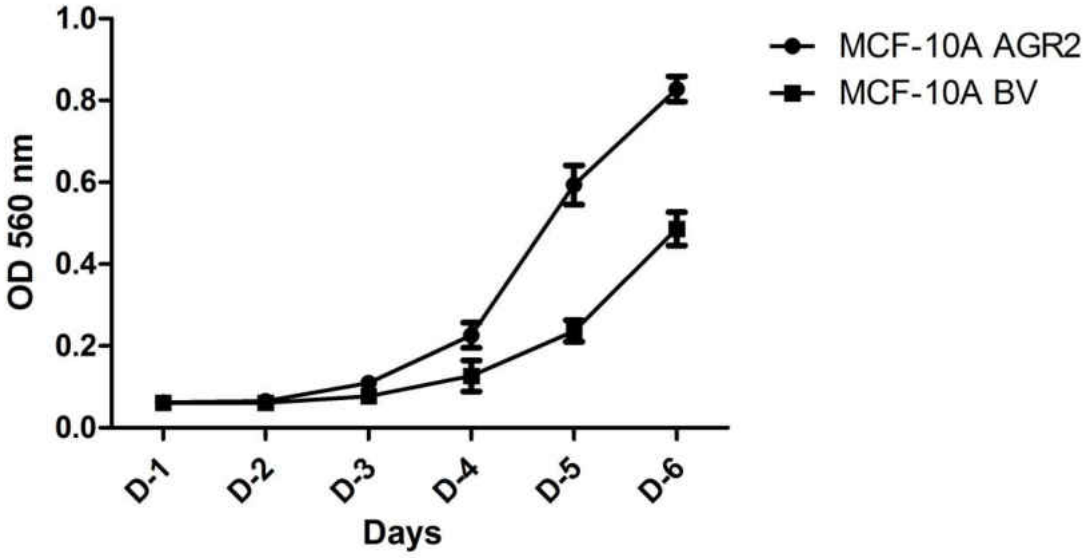

Figure 20 - Effect of AGR2 Expression on the Growth Rate of MCF-10A Cells Transfected with the Blank Vector or the AGR2 Gene. The growth rates were determined by measuring the capacity of the cells to reduce MTT to formazan. The cells were allowed to grow for 6 days and the ability of the cells to reduce MTT was determined every day. All experiments were done in triplicates and shown is the mean ± SEM absorbance values.

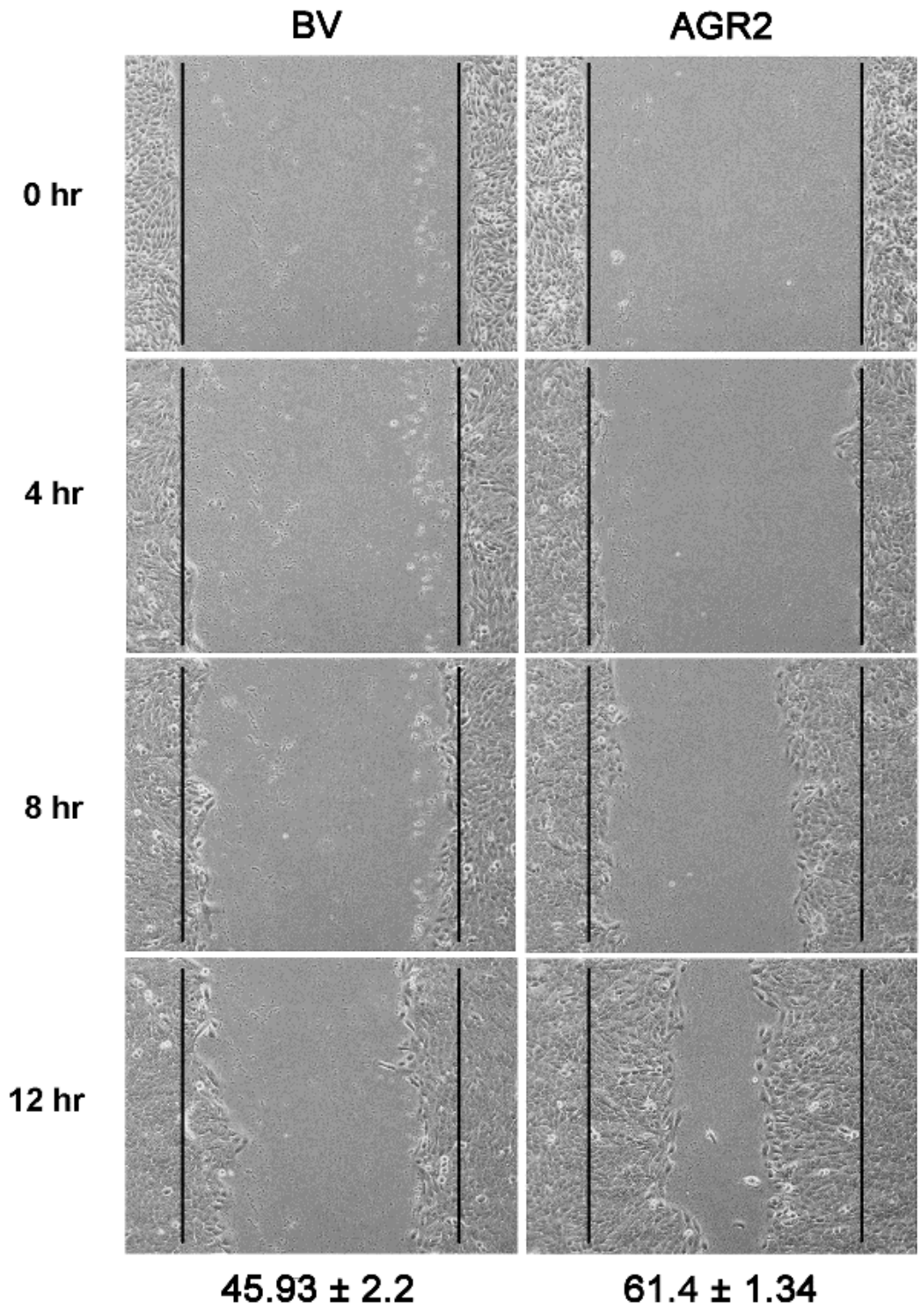

Figure 21 - Effect of AGR2 Expression on MCF-10A Cell Migration. MCF-10A cells were transfected with AGR2 or a blank vector and were scratched at confluency. The ability of the cells to grow and migrate into the wound was determined after 4, 8 and 12 hours of incubation. Percent wound closures were calculated and are presented beneath the 12 hour panels for each cell line.

3.11 Localization of AGR2 in MCF-10A Cells

Normally AGR2 is seen localized to the endoplasmic reticulum and may be secreted outside of the cell (Park et al. 2009; Bergström et al. 2014). In the case of AGR2 expression, it is of great interest to determine localization as it has been demonstrated that AGR2 localization impacts its function (Gupta, Dong, and Lowe 2012; Chevet et al. 2013; Tsuji et al. 2014; Fessart et al. 2016; Li et al. 2016). There remains a need to better understand how the cellular or extracellular localization of AGR2 impacts its function as very few studies have addressed this question so far. This study next sought to determine the localization of AGR2 in MCF-10A cells using immunofluorescence microscopy and representative images are shown in Figure 22. Parent MCF-10A cells showed weak to no AGR2 staining (Figure 22 A). While the AGR2-transfected MCF-10A cell line had cells exhibiting the strongest AGR2 staining, there were smaller clusters of cells with this strong staining rather than exhibiting staining throughout the population of cells. The intense staining had a very apparent web-like appearance which was slightly more localized to near the nucleus, indicative of endoplasmic reticulum localization (Figure 22 B). Staining in the As^{3+} and Cd^{2+}-transformed MCF-10A cell lines showed populations of cells with moderate to strong AGR2 staining also consistent with localization to the endoplasmic reticulum (Figure 22 C and D). Overall, these results indicated that AGR2 is mainly localized to the endoplasmic reticulum in each of the MCF-10A cell lines evaluated. No apparent localization of AGR2 to secretory vesicles was seen which would have exhibited a more widespread and punctate staining throughout the cytoplasm. This suggests that AGR2 is mainly localized in the endoplasmic reticulum in MCF-10A cells and likely mainly functioning as a PDI and in endoplasmic reticulum homeostasis.

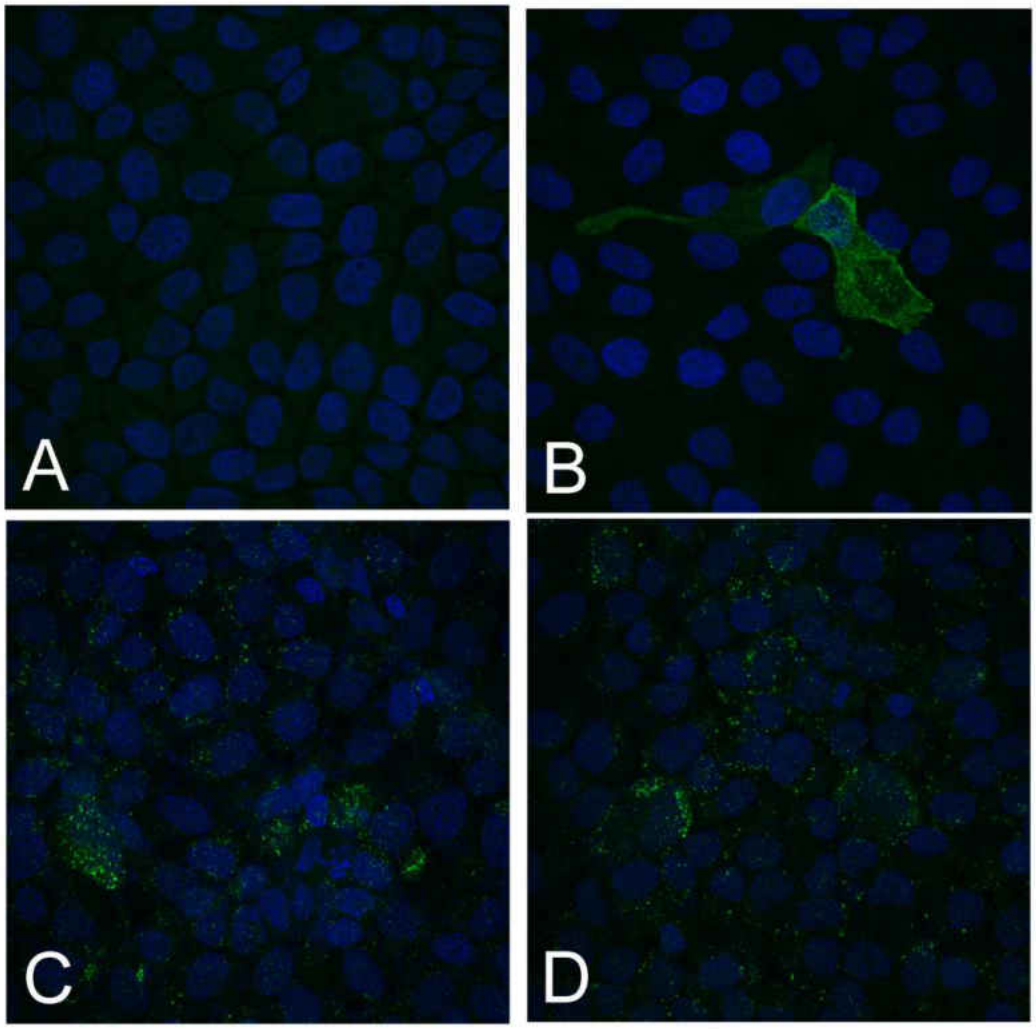

Figure 22 – AGR2 Localization in MCF-10A Cell Lines. Images of AGR2 immunofluorescence in MCF-10A cell lines. **A:** Parent MCF-10A **B:** AGR2-transfected MCF-10A **C:** As^{3+}-transformed MCF-10A **D:** Cd^{2+}-transformed MCF-10A. Blue – DAPI (nuclear) staining, Green – AGR2

3.12 Secretion of AGR2 in MCF-10A Cell Lines

Secretion of AGR2 has been shown to result in the initiation and progression of various cancers, including that of the prostate (Ramachandran et al. 2008) and to promote tumorigenic characteristics in MCF-7 cells (Li et al. 2015; Li et al. 2016). Recently it was demonstrated that AGR2 secretion may serve as a useful biomarker for bladder cancers (Ho et al. 2016). After having determined the cellular localization of AGR2 in MCF-10A

cell line, the next aim was to verify whether AGR2 is secreted in MCF-10A cells. While AGR2 did not appear to be localized to secretory vesicles, this possibility could not be completely discounted. In order to further establish whether AGR2 is secreted, conditioned media and cell monolayers were collected from As^{3+}-transformed and AGR2-transfected MCF-10A cells. Western analysis was performed in order to determine whether AGR2 was secreted and conditioned media from T47D cells was used as a positive control for secreted AGR2. Data indicated that AGR2 is not secreted in any of the MCF-10A cell lines (Figure 23). This suggests that secretion does not have a significant impact on AGR2 function in the MCF-10A cell line.

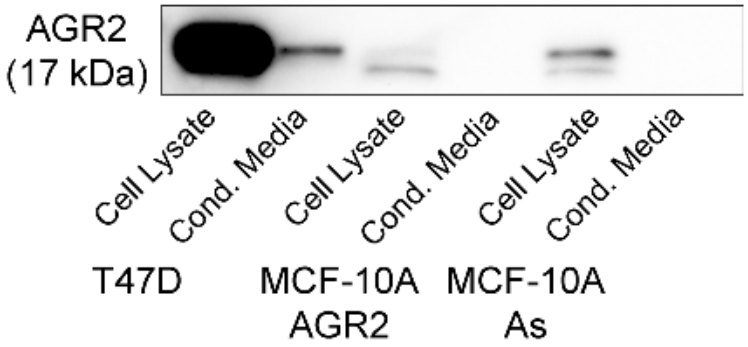

Figure 23 – AGR2 Secretion in MCF-10A cells. Western analysis of AGR2 expression in cell lysate and conditioned media from T47D and MCF-10A cells transfected with AGR2 or transformed by As^{3+}.

3.13 Expression of AGR2 in Breast Cancers

The next goal was to determine the impact of AGR2 in breast cancers and to evaluate whether AGR2 expression correlates with tumor type or grade. A panel of breast cancers archived in paraffin blocks was used for immunohistochemical staining and consisted of ductal carcinoma *in situ* (DCIS) and grade 1, 2, and 3 infiltrating ductal carcinoma (IDC). Ductal carcinoma *in situ* is a subtype of breast cancers in which tumors have arisen inside mammary ducts and has not exhibited invasion out of the duct.

Infiltrating ductal carcinoma, also known as invasive ductal carcinoma, occurs when breast cancers which originated in the mammary duct have progressed through the milk duct and has potential to spread throughout mammary tissues or to metastasize to lymph nodes. Tumors that are determined histologically to be well differentiated are classified as Grade 1. Similarly grade 2 tumors are moderately differentiated and grade 3 represents poorly differentiated tumors (AJCC 2010).

Specimens were stained for AGR2 expression using immunohistochemical techniques in order to determine whether AGR2 expression correlates to stage or progression of breast cancers. Normal breast tissues exhibited AGR2 staining in lobular and ductal epithelial cells, with no observed staining in the surrounding myoepithelial cells (Figure 24 A and B). Low grade DCIS exhibited moderate AGR2 staining while high grade DCIS showed strong staining for AGR2 (Figure 24 C and D). Grade 1 IDCs exhibited moderate to strong AGR2 staining (Figure 24 E and F). Grade 2 IDC exhibited AGR2 staining in tumor cells, either in scattered tumor cells or localized in cancer nests (black arrow) while benign ducts exhibited no AGR2 staining (Figure 25 A and B). One section with both grade 2 IDC and intermediate grade DCIS exhibited strong AGR2 staining in the affected duct (DCIS – white arrow) and in the IDC nests (black arrow) to either side the affected duct. No AGR2 staining was observed in the surrounding myoepithelial cells (Figure 25 C). In benign breast cells from the same slide as Figure 25 C, results showed luminal epithelial cells (black arrow) positive for AGR2 staining while outer myoepithelial cells did not show AGR2 staining (Figure 25 D). Another grade 2 IDC also exhibited strong AGR2 staining in cancer cells (Figure 25 E). One slide of grade 3 IDC exhibited cancer nests (black arrow) strongly positive for AGR2 and which

were moderately positive for AGR2 (Figure 25 F). Another grade 3 IDC exhibited strongly AGR2 stained cancer nests (black arrow) with no AGR2 staining in two benign ducts (white arrows) (Figure 25 G). Diffuse and strong positive AGR2 staining was also seen in another grade 3 IDC (Figure 25 H). In summary, AGR2 staining of at least moderate degree was seen in all tumor samples, as demonstrated in DCIS and Grade 1 IDC (Figure 24). The intensity of staining increased with increasing grades of breast tumors, as seen in grade 2 and 3 IDCs (Figure 25). In most instances, the myoepithelial cells surrounding the tumor did not exhibit significant AGR2 staining. Overall, this data shows that increased AGR2 expression is correlated with higher grades of IDC, suggesting that AGR2 is a biomarker for breast cancers.

The previously mentioned slides were also stained for ERα expression in an attempt to discern whether hormone receptor status may correlate with AGR2 expression and tumor subtype. Table 6 summarizes the results as determined by two pathologists. Nine of the seventeen lesions evaluated demonstrated strong AGR2 and strong ERα staining, with all but one of the grade 3 IDCs exhibiting strong staining for both. Of the seven grade 2 IDCs, four exhibited strong staining for both AGR2 and ERα and two showed moderate staining for both. There was one instance of no to weak staining for both AGR2 and ERα. One of the grade 1 IDC lesions exhibited strong staining for AGR2 and ERα while the other lesion was weakly stained for AGR2 but strongly stained for ERα. Neither the high grade or low grade DCIS lesion evaluated exhibited moderate or strong ERα staining while the high grade DCIS showed strong AGR2 positivity. Benign breast tissue exhibited moderate AGR2 and ERα staining (Table 6). This data suggests

that there may be a correlation between AGR2 expression and the ERα status of the tumor.

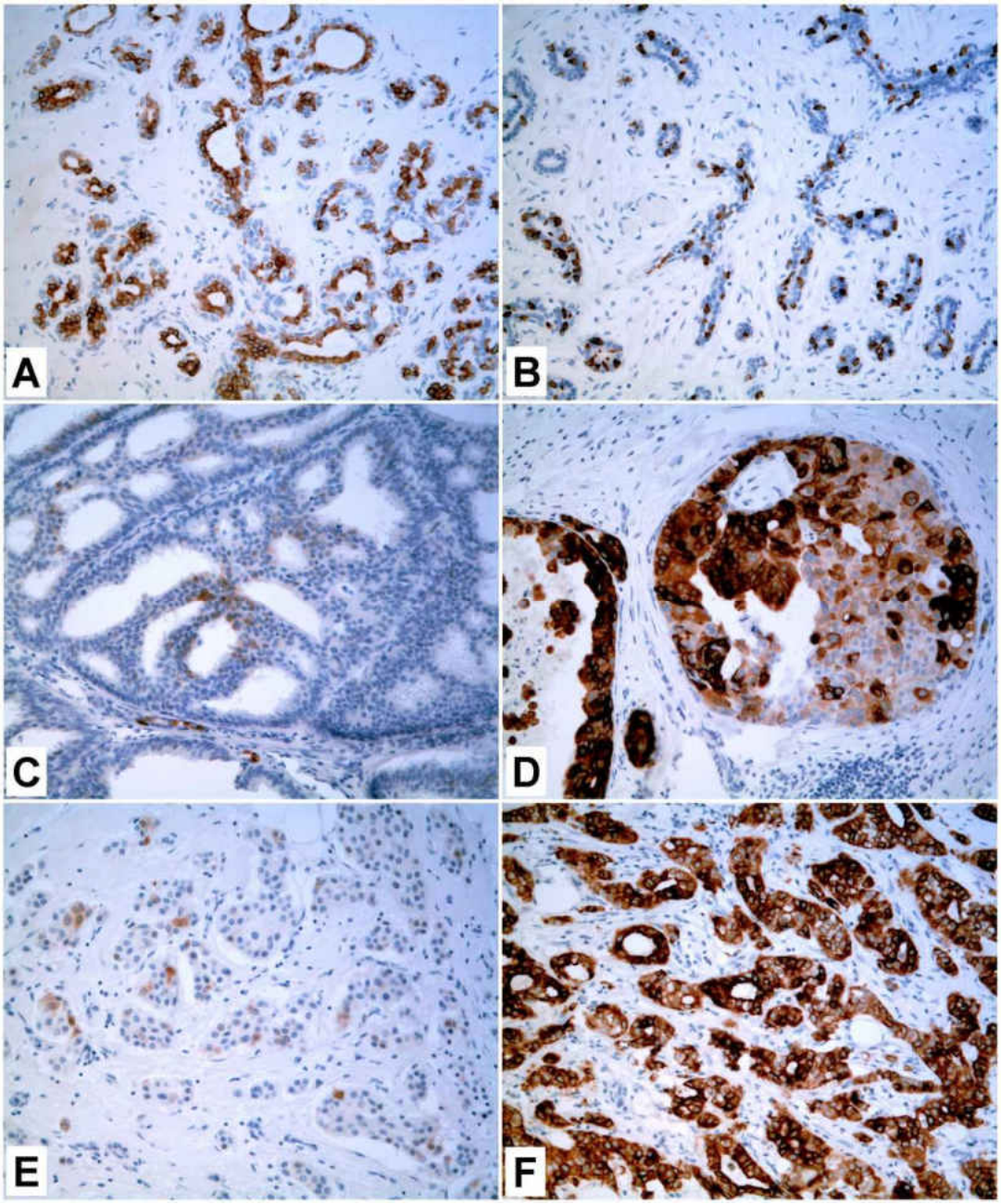

Figure 24 – AGR2 Staining in Benign, DCIS, and Grade 1 Infiltrating Ductal Carcinoma of the Human Breast. A: Human benign breast tissue. **B:** Normal human breast from breast reduction. **C:** Low grade DCIS. **D:** High grade DCIS. **E-F:** Grade 1 IDC.

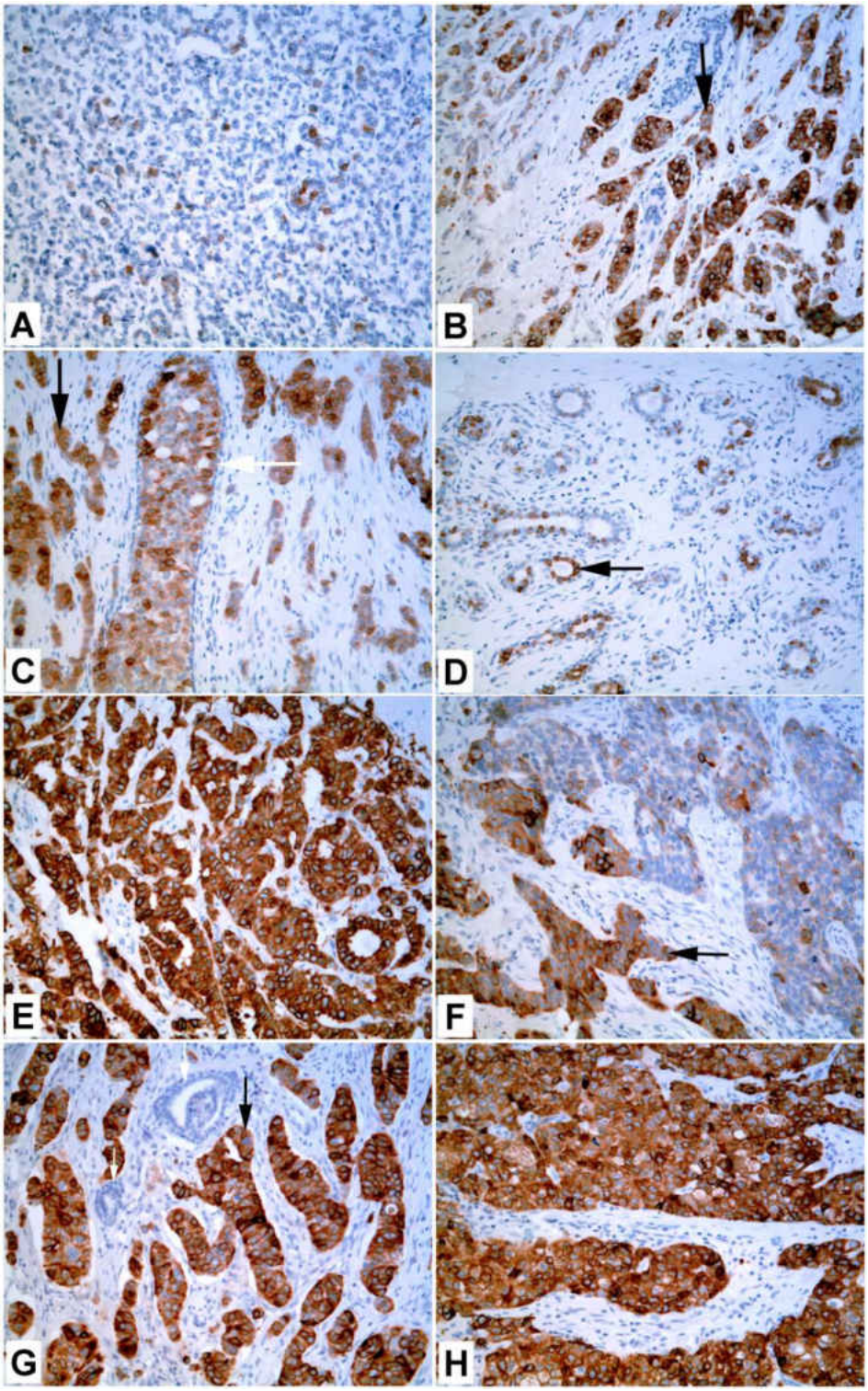

Figure 25 – AGR2 Staining in Grade 2 and 3 Infiltrating Ductal Carcinoma of the Human Breast. A-B: Grade 2 IDCs. **C:** Grade 2 IDC and intermediate grade DCIS. **D:** Benign breast tissue. **E:** Grade 2 IDC. **F-H:** Grade 3 IDCs.

Table 6 – Immunostaining of AGR2 and ERα in Human Breast Carcinomas. Summarizes AGR2 and ERα staining data from DCIS and IDC lesions as seen in Figure 24 and Figure 25. G1 – Grade 1, G2 – Grade 2, G3 – Grade 3, HG – High Grade, LG – Low Grade

	AGR2		ERα	
Lesion	Intensity	%	Intensity	%
IDC-G3	3+	90	3+	90
IDC-G3	3+	90	3+	90
IDC-G3	3+	90	2+	80
IDC-G3	3+	90	2-3+	60
IDC-G3	3+	80	2-3+	80
IDC-G3	2-3+	50	3+	90
IDC-G2	3+	90	3+	90
IDC-G2	3+	90	3+	90
IDC-G2	3+	90	3+	80
IDC-G2	2-3+	80	3+	90
IDC-G2	2-3+	70	2-3+	70
IDC-G2	3+	60	2+	60
IDC-G2	2+	<5	2+	20
IDC-G1	3+	90	3+	90
IDC-G1	2+	20	2-3+	80
DCIS-HG	3+	80	-	-
DCIS-LG	1-2+	10	2+	30
Benign	2-3+	50	3+	50

3.14 Epigenetic Regulation of AGR2 in MCF-10A and Breast Cells

At least one study has demonstrated that AGR2 expression can be regulated by DNA methylation, increasing AGR2 expression and producing more aggressive ovarian cancer phenotypes (Hirst and Marra 2009; Sung et al. 2014). This suggests a possible mechanism for the induction of AGR2 expression in breast cancers. It was therefore decided that it would be beneficial to further investigate epigenetic modifications as a possible mechanism by which As^{3+} could induce AGR2 expression. DNA methylation is considered to be associated with the decreased expression of gene transcription therefore genes regulated by DNA methylation should exhibit increased expression in the presence of DNA methylation inhibitors such as 5'-azacytidine (5-AZC) (Cedar 1988; Hirst and

Marra 2009). Histone deacetylases (HDACs) are responsible for removing acetyl groups from histones, resulting in the repression of gene expression (Struhl 1998). Inhibitors of HDACs, such as Entinostat (MS-275), can be used in an attempt to restore gene expression when regulation occurs via histone acetylation. MCF-10A cells were exposed to 1, 3, or 10 μM MS-275 or either 1 or 3 μM 5-AZC for 72 hours. Data showed increasing AGR2 expression with increasing doses of both HDAC and DMT inhibitors (Figure 26). This suggests that both histone acetylation and DNA methylation play roles in the regulation of AGR2 transcription in MCF-10A cells.

We next sought to determine whether histone acetylation or DNA methylation are also active in regulating AGR2 expression in commercially available breast cancer cell lines. In order to determine whether AGR2 expression is under epigenetic control, MDAMB-231 and Hs578T cells were exposed to 1, 3, or 10 μM MS-275, or either 1 or 3 μM 5'-azacytidine (5-AZC) for 72 hours. Real-time PCR analysis was used to determine AGR2 mRNA expression. Data indicated that AGR2 expression was not as highly induced in MDAMB-231 cells as in MCF-10A cells, suggesting that AGR2 expression is still partially regulated by both histone acetylation and DNA methylation in MDAMB-231 cells (Figure 27 A). Hs578T, cells may be partially regulated by histone acetylation but did not appear to be regulated by DNA methylation (Figure 27 B). Overall, these data suggest that histone acetylation and DNA methylation may have roles in the regulation of AGR2 transcription in various breast cancers. Further study is necessary in order to verify the specific roles that histone acetylation and DNA methylation may play in AGR2 regulation. Both 5-AZC and MS-275 are known to affect global epigenetic regulatory mechanisms as opposed to acting on specific acetylation or methylation sites. Until

further studies are performed, it is possible that the effect of histone acetylation and DNA methylation on AGR2 seen in the data presented in this study represent indirect effects.

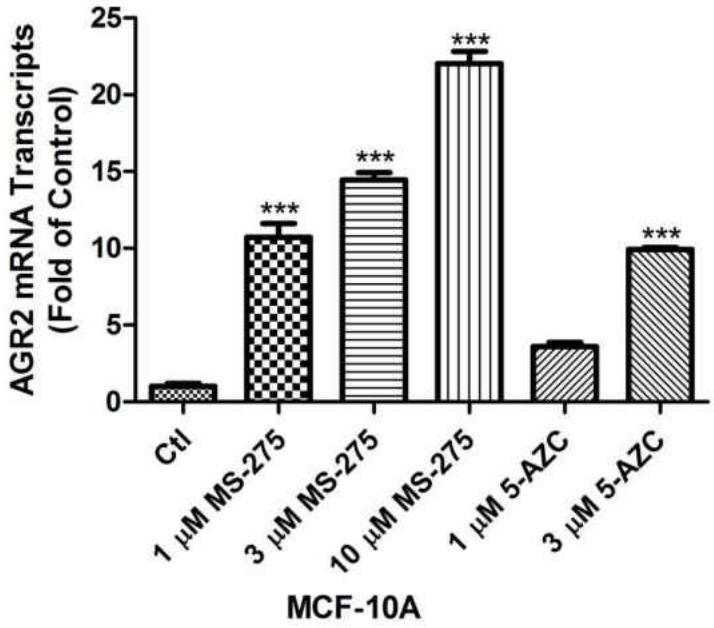

Figure 26 – MCF-10A Expression of AGR2 in Response to MS-275 or 5-AZC. Real-time PCR analysis of AGR2 transcripts in MCF-10A cells exposed to MS-275 (1, 3, or 10 μM) or 5-AZC (1 or 3 μM) for 72 hours. Asterisks denote a statistically significant difference from untreated MCF-10A cells with * ($p < 0.05$), ** ($p < 0.01$) and *** ($p < 0.001$). Real-time data is plotted as the mean ± SEM of triplicate determinations.

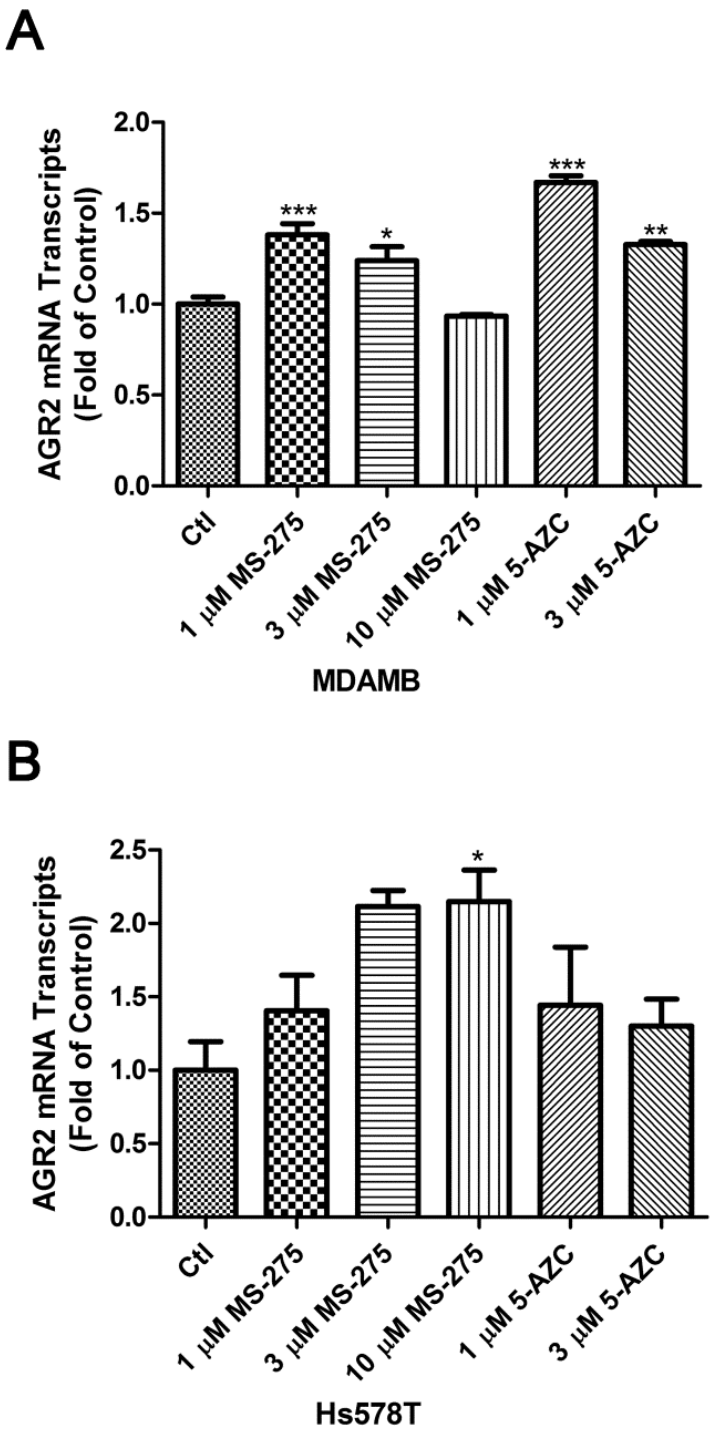

Figure 27 – Expression of AGR2 in Response to MS-275 or 5-AZC in Breast Cancer Cell Lines. Real-time PCR analysis of AGR2 transcripts in **A:** MDAMB and **B:** Hs578T cells exposed to MS-275 (1, 3, or 10 μM) or 5-AZC (1 or 3 μM) for 72 hours. Asterisks denote a statistically significant difference from untreated control (Ctl) cells with * ($p < 0.05$), ** ($p < 0.01$) and *** ($p < 0.001$). Real-time data are plotted as the mean ± SEM of triplicate determinations.

CHAPTER 4

DISCUSSION

4.1 AGR2 in the Bladder

This laboratory has examined the expression of AGR2 in a small set of archival specimens of low grade and high grade urothelial cancers and found benign urothelium and low grade tumors to have the most pronounced expression of AGR2, with high grade non-invasive and high grade invasive cancers having absent or lower expression. This finding is in agreement with the only previous study to examine AGR2 expression in urothelial cancer (Ho et al. 2016). The expression of AGR2 in breast cancer correlates with lower tumor grade, epidermal growth factor receptor negativity, and estrogen receptor alpha (ERα) positivity (Fletcher et al. 2003; Innes et al. 2006). In breast cancer, high AGR2 expression is associated with poor outcome in ERα-positive cancers and hormonally treated breast cancers (Fritzsche et al. 2006; Barraclough et al. 2009; Hrstka et al. 2010; Lacambra et al. 2015). An analysis of AGR2 mRNA expression in prostate cancer also showed AGR2 to be upregulated in all tumors in general compared to benign tissues, but with low grade tumors and prostatic intraepithelial neoplasia (PIN) lesions having the highest expression of AGR2 compared to control (Bu et al. 2011). In addition, transcripts of AGR2 were higher in Gleason score (GSC) 6 tumors when compared to GSC 8-10 tumors, suggesting expression is decreased as grade increases. An analysis of AGR2 expression in three commonly utilized human bladder cancer cell lines showed the greatest expression of AGR2 in the culture isolated from a low grade urothelial cancer.

While in general AGR2 expression appears to be lost or decreased in higher grade tumors, the previous studies in breast, prostate and urothelial cancer also suggested a poor prognosis when AGR2 expression does remain elevated in high grade cancers. In prostate cancer, AGR2 expression has been shown to be elevated in circulating tumor cells in the plasma from patients with metastatic prostate cancer (Kani et al. 2013). Anterior gradient 2 expression in circulating cells was most pronounced in tumors with neuroendocrine or anaplastic features with an aggressive clinical phenotype without elevated circulating prostate specific antigen (PSA) levels. As noted above for breast cancers, high AGR2 expression correlates to a poor prognosis in ERα-positive breast cancers, and as detailed in the introduction, findings in urothelial cancer showed tumor invasion fronts of primary tumors and lymph nodes from many of these primary tumors to express AGR2. The findings in urothelial cancer suggest the hypothesis that AGR2 expression may favor the local spread of the tumor.

In an attempt to gain insight into AGR2 expression in urothelial cancer, AGR2 expression was explored employing As^{3+} and Cd^{2+}-transformed UROtsa cells since the expression of AGR2 could be examined during cell transformation *in vitro* and in *in vivo* tumor transplants derived from these cells. Overall, the expression of AGR2 in the independent isolates of the As^{3+} and Cd^{2+}-transformed cells and derived tumors was highly variable. The expression of AGR2 mRNA and protein was variable within the independent isolates of the As^{3+} and Cd^{2+}-transformed cell lines, with five of six of the Cd^{2+} and four of seven of the As^{3+}-transformed cell lines having mRNA levels significantly elevated over control. The corresponding expression of the AGR2 protein only weakly followed the AGR2 mRNA levels, with only modest elevations of protein in

four of the six As^{3+} and in six of the seven Cd^{2+}-transformed cell lines. The expression of AGR2 mRNA and protein was also highly variable in the tumor transplants and AGR2 expression showed little or no relationship to the amount of AGR2 expressed in the initiating cell line. The % of AGR2 staining cells in the tumor transplants from the independently generated As^{3+} and Cd^{2+}-transformed UROtsa cell lines varied from 5 to 70%. This demonstrates the ability of As^{3+} and Cd^{2+} to stimulate AGR2 expression in urothelial cells.

This complements studies that have demonstrated the ability of AGR2 to have a role in stimulating tumor cell proliferation and metastasis as well as studies that have demonstrated the ability of AGR2 to impact the formation of xenograft tumors. One study demonstrated the potential for AGR2 to induce metastasis and tumor formation when transfection of a construct containing a cDNA sequence identical to that of AGR2 into Rama 37 rat mammary cells promoted a metastatic phenotype when injected in syngeneic rats (Liu et al. 2005). Anterior gradient 2 was also demonstrated to increase migration and xenograft tumor growth in two esophageal adenocarcinoma cell lines using both *in vitro* and *in vivo* assays (Wang, Hao, and Anson W. Lowe 2008). Another set of *in vitro* studies found that silencing of secreted AGR2 is capable of decreasing the ability of prostate cancer cells to grow, survive, and undergo invasion, suggesting that AGR2 plays a role in these cellular functions in prostate cancer (Ramachandran et al. 2008). Similarly, another group demonstrated that knockdown of AGR2 expression in cell lines isolated from ERα-positive breast cancers reduced the ability of the cell lines to grow, progress through the cell cycle, and undergo anchorage-independent growth (Vanderlaag et al. 2010). More recent studies have also demonstrated that IGF-1 can induce AGR2

expression and that exposure to extracellular AGR2 can stimulate increased growth, migration, and progression through the cell cycle as well as EMT in MCF-7 cells (Li et al. 2015; Li et al. 2016).

In an attempt to define a reason for the above heterogeneity in AGR2 expression, AGR2 was determined in CICs isolated as spheroids from the individual cell lines. As detailed in the results the spheroids fulfill the requirement to be defined as CICs. The results show that CICs isolated from the As^{3+} and Cd^{2+}-transformed cell lines all have expression, be it variable, of AGR2 mRNA. This appears to be one of the first observations that AGR2 is expressed in CICs isolated from transformed cells in culture. In addition, the tumors derived from the CICs isolated from two each of the As^{3+} and Cd^{2+}-transformed cell lines demonstrated moderate to strong staining of AGR2 in 20 to 30% of the cells. Taken together the findings suggest the following evolution of AGR2 expression from cell culture to tumor transplants. First, the expression of AGR2 mRNA and protein in the As^{3+} and Cd^{2+}-transformed cell cultures, while interesting, probably has very little to do with the subsequent expression of AGR2 in the tumor transplants. The rationale being that the expression of AGR2 is dictated by the small sub-population of CICs and not the overall AGR2 signature of the entire culture. In the two previous studies with CICs from the As^{3+} and Cd^{2+}-transformed cells, the expression in the tumor transplant recapitulated the expression in the CICs and not the entire culture (Sandquist et al. 2016; Slusser-Nore et al. 2016). This suggests that the tumor transplants are initiated by CICs that express the AGR2 gene. One may also speculate that AGR2 might enhance tumor initiation since AGR2 expression has been suggested in an analysis of clinical specimens to assist the local invasion of urothelial cancer cells (Ho et al. 2016).

Second, the expression pattern of AGR2 in tumor cells within the tumor transplants would be consistent with AGR2 being present at the early stages of tumor growth and then becoming dormant as the tumor undergoes differentiation into higher grade tumor cells. This is suggested by the fact that previous studies have shown tumor transplants derived from these cell lines undergo squamous differentiation, producing a tumor with a more undifferentiated cell population and one comprised of cells with squamous character (Sens et al. 2004; Cao et al. 2010; Somji et al. 2010). Squamous differentiation in urothelial cancer is associated with a poor prognosis (Logothetis et al. 1989; Martin, Jenkins, and Zuk 1989; Akdaš and Türkeri 1991; Frazier et al. 1993). In the present study the differentiated squamous components of the tumor transplants were negative for the expression of AGR2 while the more undifferentiated components stained positive for AGR2. These observations are consistent with AGR2-expressing CICs initiating the tumor transplant, undergoing initial proliferation to form the tumor, and a loss of AGR2 as the tumor differentiates/progresses to a higher grade, more aggressive cell type. What the study does not answer is if the undifferentiated AGR2 staining component is driving continued tumor growth or if the AGR2 positive cells would disappear from the tumor if growth was continued by serial passage. Overall, the results show that CICs derived from the UROtsa model system provide are useful in helping to define the role of AGR2 expression from tumor initiation through serial transplant of the tumor, which could eventually further the study of tumor initiation and metastasis to other organ sites.

4.2 AGR2 in the Breast

Breast cancer has become a focus for cancer research and represents one of the greatest health concerns for women in developed countries. One area of breast cancer research warranting further study is the significance of AGR2 expression in the breast. Even with recent advances, there remains a need to discover more accurate and informative biomarkers for breast cancers, not only to aid in early detection but to allow for more informed treatment decisions based on biomarkers which might more accurately predict a given patient's prognosis. Previously this lab has observed that the proto-oncogene AGR2 exhibits increased expression following As^{3+} or Cd^{2+}-transformation of UROtsa cells, based on microarray analysis (Garrett et al. 2014). This prompted the further evaluation and characterization of AGR2 expression in a model of As^{3+} and Cd^{2+}-induced breast cancers which was created using the MCF-10A breast epithelial cell line. Preliminary experiments demonstrated that AGR2 expression increases following transformation of MCF-10A cells with As^{3+} and that AGR2 expression is induced by exposure to As^{3+} in MCF-10A cells. These results add to previous studies linking As^{3+} exposure to breast cancer risk (Xu, Erik J Tokar, and Waalkes 2014).

A possible connection of AGR2 expression to ERα status is also of interest as AGR2 expression has previously been shown to be responsive to the presence of estrogen and ERα (Thompson and Weigel 1998; Innes et al. 2006; Salmans, Zhao, and Andersen 2013). For example, it has been previously established that AGR2 expression predicts poor prognosis when highly expressed in ERα-positive breast cancers (Barraclough et al. 2009; Hrstka et al. 2010; Lacambra et al. 2015). Other experiments have also indicated that AGR2 exhibits expression and functions that are independent of ERα status, though

this area has not been well studied (Hrstka et al. 2010). In this study, AGR2 expression was demonstrated in the ERα-positive T47D and MCF-7 cell lines and in the ERα-negative MDAMB cell line, indicating that AGR2 expression is common in some subtypes of breast cancers. In this study it was further demonstrated that ERα is not highly expressed in the MCF-10A cell lines, showing that As^{3+} and Cd^{2+}-transformed MCF-10A cells remained ERα-negative. This suggests that any effect seen as a result of AGR2 expression in transformed MCF-10A cells may be due to ERα-independent mechanisms or functions. This also suggests an explanation for why AGR2 functions and responses in the MCF-10A model may differ from what has been previously demonstrated in literature involving AGR2.

Anterior gradient 2 expression has previously been known to impact cell functions with potential to contribute to both tumorigenesis and to the progression of cancers, particularly metastasis (Liu et al. 2005; Wang, Hao, and Anson W. Lowe 2008; Park et al. 2011; Tsuji et al. 2014; Li et al. 2015; Fessart et al. 2016; Li et al. 2016). In breast and other cancers, AGR2 expression has also been shown to enable cancer progression and tumor cell survival (Vanderlaag et al. 2010; Dumartin et al. 2011; Brychtova et al. 2014). Here this study has demonstrated that As^{3+}-transformation is capable of increasing cell growth and migration in MCF-10A cells, suggesting that As^{3+} exposure can lead to cellular responses which may result in tumorigenesis or metastasis. While not fully established in this study, data suggest the possibility that the mechanism by which this process occurs could involve the induction of AGR2 expression as this study demonstrated the ability of As^{3+} to induce AGR2 expression. In this study, it was shown that AGR2 overexpression itself can induce cell proliferation and motility in

MCF-10A cells transfected with the AGR2 gene. This suggests a role for AGR2 in conferring properties to breast epithelia which have been known to contribute to tumor formation, progression, and metastasis (Wang, Hao, and Anson W. Lowe 2008; Di Maro et al. 2014). In short, the induction of AGR2 expression, by As^{3+} among other means, may stimulate growth in breast epithelia resulting in tumor formation and eventual metastasis.

The present study has demonstrated that AGR2 is localized mainly to the endoplasmic reticulum in the MCF-10A cell lines, which is consistent with the previously established AGR2 role as a PDI in breast epithelia. Functioning as a PDI, responding to endoplasmic reticulum stress, is the most well-understood role which has been established so far for AGR2 in previous studies (Higa et al. 2011). As part of its ability to function as a PDI, it has been shown that AGR2 can be secreted when the KTEL endoplasmic reticulum retention sequence is lost (Park et al. 2009; Gupta, Dong, and Lowe 2012; Bergström et al. 2014). This prompted the determination of whether or not AGR2 is being secreted in the MCF-10A model. Data revealed that AGR2 is not secreted by MCF-10A cells, even when AGR2 expression is increased due to As^{3+}-transformation or AGR2 transfection into the cell. These data further suggest that AGR2 is primarily functioning within the endoplasmic reticulum in MCF-10A cells.

Previous work has established that AGR2 expression is a predictor of poor prognosis in breast cancers and is associated mainly with more advanced breast cancers (Fritzsche et al. 2006; Barraclough et al. 2009; Hrstka et al. 2010). Evaluation of AGR2 expression in breast carcinoma specimens of low and high grade DCISs and grade 1, 2, and 3 IDCs demonstrated that AGR2 expression correlates to tumor grade with the

strongest staining seen in the higher grades of IDC. This strengthens the data supporting AGR2 expression as a useful biomarker for advanced breast cancers.

Little is known regarding the mechanisms that regulate AGR2 expression at this time. If the regulation of AGR2 were better understood, it could lead to potential targets for future cancer therapies aimed at inhibiting the progression or metastasis of AGR2 expressing cancers. As this project has demonstrated that As^{3+} exposure can induce AGR2 expression in MCF-10A cells, a potential mechanism by which AGR2 expression is regulated was evaluated. One potential regulatory mechanism for gene expression that has been previously associated with AGR2 expression involves DNA methylation (Sung et al. 2014). Another common mechanism for the epigenetic regulation of gene expression involves histone acetylation (Struhl 1998). After evaluating AGR2 expression in response to a HDAC inhibitor (MS-275) and an inhibitor of DNA methylation (5-AZC), data reveal that AGR2 expression in MCF-10A cells is regulated, at least partially, by these epigenetic mechanisms.

From this study, a picture begins to form which allows for an improved level of understanding regarding AGR2 expression and regulation, particularly in relation to those functions with the potential to affect cancers of the bladder and breast. It is possible that As^{3+} exposure induces AGR2, potentially through epigenetic means such as histone acetylation and DNA methylation. This induction of AGR2 in turn may stimulate the formation, proliferation, and eventual migration of affected epithelial cells in the breast or bladder, among others. This study demonstrates the potential usefulness of further research aimed at increasing the current understanding of the regulation and involvement of AGR2 expression in breast and bladder cancers.

ABBREVIATIONS

5-AZC	5'-azacytidine
AGR2	human Anterior Gradient 2 homolog
AKT	Protein Kinase B
ALDH1	Aldehyde Dehydrogenase 1
ANOVA	Analysis of Variance
AP-1	Activator Protein 1
AREG	Amphiregulin
As^{3+}	Arsenite
ATCC	American Type Culture Collection
ATF6	Activating Transcription Factor 6
BCG	*Bacillus Calmette-Guerin*
Cd^{2+}	Cadmium
$CdCl_2$	Cadmium Chloride
CDH1	Epithelial-cadherin
CDH2	Neuronal-cadherin
cDNA	Complementary Deoxyribonucleic Acid
CI	Confidence Interval
CICs	Cancer Initiating Cells
CIS	Carcinoma *in Situ*
CO_2	Carbon Dioxide

DAB	3,3’-diaminobenzidine
DMA	Dimethyl Arsenic
DMEM	Dulbecco’s Modified Eagle Medium
DMT	DNA Methyl-transferase
DNA	Deoxyribonucleic Acid
DTT	Dithiothreitol
EDTA	Ethylenediaminetetraacetic Acid
EGF	Epidermal Growth Factor
EGFR	Epidermal Growth Factor Receptor
EMT	Epithelial to Mesenchymal Transition
ER	Endoplasmic Reticulum
ERα	Estrogen Receptor Alpha
ErbB3	Receptor Tyrosine Protein Kinase erbB-3
ERE	Estrogen Response Element
ERK	Extracellular Signal-related Kinase
ESR1	Estrogen Receptor Alpha
FBS	Fetal Bovine Serum
GSC	Gleason Score
GSH	Glutathione
HDAC	Histone Deacetylase
HER2	Human Epidermal Growth Factor Receptor 2
hrs	Hours
IARC	International Agency for Research on Cancer

iAs	Inorganic Arsenic
IDC	Infiltrative Ductal Carcinoma
IGF-1	Insulin-like Growth Factor 1
IHC	Immunohistochemistry
I.O.D.	Integrated Optical Density
IRE1	Inositol Requiring 1
MAPK	Mitogen Activated Protein Kinase
MET	Mesenchymal to Epithelial Transition
µl	Microliter
µM	Micromolar
ml	Milliliter
min	Minute
MMA	Monomethyl Arsenic
MRI	Magnetic Resonance Imaging
mRNA	Messenger Ribonucleic Acid
MS-275	Entinostat
mTOR	Mammalian Target of Rapamycin
MTT	Thiazoyl Blue Tetrazodium Bromide
MUC2	Mucin
$NaAsO_2$	Sodium Arsenite
nM	Nanomolar
O.D.	Optical Density
OR	Odds Ratio

PBS	Phosphate Buffered Saline
PCR	Polymerase Chain Reaction
PDI	Protein Disulfide Isomerase
PERK	Protein Kinase-Like Endoplasmic Reticulum Kinase
PIN	Prostatic Intraepithelial Neoplasia
PR	Progesterone Receptor
PRK	Protein Kinase
PSA	Prostate Specific Antigen
PVDF	Polyvinylidene Difluoride
RCF	Relative Centrifugal Force
RNA	Ribonucleic Acid
RT-PCR	Real-time Polymerase Chain Reaction
SDS	Sodium Dodecyl Sulfate
SDS-PAGE	Sodium Dodecyl Sulfate Polyacrylamide Gel Electrophoresis
SEM	Standard Error of the Mean
siRNA	Small Interfering Ribonucleic Acid
TURBT	Transurethral Resection of Bladder Tumor
VIM	Vimentin
YAP1	Yes-Associated Protein 1

REFERENCES

Aberger F, Weidinger G, Grunz H, Richter K. 1998. Anterior specification of embryonic ectoderm: the role of the Xenopus cement gland-specific gene XAG-2. Mech. Dev. [Internet] 72:115–130. Available from: http://www.sciencedirect.com/science/article/pii/S0925477398000215

Ademuyiwa FO, Cyr A, Ivanovich J, Thomas MA. 2015. Managing breast cancer in younger women: Challenges and solutions. Breast Cancer Targets Ther. 8:1–12.

AJCC. 2010. AJCC Cancer Staging Manual. 7th Editio. New York, NY: Springer.

Akdaš A, Türkeri L. 1991. The impact of squamous metaplasia in transitional cell carcinoma of the bladder. Int. Urol. Nephrol. [Internet] 23:333–336. Available from: http://link.springer.com/10.1007/BF02549603

Anderson BO, Lipscomb J, Murillo RH, Thomas DB. 2015. Breast Cancer. In: Gelband H, Jha P, Sankaranarayanan R, Horton S, editors. Disease Control Priorities. 3rd Editio. World Bank Group. p. 45–68.

Arita A, Costa M. 2009. Epigenetics in metal carcinogenesis: Nickel, Arsenic, Chromium and Cadmium. Metallomics:222–228.

Bakhshaiesh TO, Armat M, Shanehbandi D, Sharifi S, Baradaran B, Hejazi MS, Samadi N. 2015. Arsenic Trioxide Promotes Paclitaxel Cytotoxicity in Resistant Breast Cancer Cells. Asian Pac. J. Cancer Prev. [Internet] 16:5191–7. Available from: http://www.ncbi.nlm.nih.gov/pubmed/26225652

Barraclough DL, Platt-Higgins A, de Silva Rudland S, Barraclough R, Winstanley J, West CR, Rudland PS. 2009. The metastasis-associated anterior gradient 2 protein is correlated with poor survival of breast cancer patients. Am. J. Pathol. [Internet] 175:1848–57. Available from: http://www.pubmedcentral.nih.gov/articlerender.fcgi?artid=2774050&tool=pmcentrez&rendertype=abstract

Bergström JH, Berg KA, Rodríguez-Piñeiro AM, Stecher B, Johansson ME V, Hansson GC. 2014. AGR2, an endoplasmic reticulum protein, is secreted into the gastrointestinal mucus. PLoS One [Internet] 9:e104186. Available from: http://www.pubmedcentral.nih.gov/articlerender.fcgi?artid=4128659&tool=pmcentrez&rendertype=abstract

Bischoff CJ, Clark PE. 2009. Bladder cancer. Curr. Opin. Oncol. [Internet] 21:272–277. Available from: http://www.sciencedirect.com/science/article/pii/S0140673609604918\nhttp://www.sciencedirect.com/science/article/pii/S0140673609604918/pdfft?md5=ddf05e50705b25ace7e436fba10c30a7&pid=1-s2.0-S0140673609604918-main.pdf

Brychtova V, Hermanova M, Karasek P, Lenz J, Selingerova I, Vojtesek B, Kala Z, Hrstka R. 2014. Anterior gradient 2 and mucin 4 expression mirrors tumor cell differentiation in pancreatic adenocarcinomas, but aberrant anterior gradient 2 expression predicts worse patient outcome in poorly differentiated tumors. Pancreas [Internet] 43:75–81. Available from: http://www.ncbi.nlm.nih.gov/pubmed/24177142

Bu H, Bormann S, Schäfer G, Horninger W, Massoner P, Neeb A, Lakshmanan V-K, Maddalo D, Nestl A, Sültmann H, et al. 2011. The anterior gradient 2 (AGR2) gene is overexpressed in prostate cancer and may be useful as a urine sediment marker for prostate cancer detection. Prostate [Internet] 71:575–87. Available from: http://www.ncbi.nlm.nih.gov/pubmed/20945500

Byrne C, Divekar SD, Storchan GB, Parodi DA, Martin MB. 2013. Metals and breast cancer. J. Mammary Gland Biol. Neoplasia 18:63–73.

Cao L, Zhou XD, Sens MA, Garrett SH, Zheng Y, Dunlevy JR, Sens DA, Somji S. 2010. Keratin 6 expression correlates to areas of squamous differentiation in multiple independent isolates of As+3-induced bladder cancer. J. Appl. Toxicol. 30:416–430.

Carter DE, Aposhian HV, Gandolfi AJ. 2003. The metabolism of inorganic arsenic oxides, gallium arsenide, and arsine: a toxicochemical review. Toxicol. Appl. Pharmacol. [Internet] 193:309–334. Available from: http://linkinghub.elsevier.com/retrieve/pii/S0041008X0300351X

Cedar H. 1988. DNA methylation and gene activity. Cell 53:3–4.

Chevet E, Fessart D, Delom F, Mulot A, Vojtesek B, Hrstka R, Murray E, Gray T, Hupp T. 2013. Emerging Roles for the Pro-Oncogenic Anterior Gradient-2 in Cancer Development. Oncogene 32:2799–2509.

Clarke C, Rudland P, Barraclough R. 2015. The metastasis-inducing protein AGR2 is O-glycosylated upon secretion from mammary epithelial cells. Mol. Cell. Biochem. [Internet] 408:245–252. Available from: http://www.ncbi.nlm.nih.gov/pubmed/26169982

Cohen SM, Arnold LL, Beck BD, Lewis AS, Eldan M. 2013. Evaluation of the carcinogenicity of inorganic arsenic. Crit. Rev. Toxicol. [Internet] 43:711–52. Available from: http://www.ncbi.nlm.nih.gov/pubmed/24040994

Darb-Esfahani S, Fritzsche F, Kristiansen G, Weichert W, Sehouli J, Braicu I, Dietel M, Denkert C. 2012. Anterior gradient protein 2 (AGR2) is an independent prognostic factor in ovarian high-grade serous carcinoma. Virchows Arch. [Internet] 461:109–16. Available from: http://www.ncbi.nlm.nih.gov/pubmed/22752467

Davey JC, Bodwell JE, Gosse JA, Hamilton JW. 2007. Arsenic as an endocrine disruptor: Effects of arsenic on estrogen receptor-mediated gene expression in vivo and in cell culture. Toxicol. Sci. 98:75–86.

Desantis C, Siegel R, Bandi P, Jemal A. 2011. Breast Cancer Statistics , 2011. Cancer 61:409–418.

Dong A, Gupta A, Pai RK, Tun M, Lowe AW. 2011. The human adenocarcinoma-associated gene, AGR2, induces expression of Amphiregulin through hippo pathway co-activator YAP1 activation. J. Biol. Chem. 286:18301–18310.

Droller MJ. 1998. Bladder Cancer : State-of-the-Art Care. 48:269–284.

Dumartin L, Whiteman HJ, Weeks ME, Hariharan D, Dmitrovic B, Iacobuzio-Donahue C a, Brentnall T a, Bronner MP, Feakins RM, Timms JF, et al. 2011. AGR2 is a novel surface antigen that promotes the dissemination of pancreatic cancer cells through regulation of cathepsins B and D. Cancer Res. [Internet] 71:7091–102. Available from: http://www.pubmedcentral.nih.gov/articlerender.fcgi?artid=3541941&tool=pmcentrez&rendertype=abstract

Ernst P, Theriault G. 1984. Known occupational carcinogens and their significance. Can Med Assoc J 130:863–867.

Feki-Tounsi M, Hamza-Chaffai A. 2014. Cadmium as a possible cause of bladder cancer: a review of accumulated evidence. Environ. Sci. Pollut. Res. 21:10561–10573.

Feki-Tounsi M, Olmedo P, Gil F, Khlifi R, Mhiri MN, Rebai A, Hamza-Chaffai A. 2013. Cadmium in blood of Tunisian men and risk of bladder cancer: Interactions with arsenic exposure and smoking. Environ. Sci. Pollut. Res. 20:7204–7213.

Fessart D, Domblides C, Avril T, Eriksson LA, Begueret H, Pineau R, Malrieux C, Dugot-Senant N, Lucchesi C, Chevet E, et al. 2016. Secretion of protein disulphide isomerase AGR2 confers tumorigenic properties. Elife [Internet] 5:1–24. Available from: http://elifesciences.org/lookup/doi/10.7554/eLife.13887

Fletcher GC, Patel S, Tyson K, Adam PJ, Schenker M, Loader J a, Daviet L, Legrain P, Parekh R, Harris a L, et al. 2003. hAG-2 and hAG-3, human homologues of genes involved in differentiation, are associated with oestrogen receptor-positive breast tumours and interact with metastasis gene C4.4a and dystroglycan. Br. J. Cancer [Internet] 88:579–85. Available from: http://www.pubmedcentral.nih.gov/articlerender.fcgi?artid=2377166&tool=pmcentrez&rendertype=abstract

Fourtouna A, Murray E, Nicholson J, Maslon MM, Pang LY, Dryden DTF, Hupp TR. 2009. The Anterior Gradient-2 Pathway as a Model for Developing Peptide-Aptamer Anti-Cancer Drug Leads that Stimulate p53 Function. Curr. Chem. Biol. 3:124–137.

Frazier HA, Robertson JE, Dodge RK, Paulson DF. 1993. The value of pathologic factors in predicting cancer-specific survival among patients treated with radical cystectomy for transitional cell carcinoma of the bladder and prostate. Cancer 71:3993–4001.

Fritzsche FR, Dahl E, Pahl S, Burkhardt M, Luo J, Mayordomo E, Gansukh T, Dankof A, Knuechel R, Denkert C, et al. 2006. Prognostic relevance of AGR2 expression in breast cancer. Clin. Cancer Res. [Internet] 12:1728–34. Available from: http://www.ncbi.nlm.nih.gov/pubmed/16551856

Garrett SH, Somji S, Sens DA, Zhang KK. 2014. Prediction of the number of activated genes in multiple independent Cd +2- And As+3-induced malignant transformations of human urothelial cells (UROtsa). PLoS One 9:1–8.

Guilbert C, Annis MG, Dong Z, Siegel PM, Miller WH, Mann KK. 2013. Arsenic trioxide overcomes rapamycin-induced feedback activation of akt and erk signaling to enhance the anti-tumor effects in breast cancer. PLoS One 8:1–12.

Gupta A, Dong A, Lowe AW. 2012. AGR2 gene function requires a unique endoplasmic reticulum localization motif. J. Biol. Chem. [Internet] 287:4773–82. Available from: http://www.pubmedcentral.nih.gov/articlerender.fcgi?artid=3281655&tool=pmcentrez&rendertype=abstract

Hartwig A. 2013. Cadmium and Cancer. In: Sigel A, Sigel H, Sigel RK, editors. Cadmium: From Toxicity to Essentiality. Vol. 11. Metal Ions in Life Sciences. Dordrecht: Springer Netherlands. p. 491–507. Available from: http://link.springer.com/10.1007/978-94-007-5179-8

Hengel SM, Murray E, Langdon S, Hayward L, O'Donoghue J, Panchaud A, Hupp T, Goodlett DR. 2011. Data-independent proteomic screen identifies novel tamoxifen agonist that mediates drug resistance. J. Proteome Res. [Internet] 10:4567–78. Available from: http://www.pubmedcentral.nih.gov/articlerender.fcgi?artid=3242698&tool=pmcentrez&rendertype=abstract

Higa A, Mulot A, Delom F, Bouchecareilh M, Nguyên DT, Boismenu D, Wise MJ, Chevet E. 2011. Role of pro-oncogenic protein disulfide isomerase (PDI) family member anterior gradient 2 (AGR2) in the control of endoplasmic reticulum homeostasis. J. Biol. Chem. [Internet] 286:44855–68. Available from: http://www.pubmedcentral.nih.gov/articlerender.fcgi?artid=3248018&tool=pmcentrez&rendertype=abstract

Hirst M, Marra M a. 2009. Epigenetics and human disease. Int. J. Biochem. Cell Biol. [Internet] 41:136–46. Available from: http://www.ncbi.nlm.nih.gov/pubmed/18852064

Ho ME, Quek S, True LD, Seiler R, Bagryanova L, Kim SR, Chia D, Goodglick L, Shimizu Y, Rosser CJ, et al. 2016. Bladder cancer cells secrete while normal bladder cells express but do not secrete AGR2. Oncotarget 7:15747–15756.

Hrstka R, Nenutil R, Fourtouna a, Maslon MM, Naughton C, Langdon S, Murray E, Larionov a, Petrakova K, Muller P, et al. 2010. The pro-metastatic protein anterior gradient-2 predicts poor prognosis in tamoxifen-treated breast cancers. Oncogene [Internet] 29:4838–4847. Available from: http://www.ncbi.nlm.nih.gov/pubmed/20531310

Innes HE, Liu D, Barraclough R, Davies MP a, O'Neill P a, Platt-Higgins a, de Silva Rudland S, Sibson DR, Rudland PS. 2006. Significance of the metastasis-inducing protein AGR2 for outcome in hormonally treated breast cancer patients. Br. J. Cancer [Internet] 94:1057–65. Available from: http://www.pubmedcentral.nih.gov/articlerender.fcgi?artid=2361240&tool=pmcentrez&rendertype=abstract

Jacobs, B.L., Lee, C.T., Montie JE. 2010. Bladder Cancer in 2010. CA Cancer J Clin 60:244–72.

Jemal A, Siegel R, Ward E, Hao Y, Xu J, Thun MJ. 2009. Cancer Statistics , 2009 BOTH SEXES FEMALE BOTH SEXES ESTIMATED DEATHS. CA Cancer J Clin 59:1–25.

Johansson SL, Cohen SM. 1997. Epidemiology and etiology of bladder cancer. Semin. Surg. Oncol. [Internet] 13:291–8. Available from: http://www.ncbi.nlm.nih.gov/pubmed/9259084

Jomova K, Jenisova Z, Feszterova M, Baros S, Liska J, Hudecova D, Rhodes CJ, Valko M. 2011. Arsenic: toxicity, oxidative stress and human disease. J. Appl. Toxicol. [Internet] 31:95–107. Available from: http://www.ncbi.nlm.nih.gov/pubmed/21321970

Kamińska M, Ciszewski T, Łopacka-Szatan K, Miotła P, Starosławska E. 2015. Breast cancer risk factors. Przegląd menopauzalny = Menopause Rev. [Internet] 14:196–202. Available from: http://www.pubmedcentral.nih.gov/articlerender.fcgi?artid=4612558&tool=pmcentrez&rendertype=abstract

Kani K, Malihi PD, Jiang Y, Wang H, Wang Y, Ruderman DL, Agus DB, Mallick P, Gross ME. 2013. Anterior gradient 2 (AGR2): blood-based biomarker elevated in metastatic prostate cancer associated with the neuroendocrine phenotype. Prostate [Internet] 73:306–15. Available from: http://www.ncbi.nlm.nih.gov/pubmed/22911164

Kellen E, Zeegers MP, Hond E Den, Buntinx F. 2007. Blood cadmium may be associated with bladder carcinogenesis: The Belgian case-control study on bladder cancer. Cancer Detect. Prev. 31:77–82.

Kim JH, Choi HJ, Kim B, Kim MH, Lee JM, Kim IS, Lee MH, Choi SJ, Kim K Il, Kim S-I, et al. 2006. Roles of sumoylation of a reptin chromatin-remodeling complex in cancer metastasis. Nat. Cell Biol. 8:631–639.

Kitchin KT, Wallace K. 2008. The role of protein binding of trivalent arsenicals in arsenic carcinogenesis and toxicity. J. Inorg. Biochem. 102:532–539.

Klaassen CD, Liu J, Choudhuri S. 1999. Metallothionein: an intracellular protein to protect against cadmium toxicity. Annu. Rev. Pharmacol. Toxicol. [Internet] 39:267–94. Available from: http://www.ncbi.nlm.nih.gov/pubmed/10331085

Klaassen CD, Liu J, Diwan BA. 2009. Metallothionein protection of cadmium toxicity. Toxicol. Appl. Pharmacol. [Internet] 238:215–220. Available from: http://dx.doi.org/10.1016/j.taap.2009.03.026

Lacambra MD, Tsang JYS, Ni Y-B, Chan S-K, Tan PH, Tse GM. 2015. Anterior Gradient 2 is a Poor Outcome Indicator in Luminal Breast Cancer. Ann. Surg. Oncol. [Internet] 22:3489–3496. Available from: http://link.springer.com/10.1245/s10434-015-4420-8

Lamm DL. 1998. Bladder cancer: twenty years of progress and the challenges that remain. CA. Cancer J. Clin. 48:263–268.

Lane MA, Romagnoli L, Cruise B, Cohn G. 1999. Spontaneous Conversion to Estrogen Receptor Expression by the Human Breast Epithelial Cell Line, MCF-10A. Oncol. Rep. 6:507–511.

Larsson SC, Orsini N, Wolk A. 2015. Urinary cadmium concentration and risk of breast cancer: A systematic review and dose-response meta-analysis. Am. J. Epidemiol. 182:375–380.

Letašiová S, Medve'ová A, Šovčíková A, Dušinská M, Volkovová K, Mosoiu C, Bartonová A. 2012. Bladder cancer, a review of the environmental risk factors. Environ. Health [Internet] 11 Suppl 1:S11. Available from: http://www.pubmedcentral.nih.gov/articlerender.fcgi?artid=3388449&tool=pmcentrez&rendertype=abstract

Li Z, Wu Z, Chen H, Zhu Q, Gao G, Hu L, Negi H, Kamle S, Li D. 2015. Induction of anterior gradient 2 (AGR2) plays a key role in insulin-like growth factor-1 (IGF-1)-induced breast cancer cell proliferation and migration. Med. Oncol. [Internet] 32:1–12. Available from: "http://dx.doi.org/10.1007/s12032-015-0577-z

Li Z, Zhu Q, Chen H, Hu L, Negi H, Zheng Y, Ahmed Y, Wu Z, Li D. 2016. Binding of anterior gradient 2 and estrogen receptor-α: Dual critical roles in enhancing fulvestrant resistance and IGF-1-induced tumorigenesis of breast cancer. Cancer Lett. [Internet] 377:32–43. Available from: http://dx.doi.org/10.1016/j.canlet.2016.04.003

Liu D, Rudland PS, Sibson DR, Platt-Higgins A, Barraclough R. 2005. Human homologue of cement gland protein, a novel metastasis inducer associated with breast carcinomas. Cancer Res. [Internet] 65:3796–805. Available from: http://www.ncbi.nlm.nih.gov/pubmed/15867376

Liu J, Xie Y, Cooper R, Ducharme DMK, Tennant R, Diwan B a, Waalkes MP. 2007. Transplacental exposure to inorganic arsenic at a hepatocarcinogenic dose induces fetal gene expression changes in mice indicative of aberrant estrogen signaling and disrupted steroid metabolism. Toxicol. Appl. Pharmacol. [Internet] 220:284–91. Available from: http://www.pubmedcentral.nih.gov/articlerender.fcgi?artid=2680420&tool=pmcentrez&rendertype=abstract

Liu J, Yu L, Tokar EJ, Bortner C, Sifre MI, Sun Y, Waalkes MP. 2008. Arsenic-induced aberrant gene expression in fetal mouse primary liver-cell cultures. Ann. N. Y. Acad. Sci. [Internet] 1140:368–75. Available from: http://www.pubmedcentral.nih.gov/articlerender.fcgi?artid=2697955&tool=pmcentrez&rendertype=abstract

Logothetis CJ, Dexeus FH, Chong C, Sella A, Ayala, Alberto G, Ro JY, Pilat S. 1989. Cisplatin, Cyclophosphaide and Doxorubicin Chemotherapy for Unresectable Urothelial Tumors: The M.D. Anderson Experience. J. Urol. 141:33–37.

Luster MI, Simeonova PP. 2004. Arsenic and urinary bladder cell proliferation. Toxicol. Appl. Pharmacol. 198:419–423.

Ma S, Wang W, Huang C, Zhang W. 2015. Anterior gradient protein 2 expression in high grade head and neck squamous cell carcinoma correlated with cancer stem cell and epithelial mesenchymal transition. Oncotarget 6.

Makki J. 2015. Diversity of Breast Carcinoma : Histological Subtypes and Clinical Relevance. :23–31.

Di Maro G, Salerno P, Unger K, Orlandella FM, Monaco M, Chiappetta G, Thomas G, Oczko-Wojciechowska M, Masullo M, Jarzab B, et al. 2014. Anterior gradient protein 2 promotes survival, migration and invasion of papillary thyroid carcinoma cells. Mol. Cancer [Internet] 13:160. Available from: http://www.pubmedcentral.nih.gov/articlerender.fcgi?artid=4094684&tool=pmcentrez&rendertype=abstract

Martelli a, Rousselet E, Dycke C, Bouron a, Moulis J-M. 2006. Cadmium toxicity in animal cells by interference with essential metals. Biochimie [Internet] 88:1807–14. Available from: http://www.ncbi.nlm.nih.gov/pubmed/16814917

Martin JE, Jenkins J, Zuk J. 1989. Clinical importance of squamous metaplasia in invasive transitional cell carcinoma of the bladder. J. Clin. Pathol. 42:250–253.

Martinez-Zamudio R, Ha HC. 2011. Environmental epigenetics in metal exposure. Epigenetics 6:820–827.

Maslon MM, Hrstka R, Vojtesek B, Hupp TR. 2010. A divergent substrate-binding loop within the pro-oncogenic protein anterior gradient-2 forms a docking site for Reptin. J. Mol. Biol. [Internet] 404:418–38. Available from: http://www.ncbi.nlm.nih.gov/pubmed/20888340

Méplan C, Mann K, Chem JB. 1999. CELL BIOLOGY AND METABOLISM : Cadmium Induces Conformational Modifications of Wild-type p53 and Suppresses p53 Response to DNA Damage in Cultured Cells Cadmium Induces Conformational Modifications of Wild-type p53 and Suppresses p53 Response to DNA Damage. 274:31663–31670.

Missiaglia E, Blaveri E, Terris B, Wang Y-H, Costello E, Neoptolemos JP, Crnogorac-Jurcevic T, Lemoine NR. 2004. Analysis of gene expression in cancer cell lines identifies candidate markers for pancreatic tumorigenesis and metastasis. Int. J. Cancer [Internet] 112:100–12. Available from: http://www.ncbi.nlm.nih.gov/pubmed/15305381

Mizuuchi Y, Aishima S, Ohuchida K, Shindo K, Fujino M, Hattori M, Miyazaki T, Mizumoto K, Tanaka M, Oda Y. 2015. Anterior gradient 2 downregulation in a subset of pancreatic ductal adenocarcinoma is a prognostic factor indicative of epithelial-mesenchymal transition. Lab. Invest. [Internet] 95:193–206. Available from: http://www.ncbi.nlm.nih.gov/pubmed/25418581

Navarro Silvera S a, Rohan TE. 2007. Trace elements and cancer risk: a review of the epidemiologic evidence. Cancer Causes Control [Internet] 18:7–27. Available from: http://www.scopus.com/inward/record.url?eid=2-s2.0-33845889501&partnerID=tZOtx3y1\nhttp://www.ncbi.nlm.nih.gov/pubmed/17186419

Nounou MI, ElAmrawy F, Ahmed N, Abdelraouf K, Goda S, Syed-Sha-Qhattal H. 2015. Breast Cancer: Conventional Diagnosis and Treatment Modalities and Recent Patents and Technologies. Breast Cancer (Auckl). [Internet] 9:17–34. Available from: http://www.pubmedcentral.nih.gov/articlerender.fcgi?artid=4589089&tool=pmcentrez&rendertype=abstract

Park K, Chung YJ, So H, Kim K, Park J, Oh M, Jo M, Choi K, Lee E-J, Choi Y-L, et al. 2011. AGR2, a mucinous ovarian cancer marker, promotes cell proliferation and migration. Exp. Mol. Med. [Internet] 43:91–100. Available from: http://www.pubmedcentral.nih.gov/articlerender.fcgi?artid=3047197&tool=pmcentrez&rendertype=abstract

Park S, Zhen G, Verhaeghe C, Nakagami Y, Nguyenvu LT. 2009. The protein disulfide isomerase AGR2 is essential for production of intestinal mucus. PNAS 106:6950–6955.

Parodi DA, Greenfield M, Evans C, Chichura A, Alpaugh A, Williams J, Martin MB. 2015. Alteration of mammary gland development and gene expression by in utero exposure to arsenic. Reprod. Toxicol. [Internet] 54:66–75. Available from: http://dx.doi.org/10.1016/j.reprotox.2014.12.011

Partridge AH, Hughes ME, Ottesen RA, Wong Y-N, Edge SB, Theriault RL, Blayney DW, Niland JC, Winer EP, Weeks JC, et al. 2012. The Effect of Age on Delay in Diagnosis and Stage of Breast Cancer. Oncologist 17:775–782.

Pershagen G. 1981. The carcinogenicity of arsenic. Environ. Health Perspect. Vol. 40:93–100.

Persson S, Rosenquist M, Knoblach B, Khosravi-Far R, Sommarin M, Michalak M. 2005. Diversity of the protein disulfide isomerase family: identification of breast tumor induced Hag2 and Hag3 as novel members of the protein family. Mol. Phylogenet. Evol. [Internet] 36:734–40. Available from: http://www.ncbi.nlm.nih.gov/pubmed/15935701

Petzoldt JL, Leigh IM, Duffy PG, Sexton C, Masters JR. 1995. Immortalisation of human urothelial cells. Urol. Res. 23:377–380.

Pizzi M, Fassan M, Balistreri M, Galligioni A, Rea F, Rugge M. 2012. Anterior gradient 2 overexpression in lung adenocarcinoma. Appl. Immunohistochem. Mol. Morphol. [Internet] 20:31–6. Available from: http://www.ncbi.nlm.nih.gov/pubmed/21768879

Pohler E, Craig AL, Cotton J, Lawrie L, Dillon JF, Ross P, Kernohan N, Hupp TR. 2004. The Barrett's antigen anterior gradient-2 silences the p53 transcriptional response to DNA damage. Mol. Cell. Proteomics [Internet] 3:534–47. Available from: http://www.ncbi.nlm.nih.gov/pubmed/14967811

Ramachandran V, Arumugam T, Wang H, Logsdon CD. 2008. Anterior gradient 2 is expressed and secreted during the development of pancreatic cancer and promotes cancer cell survival. Cancer Res. [Internet] 68:7811–8. Available from: http://www.ncbi.nlm.nih.gov/pubmed/18829536

Reid LM, Leav I, Kwan PW, Russell P, Merk FB. 1984. Characterization of a human, sex steroid-responsive transitional cell carcinoma maintained as a tumor line (R198) in athymic nude mice. Cancer Res. 44:4560–4573.

Reinert T, Barrios CH. 2015. Optimal management of hormone receptor positive metastatic breast cancer in 2016. Ther. Adv. Med. Oncol. [Internet] 7:304–320. Available from: http://tam.sagepub.com/cgi/doi/10.1177/1758834015608993

Riener M-O, Thiesler T, Hellerbrand C, Amann T, Cathomas G, Fritzsche FR, Dahl E, Bahra M, Weichert W, Terracciano L, et al. 2014. Loss of anterior gradient-2 expression is an independent prognostic factor in colorectal carcinomas. Eur. J. Cancer [Internet] 50:1722–30. Available from: http://www.ncbi.nlm.nih.gov/pubmed/24794000

Rossi MR, Masters JRW, Park S, Todd JH, Garrett SH, Sens MA, Somji S, Nath J, Sens DA. 2001. The immortalized UROtsa cell line as a potential cell culture model of human urothelium. Environ. Health Perspect. 109:801–808.

Saint-Jacques N, Parker L, Brown P, Dummer TJ. 2014. Arsenic in drinking water and urinary tract cancers: a systematic review of 30 years of epidemiological evidence. Environ. Health [Internet] 13:44. Available from: http://www.pubmedcentral.nih.gov/articlerender.fcgi?artid=4088919&tool=pmcentrez&rendertype=abstract

Salmans ML, Zhao F, Andersen B. 2013. The estrogen-regulated anterior gradient 2 (AGR2) protein in breast cancer: a potential drug target and biomarker. Breast Cancer Res. [Internet] 15:204. Available from: http://www.pubmedcentral.nih.gov/articlerender.fcgi?artid=3672732&tool=pmcentrez&rendertype=abstract

Sandquist EJ, Somji S, Dunlevy JR, Garrett SH, Zhou XD, Slusser-Nore A, Sens DA. 2016. Loss of N-Cadherin Expression in Tumor Transplants Produced From As+3- and Cd+2-Transformed Human Urothelial (UROtsa) Cell Lines. PLoS One [Internet] 11:e0156310. Available from: http://dx.plos.org/10.1371/journal.pone.0156310

Satarug S, Garrett SH, Sens MA, Sens D a. 2010. Cadmium, environmental exposure, and health outcomes. Environ. Health Perspect. [Internet] 118:182–90. Available from: http://www.pubmedcentral.nih.gov/articlerender.fcgi?artid=2831915&tool=pmcentrez&rendertype=abstract

Sens D a, Park S, Gurel V, Sens MA, Garrett SH, Somji S. 2004. Inorganic cadmium- and arsenite-induced malignant transformation of human bladder urothelial cells. Toxicol. Sci. [Internet] 79:56–63. Available from: http://www.ncbi.nlm.nih.gov/pubmed/14976345

Shen J, Liu J, Xie Y, Diwan B a, Waalkes MP. 2007. Fetal onset of aberrant gene expression relevant to pulmonary carcinogenesis in lung adenocarcinoma development induced by in utero arsenic exposure. Toxicol. Sci. [Internet] 95:313–20. Available from: http://www.pubmedcentral.nih.gov/articlerender.fcgi?artid=2692318&tool=pmcentrez&rendertype=abstract

Shishkin SS, Eremina LS, Kovalev LI, Kovaleva MA. 2013. AGR2, ERp57/GRP58, and Some Other Human Protein Disulfide Isomerases. Biochem. Biokhimiĭa [Internet] 78:1415–30. Available from: http://www.ncbi.nlm.nih.gov/pubmed/24490732\nhttp://link.springer.com/10.1134/S000629791313004X

Slusser-Nore A, Larson-Casey JL, Zhang R, Zhou XD, Somji S, Garrett SH, Sens DA, Dunlevy JR. 2016. SPARC Expression Is Selectively Suppressed in Tumor Initiating Urospheres Isolated from As+3- and Cd+2-Transformed Human Urothelial Cells (UROtsa) Stably Transfected with SPARC. PLoS One [Internet] 11:e0147362. Available from: http://dx.plos.org/10.1371/journal.pone.0147362

Smith AH, Hopenhayn-Rich C, Bates MN, Goeden HM, Hertz-Picciotto I, Duggan HM, Wood R, Kosnett MJ, Smith MT. 1992. Cancer risks from arsenic in drinking water. Environ. Health Perspect. 97:259–267.

Soh M a, Garrett SH, Somji S, Dunlevy JR, Zhou XD, Sens MA, Bathula CS, Allen C, Sens D a. 2011. Arsenic, cadmium and neuron specific enolase (ENO2, γ-enolase) expression in breast cancer. Cancer Cell Int. [Internet] 11:41. Available from: http://www.pubmedcentral.nih.gov/articlerender.fcgi?artid=3233504&tool=pmcentrez&rendertype=abstract

Somji S, Zhou XD, Mehus A, Sens MA, Garrett SH, Lutz KL, Dunlevy JR, Zheng Y, Sens DA. 2010. Variation of keratin 7 expression and other phenotypic characteristics of independent isolates of cadmium transformed human urothelial cells (UROtsa). Chem. Res. Toxicol. 23:348–356.

Steinmaus C, Moore L, Hopenhayn-Rich C, Biggs ML, Smith AH. 2000. Arsenic in drinking water and bladder cancer. Cancer Invest. 18:174–182.

Struhl K. 1998. Histone acetylation and transcriptional regulatory mechanisms. Genes Dev. 12:599–606.

Sung HY, Choi EN, Lyu D, Park AK, Ju W, Ahn JH. 2014. Aberrant hypomethylation-mediated AGR2 overexpression induces an aggressive phenotype in ovarian cancer cells. Oncol. Rep. 32:815–820.

Talaat S, Somji S, Toni C, Garrett SH, Zhou XD, Sens MA, Sens DA. 2011. Kindlin-2 expression in arsenite- and cadmium-transformed bladder cancer cell lines and in archival specimens of human bladder cancer. Urology [Internet] 77:1507.e1-1507.e7. Available from: http://dx.doi.org/10.1016/j.urology.2011.02.040

Thompson D a, Weigel RJ. 1998. hAG-2, the human homologue of the Xenopus laevis cement gland gene XAG-2, is coexpressed with estrogen receptor in breast cancer cell lines. Biochem. Biophys. Res. Commun. [Internet] 251:111–6. Available from: http://www.ncbi.nlm.nih.gov/pubmed/9790916

Tsuji T, Satoyoshi R, Aiba N, Kubo T, Yanagihara K, Maeda D, Goto a., Ishikawa K, Yashiro M, Tanaka M. 2014. Agr2 Mediates Paracrine Effects on Stromal Fibroblasts That Promote Invasion by Gastric Signet-Ring Carcinoma Cells. Cancer Res. [Internet] 75:356–366. Available from: http://cancerres.aacrjournals.org/cgi/doi/10.1158/0008-5472.CAN-14-1693

Vanderlaag KE, Hudak S, Bald L, Fayadat-Dilman L, Sathe M, Grein J, Janatpour MJ. 2010. Anterior gradient-2 plays a critical role in breast cancer cell growth and survival by modulating cyclin D1, estrogen receptor-alpha and survivin. Breast Cancer Res. [Internet] 12:R32. Available from: http://www.pubmedcentral.nih.gov/articlerender.fcgi?artid=2917027&tool=pmcentrez&rendertype=abstract

Verma S, Salmans ML, Geyfman M, Wang H, Yu Z, Lu Z, Zhao F, Lipkin SM, Andersen B. 2012. The estrogen-responsive Agr2 gene regulates mammary epithelial proliferation and facilitates lobuloalveolar development. Dev. Biol. [Internet] 369:249–60. Available from: http://www.pubmedcentral.nih.gov/articlerender.fcgi?artid=3465459&tool=pmcentrez&rendertype=abstract

Wang Z, Hao Y, Lowe AW. 2008. The adenocarcinoma-associated antigen, AGR2, promotes tumor growth, cell migration, and cellular transformation. Cancer Res. [Internet] 68:492–7. Available from: http://www.ncbi.nlm.nih.gov/pubmed/18199544

Wang Z, Hao Y, Lowe AW. 2008. The adenocarcinoma-associated antigen, AGR2, promotes tumor growth, cell migration, and cellular transformation. Cancer Res. 68:492–497.

Wolf C, Strenziok R, Kyriakopoulos A. 2009. Elevated metallothionein-bound cadmium concentrations in urine from bladder carcinoma patients, investigated by size exclusion chromatography-inductively coupled plasma mass spectrometry. Anal. Chim. Acta 631:218–222.

Wright TM, Wardell SE, Jasper JS, Stice JP, Safi R, Nelson ER, McDonnell DP. 2014. Delineation of a FOXA1/ER /AGR2 Regulatory Loop That Is Dysregulated in Endocrine Therapy-Resistant Breast Cancer. Mol. Cancer Res. [Internet] 12:1829–1839. Available from: http://mcr.aacrjournals.org/cgi/doi/10.1158/1541-7786.MCR-14-0195

Xu C, Liu Y, Xiao L, Guo C, Deng S, Zheng S, Zeng E. 2015. The involvement of anterior gradient 2 in the stromal cell-derived factor 1-induced epithelial-mesenchymal transition of glioblastoma. Tumor Biol.:1–7.

Xu Y, Tokar EJ, Waalkes MP. 2014. Arsenic-induced cancer cell phenotype in human breast epithelia is estrogen receptor-independent but involves aromatase activation. Arch. Toxicol. 88:263–274.

Xu Y, Tokar EJ, Waalkes MP. 2014. Arsenic-induced cancer cell phenotype in human breast epithelia is estrogen receptor-independent but involves aromatase activation. Arch. Toxicol. [Internet] 88:263–74. Available from: http://www.ncbi.nlm.nih.gov/pubmed/24068038

Zhang J-S, Gong A, Cheville JC, Smith DI, Young CYF. 2005. AGR2, an androgen-inducible secretory protein overexpressed in prostate cancer. Genes. Chromosomes Cancer [Internet] 43:249–59. Available from: http://www.ncbi.nlm.nih.gov/pubmed/15834940

Zhang W, Wang L, Fan Q, Wu X, Wang F, Wang R, Ma Z, Yang J, Lu SH. 2011. Arsenic trioxide re-sensitizes ERα-negative breast cancer cells to endocrine therapy by restoring ERα expression in vitro and in vivo. Oncol. Rep. 26:621–628.

Zhang Y, Ali TZ, Zhou H, D'Souza DR, Lu Y, Jaffe J, Liu Z, Passaniti A, Hamburger AW. 2010. ErbB3 binding protein 1 represses metastasis-promoting gene anterior gradient protein 2 in prostate cancer. Cancer Res. 70:240–248.

Zweitzig DR, Smirnov D a, Connelly MC, Terstappen LWMM, O'Hara SM, Moran E. 2007. Physiological stress induces the metastasis marker AGR2 in breast cancer cells. Mol. Cell. Biochem. [Internet] 306:255–60. Available from: http://www.ncbi.nlm.nih.gov/pubmed/17694278